Graphite from the University of Idaho Thermolyzed Asphalt Reaction (GUITAR): Fundamental Electrochemical Characterizations

A Dissertation

Presented in Partial Fulfillment of the Requirements for the

Degree of Doctorate of Philosophy

with a

Major in Chemistry

in the

College of Graduate Studies

University of Idaho

by

Isaiah Owusu Gyan

Major Professor: I. Francis Cheng, Ph.D.

Committee Members: Eric B. Brauns, PhD.; David N. McIlroy, Ph.D.; Rick Watts, Ph.D.

Department Administrator: Ray von Wandruszka, Ph.D.

May 2015

Authorization to Submit Dissertation

This dissertation of Isaiah Owusu Gyan, submitted for the degree of Doctor of Philosophy with a Major in Chemistry and titled "Graphite from the University of Idaho Thermolyzed Asphalt Reaction (GUITAR): Fundamental Electrochemical Characterizations," has been reviewed in final form. Permission, as indicated by the signatures and dates given below, is now granted to submit final copies to the College of Graduate Studies for approval.

Major Professor:

_____ Date: _____
I. Francis Cheng, Ph.D.

Committee Members:

_____ Date: _____
Eric B. Brauns, Ph.D.

_____ Date: _____
David N. McIlroy, Ph.D.

_____ Date: _____
Rick Watts, Ph.D.

Department Administrator: _____ Date: _____
Ray von Wandruszka, Ph.D.

Abstract

This dissertation details electrochemical characterization of GUITAR (Graphite from the University of Idaho Thermolyzed Asphalt Reaction), a new allotrope of carbon. Applications based on fundamental electrochemical properties of this material are also presented. The dissertation is presented in five chapters. Chapter one presents a summary of the discovery and physical characterizations of GUITAR and how its physical properties position it among carbon materials. In chapter two, fundamental electrochemical properties covering aqueous potential window and electron transfer kinetics with common dissolved redox couples are presented. This chapter highlights significant electrochemical differences between GUITAR and other sp^2 carbon materials, notably, fast electron transfer across basal plane GUITAR, contrary to reports at basal planes of graphite and graphene electrodes. In chapter three, the concept of electron transfer facility is extended with biologically relevant molecules. GUITAR is shown to be suitable for biosensing with properties such as; facile electron transfer, low detection limit, high resistance to fouling and stability to anodic regeneration procedures. Chapter four presents further exploration of GUITAR's wide cathodic potential limits in other aqueous electrolytes and preliminary studies towards the exploitation of this property in the negative half of vanadium redox flow battery, where GUITAR-based electrodes are expected to increase coulombic efficiency and increase battery performance due to low hydrogen evolution. Chapter five concludes this dissertation with point-by-point presentation of significant discoveries that highlights GUITAR's uniqueness. This chapter also describes how the various fundamental electrochemical properties of GUITAR make it useful for various applications.

Acknowledgements

My deepest appreciation goes to Dr. I. Francis Cheng, for his guidance and mentorship throughout my Ph.D study. I would also like to appreciate my committee members: Dr. Eric B. Brauns, Dr. David N. McIlroy and Dr. Rick Watts for dedicating their time, knowledge and experience to help shape my academic pursuit.

To Dr. Eric Aston, Dr. David McIlroy, Dr. Blaise-Alexis Fouetio Kengne, thank you for your contributions to my knowledge and understanding of various topics and instrumentation and together with Dr. Armando McDonald, thank you for making your instruments and other resources available to me for the advancement of my research. I am very thankful to the faculty and staff, who in diverse ways have created a friendly research environment at the Chemistry department, University of Idaho. In addition, I would like to thank Dr. and Mrs. Renfrew and Thomas F. Harland for all the scholarships. Many thanks to my friends, the African community of UI, former and current lab mates : Dr. Yuqun Xie, Dr. Nolan Nicholas, Simon McAllister, Haoyu Zhu, Charles Nwamba, Md. Kabir, Jeremy Foutch, Matthew Jones, Hailey Smith, Peng Ma and Nicholas Renn. It was really great working together and knowing each other.

Dedication

This dissertation is dedicated to the Gyan family (David, Cecilia, Rebecca, Lot, Isaac, Dorcas and Faustina) of Ghana. Thank you for your support. It is also dedicated to my wife, Bridget Gyan, and our future children.

Table of Contents

List of Figures

List of Tables

Chapter 1: Introduction: Carbon Materials and Their Electrochemistry*

1.1 Forms of Carbon Materials

The tetravalent nature of carbon permits availability of four electrons which could be distributed amongst sigma and pi bonds. Hybridization of the valence electrons in carbon determine the bonding system between adjacent carbon atoms. This bonding system and atomic arrangement also define various forms of carbon with different chemical structures, called allotropes. [1,2] The most common allotropes of carbon include; (1) graphite, in which each carbon atom is sp^2 hybridized, forming hexagonal rings joined together in the likeness of a perfect chicken wire and stacked on top of each other in a 3-dimensional arrangement and (2) diamond, in which all carbon atoms are sp^3 hybridized, forming tetrahedral single bonds with each other (Figure 1.1). [1,3] Both forms of carbon materials exist in nature and are considered the main allotropes of carbon. [1] Similar to the bonding system in graphite, other forms of carbon materials including graphene and carbon nanotube have also been discovered and studied (Figure 1.1). [4]

Varieties of carbon materials are as a result of carbon bonding system (sp^2, sp^3 or both), crystallite/grain/domain size (Figure 1.2) and structure, which affect performance. Whether or not a carbon material is electrically conductive depends on the bonding system. [1] The differences in structure and other properties introduce varieties in performance as well. A brief description of the synthesis and properties of carbon materials commonly used for

* Portions of this chapter are included in a chapter accepted for publication in Graphene Science Handbook, CRC Press, with authorship; Isaiah O. Gyan, Haoyu Zhu and I. Francis Cheng.

electrochemical studies are presented below. Figure 1.1 shows the structure of various carbon materials.

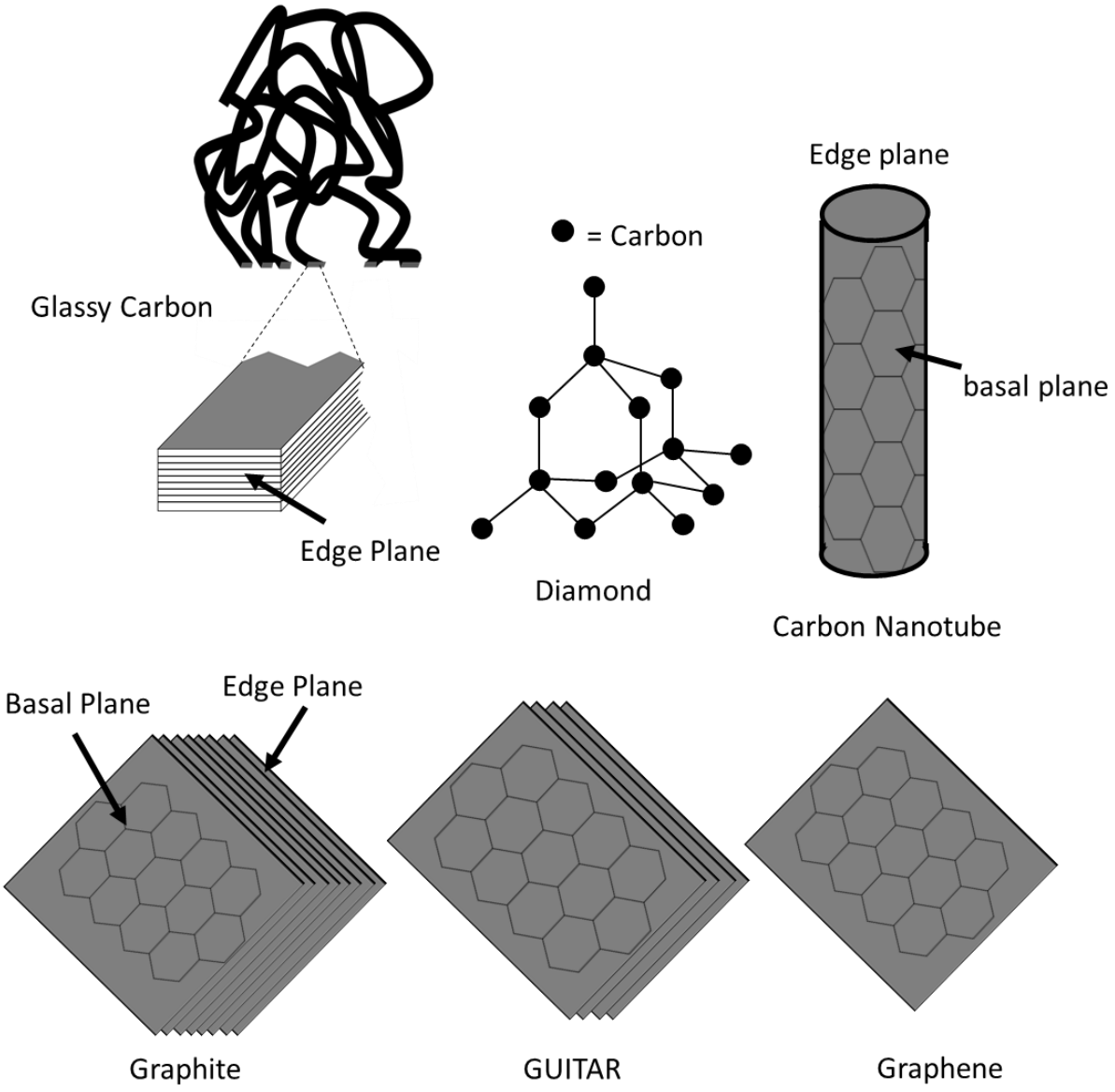

Figure 1.1. Schematic of various forms of carbon materials commonly encountered in literature and GUITAR. GUITAR, graphene and carbon nanotube are of graphitic backbone, with sp^2 hybridized carbon structure. Glassy carbon is graphitic but is composed of interwoven nanoribbons whereas diamond has purely sp^3-bonded carbon atoms.

1.1.1 Pyrolytic graphite

Graphite is perhaps the most common carbon material. In graphite, each carbon atom is sp^2 hybridized and bonded to three other carbon atoms. These carbon atoms are bonded in a hexagonal ring to form a large sheet of material called a plane or graphene sheet/layer. The planes are stacked on top of each other and held by weak attractive intermolecular forces to form a 3-dimensional block (Figure 1.1). Between every two planes is a distance of 3.354 Å (0.3354 nm), called interlayer spacing (d-spacing). [1,5] Figure 1.2 is a schematic of the interlayer spacing in graphite as well as the in-plane and out-of-plane dimensions discussed below.

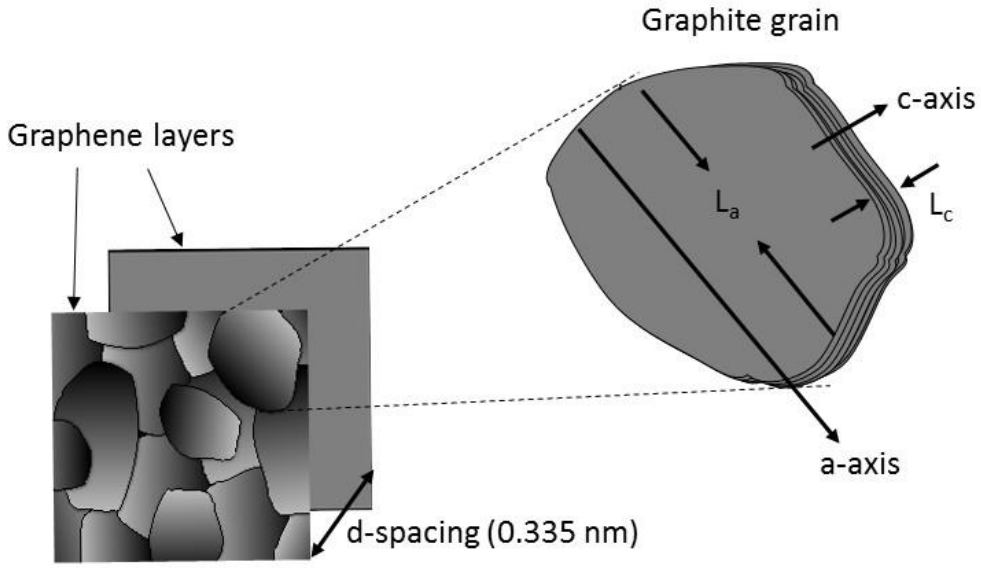

Figure 1.2. Schematic showing the distance between graphene planes in graphite (d-spacing) and the in-plane (a-axis) and out-of-plane (c-axis) dimensions of a graphite grain.

Pyrolytic graphite (PG) is a polycrystalline artificial graphite which can be prepared by the pyrolysis of light hydrocarbons unto a hot stage followed by high-temperature heat treatments. [5]

The high temperatures applied permit orientation of the layers parallel to each other. The extent of ordering of these planes is often expressed as mosaic spread, with the lowest mosaic spread value representing a high degree of ordering. [1] The most ordered graphite, highly ordered pyrolytic graphite (HOPG) could be obtained from pyrolytic graphite (not highly ordered) by pressure annealing under high temperature (ca 3000 ^{o}C) and pressure (> 10 GPa). [5,6] The consequence of the extra treatment of PG to produce HOPG is the presence of little or no defects in HOPG compared to PG. [7] This property has been shown to greatly affect the electrochemical usefulness of HOPG, especially in electron transfer kinetics. [6,8] Physically, HOPG has a smooth, shiny basal surface, while PG is mottled and dull. Apart from PG and HOPG, other forms of graphite with unique features are also known. Glassy carbon (GC) is a form of graphite slightly different in structure. It is made by heating (1000 – 3000 ^{o}C) various polymers, often polyacrylonitrile, under conditions of inert atmosphere. [6,8] Under such pyrolysis, the C-C bonds remain unbroken giving rise to a randomly intertwined ribbon structure as a result of incomplete development of the graphite structure (Figure 1.1). [1,6] The interlayer spacing in GC is 0.36 nm, slightly larger than pyrolytic graphite. [6] Graphitic materials are characterized by the dimensions of their grains (crystallites). The dimension of the grain that is in-plane (a-axis) is often referred to as L_a whereas that perpendicular to the layers (c-axis) is L_c (Figure 1.2). The plane that corresponds to L_a is known as the basal plane whereas that which corresponds to L_c is known as the edge plane

(Figure 1.1). Both L_a and L_c can range from 1 µm to 10 µm in HOPG and 2 nm – 7 nm for glassy carbon. [6,8] A significant difference between glassy carbon and PG/HOPG is that, the structure of GC permits relatively high density of edge plane for use in electrochemical studies (Figure 1.1). Because of this, GC is known to exhibit relatively fast electrochemical kinetics than especially HOPG. [6,7,8] Pyrolytic graphite (PG) has less ordering than HOPG and this property has been shown to favor electrochemical applicability of PG over HOPG. [7]

1.1.2 Graphene

In describing graphene, it is expedient to distinguish the various forms depending on synthesis technique and microstructure. Ideally, graphene is a 2-dimensional (2D) single layer of graphite (monolayer graphene), however bilayer (two layers), few layer (three to ten layers) and graphene platelets/nanoplatelets (ten to hundred layers) are also known. [9,10] The carbon atoms are sp^2 hybridized, in a hexagonal array. The ideal form of graphene (monolayer graphene) was isolated by Geim and Novoselov by mechanical exfoliation of graphite. [11,12] Since then, various attempts have been made to synthesize this material. Currently, many methods have been developed to achieve this goal and graphenes are distinguished according to the method of synthesis. Bottom-up synthesis methods produce graphene from scratch. These methods use carbon precursors that are not already layered or that do not exist in the form of graphite and convert them into graphene. [10,13] Typical examples of bottom-up synthesis methods include; chemical vapor deposition (CVD) and epitaxial growth on SiC. [10,14] In top-down synthesis methods, graphene is produced from precursors that already contain the graphene structure. These precursors are mostly graphite and carbon nanotubes. Top-down synthesis of graphene from graphite could be

achieved by mechanical exfoliation or a process that involve oxidative and reductive treatments that are able to split graphite into graphene layers (often multilayer graphene). [10,14,15] Top-down synthesis of graphene from carbon nanotube is achieved by unzipping the tube. [10] It is worth mentioning that, graphenes differ in properties depending on the method of synthesis. Two of the methods commonly used and the characteristics of their graphene products are described below;

1.1.2.1 Bottom-up: Graphene from chemical vapor deposition (CVD-grown graphene)

In the CVD method of graphene synthesis, carbon precursors (e.g. methane) are pyrolyzed into a chemical vapor that deposits on a catalytic metal substrate (Co, Ni, Cu, Pt, etc.).[16,17,18] The mechanism is thought to involve (1), direct catalytic decomposition of the carbon precursor on the metal surface and/or (2), surface segregation of carbon dissolved in the bulk of the metal substrate. The solubility of carbon in the metal substrate determines which growth mechanism occurs.[16,19]

Even though the growth of a continuous multilayer graphene has been reported with the chemical vapor deposition method, [20] the method is also reported to produce multilayer graphene regions that are randomly scattered on a single layer graphene such that the former acts like graphitic islands and becomes responsible for electrochemical activity, i.e. fast heterogeneous electron transfer (HET). [21] The CVD method can achieve large graphene sizes, however it requires expensive apparatus, high temperatures ($\geq 1000^{o}C$), which affords selectivity in substrates on which the product could be deposited. [17,22]

The quality of graphene from this process also depends on the solubility of carbon in the metal substrate and deposition conditions such as pressure and temperature.[16,19]

1.1.2.2 Top-down: Graphene from chemical oxidation and reduction of graphite

This method of graphene synthesis begins with the treatment of graphite in a mixture of solvents under strong oxidizing conditions to obtain graphite oxide.

Graphite oxide is formed by the combined effect of graphite bulk oxidation and intercalation of ions into the layers of graphite, forming graphite intercalation compounds (GICs).[13,14,15] The oxidation step could be achieved with mixtures of strong acids and oxidants; conc. H_2SO_4/$NaNO_3$/$KMnO_4$ (Hummers method), conc. H_2SO_4/conc. H_3PO_4/$KMnO_4$ (Tour method), conc. H_2SO_4/conc. HNO_3/$KClO_3$ (Hofmann method) and conc. H_2SO_4/fuming HNO_3/$KClO_3$ (Staudenmaier method). [23] Sonication of graphite oxide then disperses the oxidized graphene layers of graphite, producing graphene oxide (GO). The latter is subsequently reduced chemically, thermally (1000^{o}C) and/or photolytically. [24,25,26,27,28] Graphene produced by this method is called reduced graphene oxide (r-GO) or graphene paper and may contain residual oxygen species along the basal and edge planes. Characteristics of the product, including electrochemical applicability depend on the oxidation bath used. [23,28] Solvent based methods described above require as long as 96 hour processing time, is prone to the danger of sudden increment in temperature and the formation of explosive chlorine dioxide gas and eventually results in non-crystalline products. [14,28,29]

1.1.3 Carbon nanotubes (CNTs)

Not only does carbon form planar structures, there also exist structures with closed and open cages based on sp^2 hybridization of the carbon atoms (Figure 1.1). Carbon nanotubes are one kind of such non-planar carbon structures. [2,4] The structure of carbon nanotube is similar to graphene that has been rolled up into a cylinder that can achieve tubes with 2 – 30 nm in diameter and length in micron ranges. [30,31] The tube could be fabricated from a single graphene sheet (single-walled carbon nanotube) or could consist of several graphitic shells (multi-walled carbon nanotube) stacked into one another and separated by 0.34 nm, which is the typical distance between two graphene layers. [31]

Carbon nanotubes are synthesized by three main methods; (1), arc-discharge: in which direct current, applied to two graphite electrodes under inert gas atmosphere, deposits the tube by evaporation of the graphite electrode. (2), laser ablation: in which a laser beam is used to vaporize a mixture of graphite and metal catalyst in a horizontal tube under conditions of inert gas, controlled pressure and temperature. The nanotubes are deposited on a water-cooled collector outside of the furnace. (3), the chemical vapor deposition (CVD) method in which hydrocarbons (typically acetylene and ethylene) are decomposed in the presence of metal catalysts and under controlled conditions. Irrespective of the synthesis method used, CNTs are always produced with impurities that include nanographite, amorphous carbon and the metal catalysts. [31,32,33,34]

The tube-like structure of CNTs results in a material that is one-dimensional with a basal plane (the wall) and edge plane (the tube ends) (Figure 1.1). As observed with graphite and

graphene, these two surfaces of CNTs exhibit different electrochemical activities, with the edge plane reported to exhibit favorable electrochemical kinetics than the basal plane.[30,35]

1.1.4 Diamond and doped diamond

Diamond is known for its unusual hardness and high resistivity. [36] Amongst carbon materials, diamond is regarded to possess the highest hardness, thermal conductivity and density. [37] The purely sp^3 bonding system in diamond makes this material non-conductive, however a variant of diamond, in which boron atoms have been incorporated (boron-doped diamond, BDD) is conductive and widely used in electrochemistry. [1,36,37] Amongst other methods, doped diamond are commonly synthesized by chemical vapor deposition unto conductive substrates, using hydrocarbons as carbon source (typically, methane or acetone/methane mixture), hydrogen as a carrier gas and other gases to provide the dopant.[38] The hydrogen atoms are used to terminate the carbon bonding and prevent graphitization (formation of sp^2 bonded carbon). [39] The boron doping level and the presence of non-diamond carbon impurities affects the characteristics of BDD in electrochemical applications. [40]

Between the structural and bonding (sp^2 and sp^3) extremes in graphite(s) and diamond respectively, various forms of carbon materials are known and studied in literature. Of most interest among these is diamond-like carbon (DLC), which has been defined as amorphous carbon with a high fraction of sp^3 carbon bonds. DLCs also contain sp^2 carbon bonds, however, dominance of the sp^3 bonding makes them possess similar properties as diamond. DLCs can either be synthesized from pure hydrocarbon sources or solid carbon sources such as graphite and fullerenes, with the possibility of doping just like doped diamonds. [1,41]

1.2 Discovery of GUITAR

In the spring of 2008 an interesting carbon film was encountered during sample preparation of a Piceance Basin (Colorado) oil shale for atomic absorption analysis. In an effort to remove the crude oil matrix, flame heat was applied to the sample in a crucible. Upon cooling it was discovered that, under conditions of partial enclosure a film with a metallic sheen coated the interior of the ceramic crucible. Careful removal of the material resulted in flakes (Figure 1.3). Because of its layered characteristics, it was surmised that the material was a form of graphite. [42]

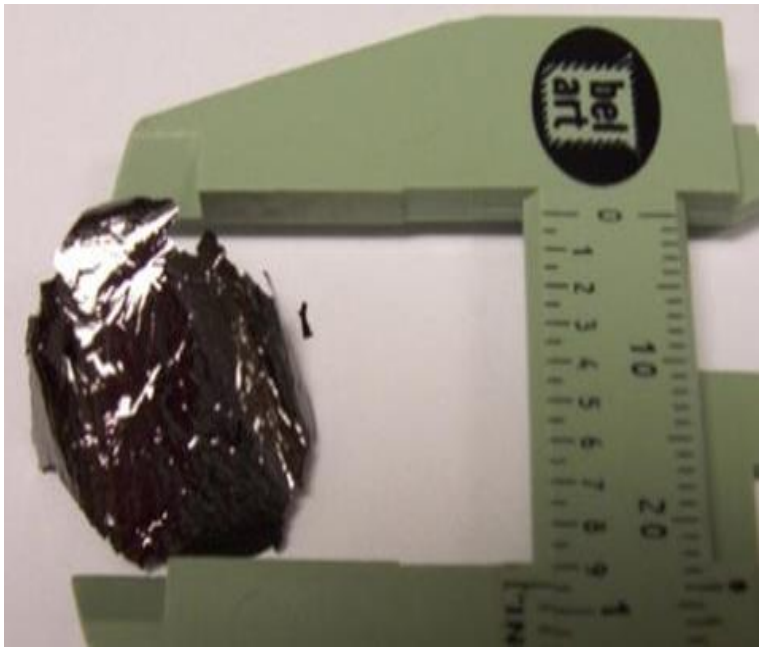

Figure 1.3. A photograph of a flake of GUITAR (approximately 25 mm in diameter) exfoliated from the crucible used in the oil shale sample preparation.

1.2.1 The Thermolyzed Asphalt Reaction (TAR) process

Taking after the setup used in the sample preparation described above, the thermolyzed asphalt reaction was developed with porcelain crucibles supported on clay triangles and

heated by a burner. The oil shale samples were used as carbon precursors. Since the discovery of this material, the method of synthesis has been under development. Beside the crucible method, current synthesis also employs a tube furnace, which allows for temperature control and more rapid synthesis rates. A schematic of both crucible and tube furnace methods are illustrated in Figure 1.4. The GUITAR process is a form of chemical vapor deposition (CVD), in which gas phase reactions deposit layers of GUITAR unto the substrate and often, also unto the reaction vessel (crucible or glass tube). In the crucible method, it is hypothesized that chemical vapor from the pyrolysis of the starting material first exit the inner crucible and disperses towards the sides of the porcelain crucible, where it encounters the substrate and deposits layers of GUITAR (Figure 1.4A). With the tube furnace method, one end of the glass tube it sealed with a paper plug whereas the other end is partially sealed. This is done to concentrate the chemical vapor within the glass chamber for effective deposition and also to direct the flow of the chemical vapor, depending on the position of the substrate (Figure 1.4B).

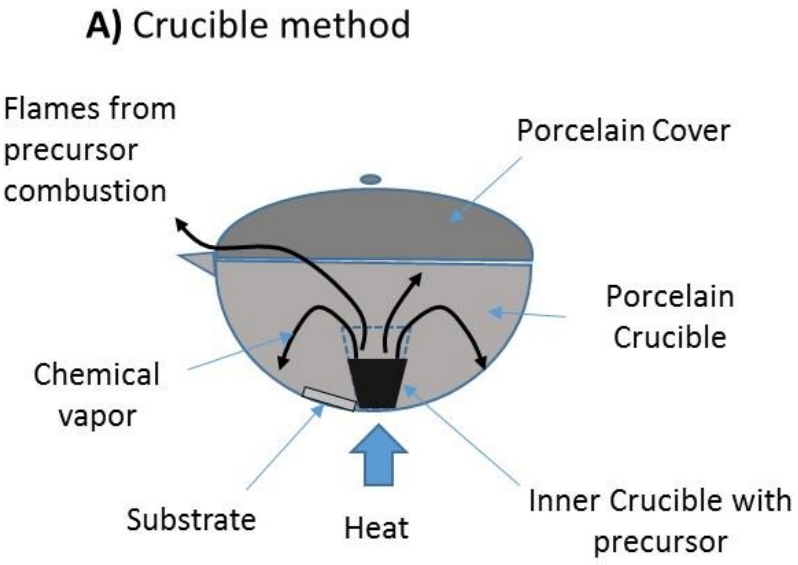

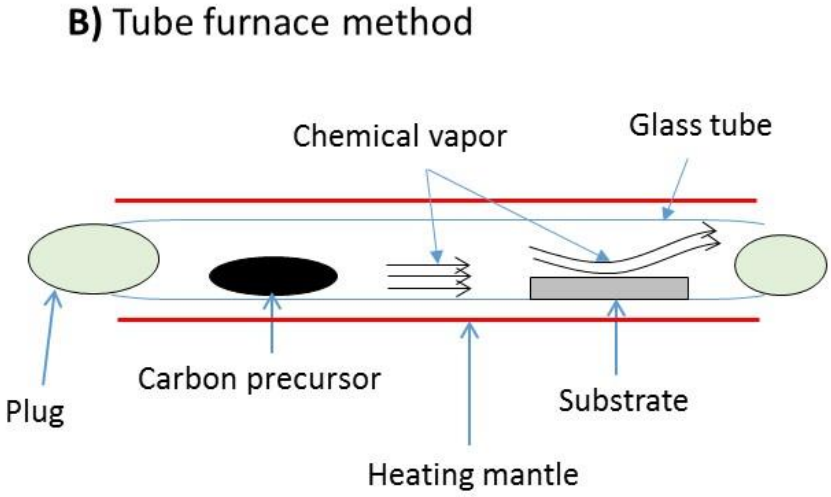

Figure 1.4. Photographs and illustrations of the two methods applied in the GUITAR process. A), crucible method and B), tube furnace method. Both methods are able to deposit GUITAR unto a variety of substrates.

It is worth mentioning that whether crucible or tube furnace method, bulk synthesis of GUITAR can be achieved. Bulk synthesis of GUITAR is unique to this process and affords unique advantages in the area of scalable production for mass applications.

Observations from our laboratories indicate many starting materials produced similar results. These include crude or refined oils and food products such as tortilla chips, red beans and candy bars (Figure 1.5).

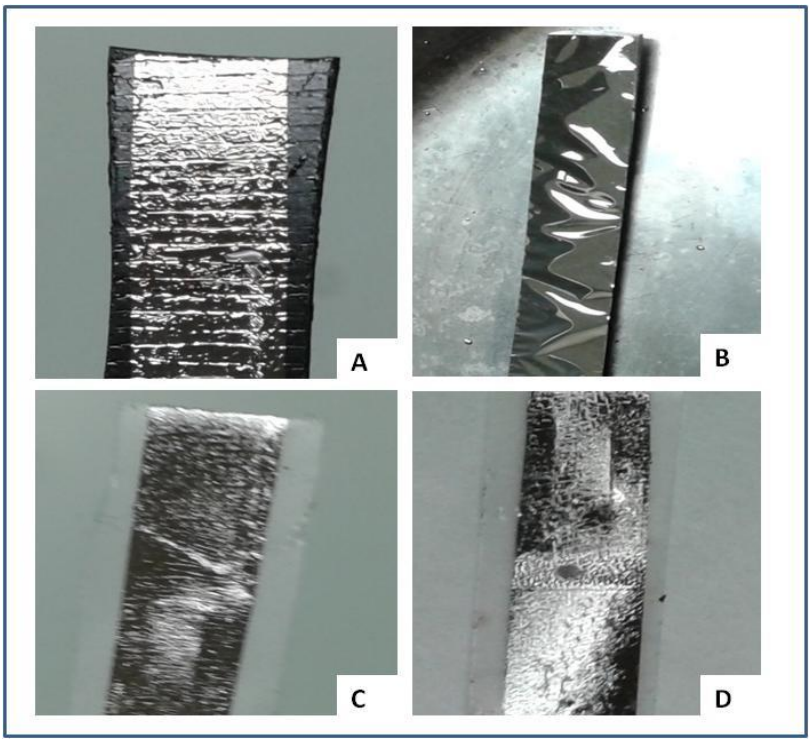

Figure 1.5. Photographs of GUITAR synthesized from various starting materials; GUITAR from red beans (A), roofing tar (B), petroleum jelly (C) and tortilla chips (D).

It was also discovered that sulfur is an Important co-factor in the GUITAR process, acting as a cross linker, according to the scheme shown in Figure 1.6. [43] Sulfur could be added to the starting materials or be incorporated in the carbon precursor. Sulfur is important in the growth of graphitic planes in carbon steel and nanotubes, vulcanization and in the dehydrogenation and dehydration of organics and coal. [44,45,46,47,48]

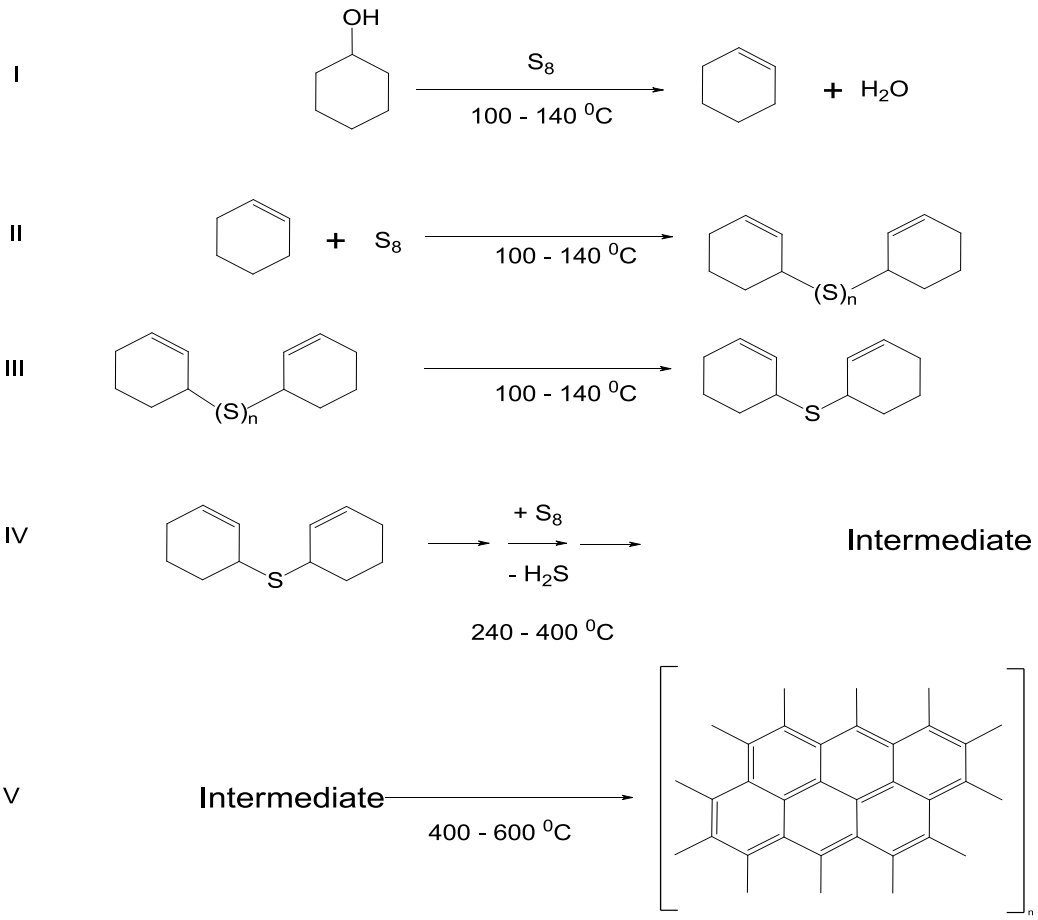

Figure 1.6. Proposed overall scheme for GUITAR formation from sulfur and cyclohexanol based on thermogravimetric analyses. Steps I-III occur concurrently between 100-140 ^{0}C. Above 240 ^{0}C a sequence of sulfur based dehydration steps occur to give an intermediate (as detected by Raman), that rearranges to give GUITAR between 450-600 ^{0}C.

Among the starting materials applicable, asphalt (roofing tar) is a common choice because it is a mixture of high molecular weight hydrocarbons, which result in thicker flakes. It is worth highlighting the simplicity of the GUITAR process, which only requires simple and inexpensive carbon precursors such as roofing tar, casserole crucible, common laboratory apparatuses (burner and clay triangle) and a synthesis temperature that does not exceed 900 ^{o}C. In this process, little skill is required, no flow or restriction of an inert or reactive gas

is necessary and there is no need for pressure control however, bulk synthesis of the product can be achieved. The relatively low temperature has made it possible to deposit GUITAR on a wide range of substrates including glass fibres, nanosprings and diatomaceous earth. [42] The ability to produce graphenic nanostructures is a unique characteristic of the GUITAR process. The GUITAR process also affords a simple, low cost method for synthesizing a material that is very unique and demonstrates electrochemical properties superior to graphene and other carbon materials.

1.2.2 Physical Characterizations of GUITAR

Details of the fabrication process and mechanism of GUITAR formation, as well as physical characterizations have been published and also presented in a previous dissertation. [42,43,49,50] A summary of these physical properties and recent results that make GUITAR similar to or different from other carbon materials are therefore presented here;

1.2.2.1 Optical and electron microscopies

GUITAR has featureless surface to the resolution of scanning electron microscopy (SEM) and optical microscopy (OM) (Figure 1.7), however, recent atomic force microscopy (AFM) results show semi-random circular pits that are 10-50 nm in diameter and 20 nm amplitude (see chapter two for details). [51] SEM images of the edge plane also show that GUITAR is layered (Figure 1.7B). GUITAR has semblance with highly ordered pyrolytic graphite (HOPG) in its atomically flat surface and layered edge however, the AFM results show no evidence of step defects with GUITAR as is apparent with AFM images of HOPG. [52,53] The layered characteristic is also been confirmed with transmission electron (Figure 1.7C) and optical microscopies (TEM & OM). The transmission electron micrograph demonstrates that this

layered feature extends to the nano scale. The layered feature is also shared by graphene paper (also known as reduced graphene oxide, r-GO) and graphites (other than HOPG). [54]

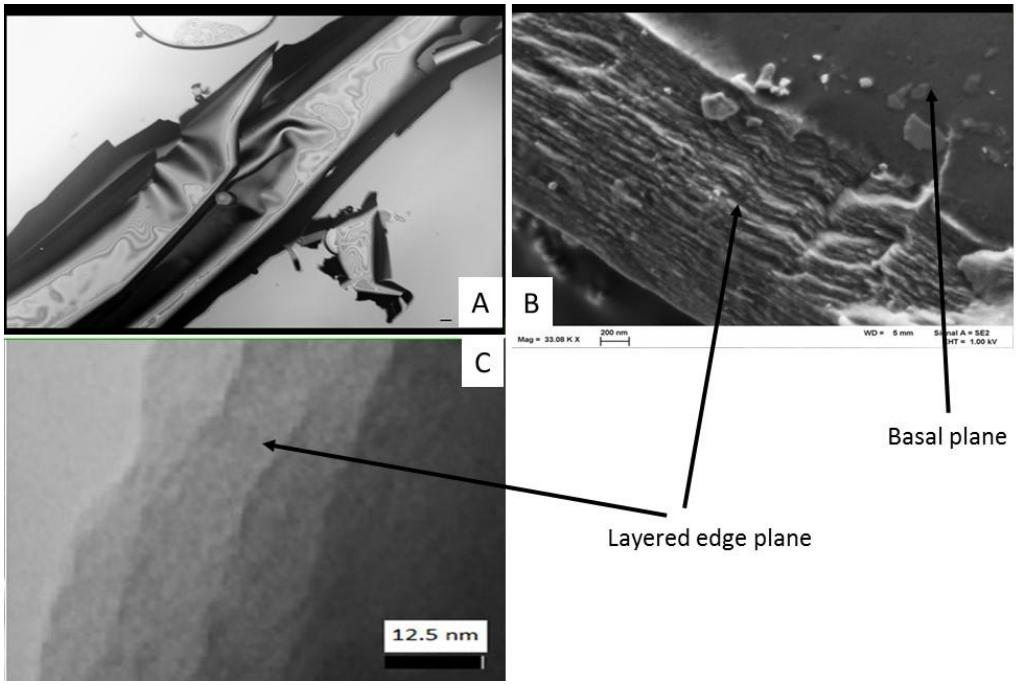

Figure 1.7. An optical micrograph (400x) of GUITAR dispersed in water (A), 23.08K x SEM showing layered characteristics (B) and a TEM showing layered characteristics on the nanometer scale (C).

1.2.2.2 Raman spectroscopy

The Raman spectrum of GUITAR shows a D-band at 1354 cm^{-1} and a G-band at 1593 cm^{-1} (Figure 1.8). The intensity ratio of D to G (I_D/I_G) is 0.93. This ratio is an indication of the presence of significant defects in this material. At this moment, the nature of the defects and how it is propagated within the structure of GUITAR is unknown. It is surmised that non-hexagonal carbon rings (five and/or seven membered rings) may be present. When compared with HOPG, GUITAR is very defective and the D/G ratio is consistent with multilayer and disordered graphene. [55,56,57]

Analyses of GUITAR's Raman spectrum shows that, this material has nanocrystalline grains of 5 nm, is positioned between graphite and nanocrystalline graphite, and has no sp^3 hybridization character. [58,59] The 5 nm grain size of GUITAR is closest to graphene paper and unlike HOPG, which has grains with 1 µm to 10 µm sizes and chemical vapor deposition (CVD) grown graphene, with sizes of 250 nm. [30,60,61]

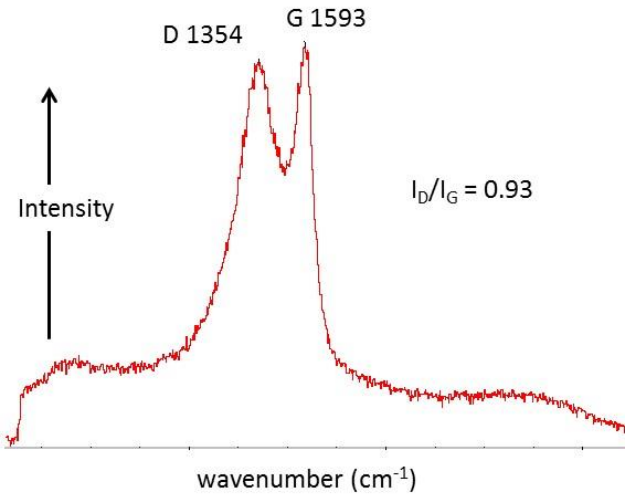

Figure 1.8. Raman spectrum of GUITAR acquired in ambient air using 532 nm excitation; G mode peak at 1593 cm^{-1}, D mode peak at 1354 cm^{-1} at maximum intensity. Intensity ratio (I_D/I_G) is 0.93.

1.2.2.3 X-ray photoelectron spectroscopy (XPS)

Surface elemental analysis with XPS shows that, it is almost pure sp^2 carbon. This information is obtained from analysis of the C1s peak. Deductions from Raman spectroscopy (0% sp^3) confirms this. The elemental ratio of oxygen to carbon (O/C) of 4% is similar to high quality graphene. [62] The sp^2 hybridization property of GUITAR is similar to HOPG and graphene.

1.2.2.4 X-ray diffraction (XRD)

Initial investigations of the diffraction pattern of GUITAR showed an inter-layer spacing (d-spacing) of 0.335 nm, which matches the distance between planes in graphites. [6,42] However, most recent investigations with more advanced x-ray techniques have shown this distance to be much wider (0.376 nm).

1.3 Electrochemistry at carbon electrodes

Carbon materials are probably the most common electrodes used across electrochemistry. Given the wide forms, various carbon electrodes have been applied as either electrodes or substrates in fuel cells and batteries, waste water treatment, ultracapacitors, transistors, electrochemical synthesis, nanomedicine and detection of compounds. [6,63,64,65,66]

The diversity in carbon materials gives rise to variable responses and performances in these applications. Depending on the application, one or more properties of a particular carbon material may be exploited. These properties may involve bulk or surface characteristics. For most electrochemical applications, the success of a carbon material depends on (i) facility of electron exchange between the electrode and a dissolved redox species and (ii) the electrolyte-dependent potential window of the material. The latter encompasses solvent breakdown as well as stability of the electrode material. In most cases, both (i) and (ii) are of great consideration when applying a particular carbon material as electrode. [6,64,65,66]

1.3.1 Heterogeneous Electron Transfer (HET) Kinetics

Exchange of electrons between a solid electrode and a dissolved species is a heterogeneous process whose rate could easily be determined.

In electrochemical assessment of kinetic facility, cyclic voltammetry is a commonly used technique. In cyclic voltammetry, the potential of an electrode is swept through one direction, reversed and swept back. This potential control is in the form of a triangular wave (Figure 1.9). [67,68,69] The potential window of the sweep should enclose the redox potential of the dissolved redox species. In cyclic voltammetry, the solution is not stirred and a large excess of supporting electrolyte is added to the analyte solution. These are needed to exclude mass transport by convection and migration respectively. Mass transport to and from the surface of the electrode is therefore by diffusion. [67,69]

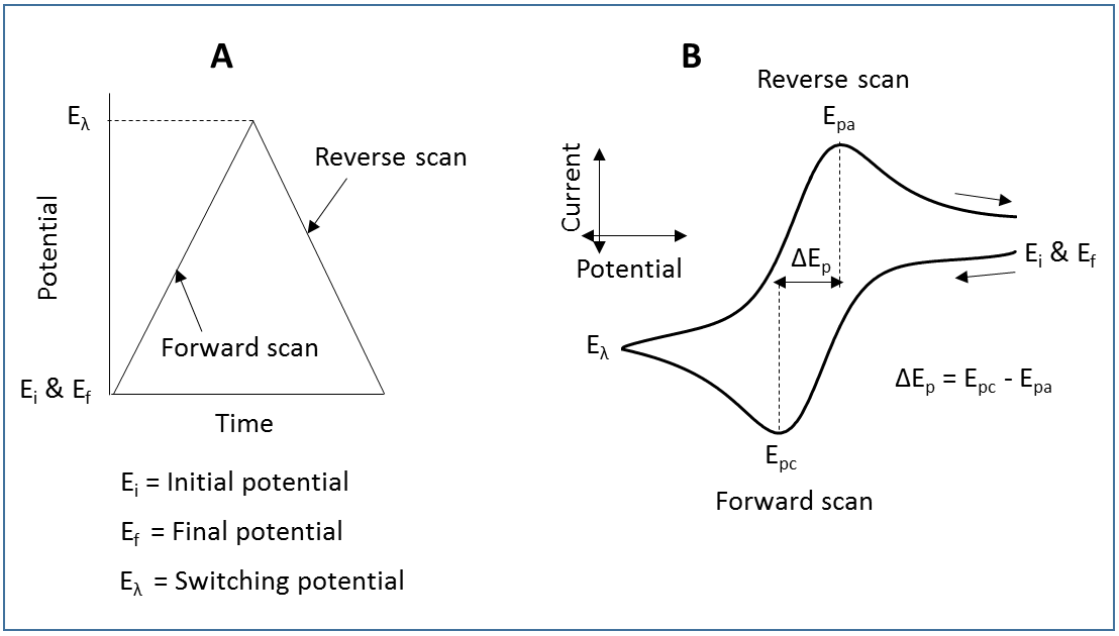

Figure 1.9. A) Triangular wave applied to an electrode during cyclic voltammetry and B) typical cyclic voltammogram showing cathodic and anodic peak potentials (E_{pc} and E_{pa} respectively).

The potential waveform applied in cyclic voltammetry and a sample voltammogram are shown in Figure 1.9A & B respectively. For Figure 1.9B, the IUPAC convention, in which positive potentials are plotted to the right of the x-axis and oxidation currents are positive and plotted at the top of the y-axis, is used in this example.

In most studies the ferri/ferrocyanide redox couple ($Fe(CN)_6^{3-/4-}$) is used as a benchmark redox probe. This redox couple involves a simple one-electron transfer redox process (equation 1). [51]

$$Fe(CN)_6^{3-} + e^- = Fe(CN)_6^{4-} \qquad (1)$$

From the cyclic voltammetry, the separation of the anodic and cathodic peaks (ΔE_p) is used to evaluate how fast electrons are exchanged between the electrode and the redox analyte. For a one-electron process, an electrode demonstrating fast electron transfer kinetics is expected to produce ΔE_p = 57 mV. [67,68,69] Such processes are called reversible. Irreversible electron transfer processes are characterized by much wider peak separations and other properties including relatively low peak currents and a shift in the peak positions with scan rate. Between these two kinetic extremes, are quasi-reversible reactions whose kinetics can either be driven towards reversibility at slow scan rates or towards irreversibility at fast scan rates. [67,68,69] The cyclic voltammogram can be compared to simulations to extract kinetic information or most commonly, electron transfer rate constant (k°, cm/s) is calculated from the relationship between potential peak separation and a kinetic parameter, ψ (see reference 70 for values of ψ), according to equation 2, as developed by Nicholson. [69,70]

$$k^{0} = \frac{\psi\left(\pi D_O v\left({}^{nF}/_{RT}\right)\right)^{1/2}}{\left(\frac{D_O}{D_R}\right)^{\alpha/2}} \qquad (2)$$

Where α is the transfer coefficient, D_O & D_R are diffusion coefficients for the oxidized and reduced forms of the redox probe respectively (cm^2/s), v is the scan rate (V/s), n = number of electrons in the redox process, F = Faraday's constant (96,485 C/mol) and R = universal gas constant = 8.314 J/mol K and T = temperature (K). [67,69] For totally irreversible reactions, the Klingler and Kochi method is used to obtain k°.[71]

1.3.1.1 Factors that affect electron transfer kinetics

A number of factors have been reported to influence the kinetics of electron transfer at carbon surfaces. These factors could be divided into those that are electrode-specific and others that are specific to the redox species.[72] Whether or not a redox species undergoes inner or outer sphere electron transfer, determines whether it requires interactions with sites on the electrode surface to effect electron transfer. [73,74] For inner sphere electron transfer, specific interactions of the dissolved species with sites on the electrode surface are required to speed electron transfer. The sites on the electrode can include species such as oxides. [68,69,74] The latter has been shown to be the case for most metal redox species such as Iron ($Fe^{2+/3+}$) and $Fe(CN)_6^{3-/4-}$. [6,74] In such cases, electrode pretreatments such as application of anodic potentials are able to increase electron transfer kinetics by oxidizing the surface of the electrodes, creating oxide sites for interaction with the redox species. [6,74] Outer sphere redox couples such as $Ru(NH_3)_6^{2+/3+}$ and $IrCl_6^{2-/3-}$ are considered to lack any electrocatalytic or adsorption effects with the electrode.[72] In such cases, modification of the surface of the electrode by physi- or chemisorption of a monolayer (< 1-2 nm) of e.g bis(methyl

styryl)benzene, has no effect on the heterogeneous electron transfer rate constant, since the electron transfer is considered to involve a tunneling mechanism. Rate of electron exchange with such species is considered to depend primarily on the electronic structure of the electrode, specifically, density of electronic states of the electrode (DOS). [6,8,69]

Whether inner or outer sphere electron transfer, the DOS of the electrode is necessary for electron transfer.[75] The electronic DOS of an electrode is potential-dependent and could be described as the density of filled electronic levels/states with the right energy to donate to or the density of vacant electronic levels/states of the right energy to receive electrons from the dissolved species.[68,76] The DOS of carbon electrodes have been shown to be highly dependent on microstructure. At step edges (edge plane) and defects, the DOS of carbon materials (especially graphitic materials) are reported to be higher than at the basal plane.[75] This makes it relatively easier to exchange electrons at edges planes/defect sites. Amongst the evidences leveled in favor of this, are (1), a decrease in the C1s binding energy for carbon atoms at edge planes and (2), a lower barrier to the tunneling current measured at the edge plane from a scanning tunneling microscopy (STM) study.[77] The higher DOS at the edge plane over basal plane, is one of the reasons for the relatively fast electron transfer kinetics at edge plane graphite over basal plane (Figure 1.10). The edge plane also affords easy interaction with inner sphere redox probes.

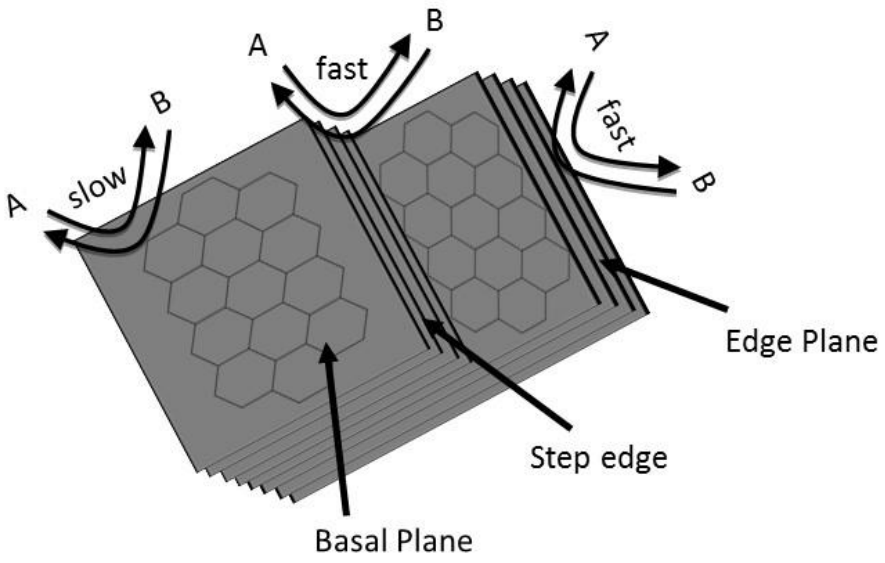

Figure 1.10. Schematic illustration of electron exchange at the different microstructures of graphite and a dissolved redox couple (A and B). Relatively fast electron transfer is achieved at edge and step edge planes of graphitic materials over basal planes due to a number of factors that include a higher density of states at the edge planes/defect sites.

1.3.1.2 Electron transfer kinetics at carbon materials

Typically, basal plane graphite and graphene have electron transfer rates on the order of 10^{-9} cm/s with ferri/ferrocyanide whereas the edge plane can achieve 10^{-2} cm/s. [9] The latter rate is common at glassy carbon, given that it is an edge plane material. [51] The basal plane is inferior to the edge plane by about 1-8 orders of magnitude. In fact, arguments have been leveled towards the fact that, any electron transfer recorded on basal plane HOPG is actually due to residual step edges and that, true basal plane has $k^o \approx 0$ cm/s. [52,68] Treatment of the basal plane such as application of anodic potentials and laser treatment, increases the electron transfer kinetics significantly into the range of edge plane. [77,78] The pretreatment introduces edge defects on the basal plane that increases the electron transfer ability. At graphene electrodes the electron transfer kinetics has also been shown to be highly

dependent on the method of synthesis. [28] The difference in kinetics is due to either residual oxides or fraction of edges/active sites that results from a particular synthesis method. In one report, electron transfer at graphene synthesized by Hummers method was found to be 3.5 and 4.5 times faster than graphenes from the Staudenmaier and Hofmann methods respectively for the ferri/ferrocyanide redox couple. [28] When CVD graphene is used as an electrode whiles still on the metal substrate, the electroactivity of the underlying substrate can complicate the electrochemistry, especially along areas where non-continuous graphene sheets exposes the substrate. [79] Nonetheless, the electrochemistry of CVD graphene is reported to occur at graphitic islands that are randomly scattered on its surface.[79] These islands are as a result of non-uniform growth of multilayer patches of graphene on top of a uniform single layer. The edge planes of the multilayer graphene regions are responsible for the improved electron transfer kinetics. [21,79] Graphene has been reported to be no better electrode and under right edge plane conditions, its performance can only be as good as edge plane pyrolytic graphite (EPPG). [62,68,79]

At carbon nanotubes, the kinetically facile electrochemical performance which made CNTs superior to other carbon materials, has been shown to be due to nanographite impurities and residues of the metals that are used as catalysts in the synthesis process. [80] It has been shown that, even extreme treatment of CNTs in nitric acid is unable to rid the tubes of these metal catalysts. [81] Recent reports show that electron transfer kinetics at pure CNTs, is not any better than graphite, with the edge over basal dominance effect seen too. [82] A rate constant of 10^{-4} cm/s has been reported for pure MWCNT (without metal or carbon impurities) for the redox of ferro/ferricyanide. [80]

Boron doped diamond surfaces are other carbon platforms for electrochemical studies. In place of the edge vs basal plane phenomena in graphite and graphene, there is the effect of the kind of atom terminating the surface bonds. [40,83] Hydrogen-terminated BDD is the common configuration however, oxidative treatments are able to produce oxygen-terminated ones.[40] At pristine BDD, the rate of electron transfer is affected by the concentration of boron dopant and the presence of non-diamond carbon impurities.[40] Oxidatively treated BDD has been found to exhibit slower kinetics towards ferri/ferrocyanide.[40,83] This is in contrary to observations at graphites and graphenes. The reason is that, unlike graphite and graphene, there is no edge defects in BDD to be activated during treatment. Besides, repulsion between the negative charges of the ferri/ferrocyanide and the oxides on the BDD surface cannot be ruled out.[83] Lastly, others report the possible elimination of sp^2 impurities during treatment.[40] A rate constant of 10^{-4} cm/s has been reported for the ferro/ferricyanide redox couple at a pristine BDD surface and 10^{-5} cm/s for the same surface after anodic pretreatment.[40] The oxidation is only beneficial in catalyzing redox of dissolved species that are sensitive to surface oxides.

A striking exception to the edge and basal plane kinetics trend at graphites and graphenes is electron transfer at GUITAR electrodes. A study that looked at electron transfer at basal and edge planes of GUITAR with ferri/ferrocyanide discovered fast kinetics ($k^o = 10^{-2}$ cm/s) at both planes, unlike reports at graphite and graphene. A complementary physical characterization that included AFM showed no steps on the basal surface of GUITAR. Details of this study are presented in chapter two of this dissertation and highlights significant differences between GUITAR and other graphitic carbon materials. [51]

1.3.2 Electrochemical Potential Window

During potential cycles in aqueous electrolytes, two very common reactions are hydrogen evolution (equation 3) and oxygen evolution (equation 4).[84]

$$2H^+ + 2e^- = H_2 \qquad E^o = 0.00 \text{ V vs SHE} \qquad (3)$$

$$2H_2O = 4H^+ + O_2 + 4e^- \qquad E^o = 1.23 \text{ V vs SHE} \qquad (4)$$

Hydrogen generation is a reduction process (cathodic) whereas oxygen evolution is an oxidation process (anodic). At carbon electrodes, a third undesirable reaction at anodic potentials is corrosion of the electrode (equation 5); [85]

$$C + 2H_2O = CO_2 + 4H^+ + 4e^- \qquad E^o = 0.207 \text{ V} \qquad (5)$$

The potentials at which reactions 3 and 4 occur are termed the hydrogen and oxygen evolution potentials respectively and the sum is an indication of the useful potential window within which the electrode could be used without interference from gas evolution. [84] These potentials are commonly evaluated with cyclic voltammetry in bare supporting electrolytes. For applications such as water splitting, in which oxygen and hydrogen are generated by electrolysis, electrodes with low overpotentials for such processes are required, [86,87] however, for studies in anodic stripping voltammetry, cathodic electrochemiluminescence, and vanadium redox flow battery (negative half), an ideal electrode is required to possess a high overpotential for hydrogen evolution.[88,89] In aqueous ultracapacitors, cell voltages are limited to 1.0 to 2.0 V, [66,90,91] based on the 1.23 V required for water breakdown (Reaction 3 and 4). Even though organic solvents offer up to 5 V of cell potential, the advantages of

aqueous electrolytes in ultracapacitors are superior ionic conductivity, nonflammability, lower costs and green solvent considerations.[92,93,94]

In characterizing electrode materials, a wide potential window is desired. In this way, the electrode approaches an ideal polarizable electrode.[69] Graphitic carbon materials have potential windows mostly limited to ≈ 2.0 V in acidic media. In sulfuric acid medium, graphitic materials (HOPG, PG and GC) have windows in the range of 1.97 V to 2.2 V.[95,96,97] These windows break down to +1.5 V to +1.8 V and -0.3 V to -0.5 V versus the standard hydrogen electrode (SHE) on the anodic and cathodic potential halves respectively. Boron-doped diamond (BDD) has been reported to exhibit the widest aqueous potential window reported for carbon materials. Even though this window varies depending on the source, boron doping level and surface termination, values in the range of 2.3 V to 3.5 V are reported. [96,97,98,99] A variant of BDD in which fluoride ions have been bonded to carbon (fluorinated BDD), has been shown to extend even wider (up to 5 V).[100,101] At GUITAR electrodes, potential windows from 3.0 V to 3.4 V have been discovered in various aqueous electrolytes. In sulfuric acid medium, the potential window at GUITAR electrodes is 3.0 V, which breaks down to +2.1 V and -0.9 V at the anodic and cathodic limits respectively.[51] Potential window at GUITAR electrodes exceed that of graphite (HOPG, PG, GC) by at least 0.8 V and compares with BDD (2.3 V to 3.5 V). In this case, GUITAR possesses the largest window reported for a graphitic carbon material. The result of this, is the ability of GUITAR to be used at potentials where typical graphite electrodes are unstable or have their performance obscured by gas evolution. This feature of GUITAR also marks another

significant difference between this material and other graphitic carbon materials and the details are presented in chapters two and four of this dissertation.

1.3.2.1 Potential Window-Limiting Reactions

It is worth mentioning that, besides the potential limits defined by reactions 3 and 4 (water breakdown reactions), inherent properties of certain materials could also limit their applicability at or beyond certain potentials. For example, considering the two anodic reactions above (equations 4 and 5), corrosion of carbon is a more accessible process and should limit the application of carbon materials, since the process involves consumption of the electrode (conversion to CO_2). [85] This phenomenon is seen at graphite electrodes during anodic cycles in some aqueous solutions. During anodic potential cycling of graphite in sulfuric acid (and other electrolytes), a process called intercalation, which involves insertion of ions and electrolyte into the layers of graphite is reported to occur. [102,103,104]

Intercalation in graphite is reported to proceed according to equation 6 and is accompanied by side reactions that include graphite oxide formation (equation 7), oxygen and carbon dioxide evolution (equations 4 and 5).[103,104,105]

$$[C_x] + [A^-] + y(\text{solvent}) = [C_x^+ A^-]y(\text{solvent}) + e^- \qquad (6)$$

$$C_x + 2H_2O = C_xO_2H_y + (4\text{-}y)H^+ + (4\text{-}y)e^- \qquad (7)$$

It is obvious that, the combined effects of oxygen evolution (equation 4), graphite oxidation (equations 5 and 7) and intercalation (equation 6), limits the anodic applicability of graphite.[105] Intercalation in graphite is also accompanied by blister formation and eventually

corrosion. This is an indication of the lack of stability of typical graphitic materials at higher anodic potentials.

At graphene electrodes, it is also reported that both the anodic and cathodic potential limits depend on the method of graphene synthesis. [23,106] It is reported that, graphene prepared by chemical reduction of graphene oxide contains residual oxygen moieties whose reduction during cathodic potential cycling, limits the cathodic applicability of this material.[106] In a typical case, the cathodic potential limit of chemically reduced graphene was limited to about -0.5V vs SHE in borate buffer, making it unable to be used for the electroanalytical determination of 2-Nitrotoluene. [106] In another report, graphene prepared by the reduction of permanganate-oxidized graphite is found to possess limited anodic potential limit.[23] It is interesting to note that at GUITAR electrodes, there is neither intercalation nor any inherent surface properties that limit the potential window.[51] In other words, the aqueous potential window at GUITAR electrodes are controlled only by water breakdown. Lack of intercalation at GUITAR electrodes have been verified in H_2SO_4, KNO_3, $LiClO_4$, $(NH_4)_2SO_4$ electrolytes, in all of which, HOPG has been reported to experience the intercalation effect. [102,103,104] In the same way, there is the lack of inherent features that are reported to limit both the anodic and cathodic limits at graphene. The sum of these (lack of both intercalation and potential window-limiting reactions) is the reason for the wider potential limits at GUITAR electrodes. Most importantly, it is also the reason for GUITAR's anodic stability over typical graphitic materials. Both properties distinguish GUITAR from graphitic materials.

1.4 GUITAR versus other graphitic materials

Since the discovery of GUITAR, both physical and electrochemical studies have been directed towards understanding its properties in order to identify the position of this material within the list of carbon materials. Initial physical characterizations hinted that the structure of GUITAR is graphitic, which means that, the carbon atoms in this material are all sp^2 bonded to each other. This information was obtained from analyses of x-ray photoelectron spectroscopy (XPS) data. Looking at electron and optical micrographs, further understanding indicates that, GUITAR is multilayered, with typical thickness that reaches up to 1 µm but can vary with deposition conditions (specifically quantity of starting material used).

The presence of a d-band in the Raman spectrum of GUITAR is an indication of a disordered graphitic material. Analysis of the same Raman data supported the purely sp^2 hybridization of the carbon atoms in GUITAR. In determining as to whether the new material was graphene paper or HOPG, we began to call it GUITAR for graphene/graphite from the University of Idaho Thermolyzed Asphalt Reaction. It is apparent that GUITAR is a form of pyrolytic graphitic carbon material however, at this moment, it is been identified to be unique in its characteristics, though it has semblance to especially graphite and graphene paper.

Mechanical examination shows that GUITAR is brittle and very easy to squash into pieces however, attempts to isolate its layers by scotch tape exfoliation is almost impossible. Unlike HOPG whose layers can be separated easily and uniformly by exfoliation, attempts to exfoliate GUITAR layers hardly results in a uniform transfer of material and often produces patches of randomly detached material. Though unconfirmed, it is possible that the defects

in GUITAR are involved in interlayer bonding that prevents easy exfoliation of its planes.[107] This hypothesis will explain some electrochemical findings explained in later chapters of this dissertation.

In comparison with graphites, including HOPG, and graphene, GUITAR exhibits markedly different physical, chemical and electrochemical properties. Similarities in appearance led us to believe initially that GUITAR was a form of HOPG or graphene. These are outlined in the summary of physical characteristics; however a prominent Raman d-band indicates a small grain size of 5 nm. When compared to 1 – 10 μm for graphite and 50 to 3000 nm for CVD grown graphene,[22] GUITAR should be precluded from consideration as a form of either.[30] Also noteworthy is that although GUITAR has a similar grain size as r-GO they are dissimilar in that this material has a wavy and textured surface from its agglomeration of graphene platelets,[54] whereas GUITAR's surface appears to be almost atomically flat to the resolution of SEM. Highly oriented pyrolytic graphite (HOPG) has morphological features that include a flat surface with layered graphene planes. GUITAR is also hydrophobic and tends to curl upon itself in aqueous solutions (Figure 1.7A).

Perhaps the largest deviation from HOPG and graphene is in terms of electrochemical characteristics, which are presented in detail in further chapters of this dissertation. We hypothesize that nature of the defects between the grains and/or layers of GUITAR are fundamentally different from those with graphite and graphene. The lack of electrolyte intercalation and relatively fast electron transfer rates from its basal planes with dissolved redox species (chapter two) indicate that the defects may give rise to higher density of states (DOS) than with HOPG or graphene. GUITAR is a much better electrode than either

material.[62] Furthermore, GUITAR has a larger aqueous electrochemical potential window (chapters two and four). We propose GUITAR to be a unique material, perhaps a new allotrope of carbon, which has an ordered layered structure across planes giving rise to atomically flat graphene planes, but with a great degree of disorder within those planes. Furthermore, although Raman spectroscopy suggests that it has nano-grains of 5 nm, we suggest that these grains are bound together in non-hexagonal arrangements of sp^2 carbon. This is in contrast with graphites including HOPG and graphene where the crystalline grains are in only physical contact.

1.5 Research overview and significance

In this dissertation, studies on the electrochemical characteristics of GUITAR are presented. The projects reported in this work were performed to complement the physical characterizations of this material, in order to fully understand its properties and performance, and the relationships between these parameters. GUITAR used in the studies presented here were synthesized mostly by the crucible method, using asphalt as carbon precursor and pieces of silicon wafer as substrates. Once synthesized, GUITAR electrodes were fabricated by using a thin film of vacuum grease to immobilize the flake unto a non-conductive substrate, mostly transparent plastic sheets. Electrical contact was established with a copper alligator clip. A schematic of GUITAR electrode fabrication is presented in Figure 1.11. Prior to use, geometric areas of the electrodes could be isolated with molten wax (see chapter two for details).

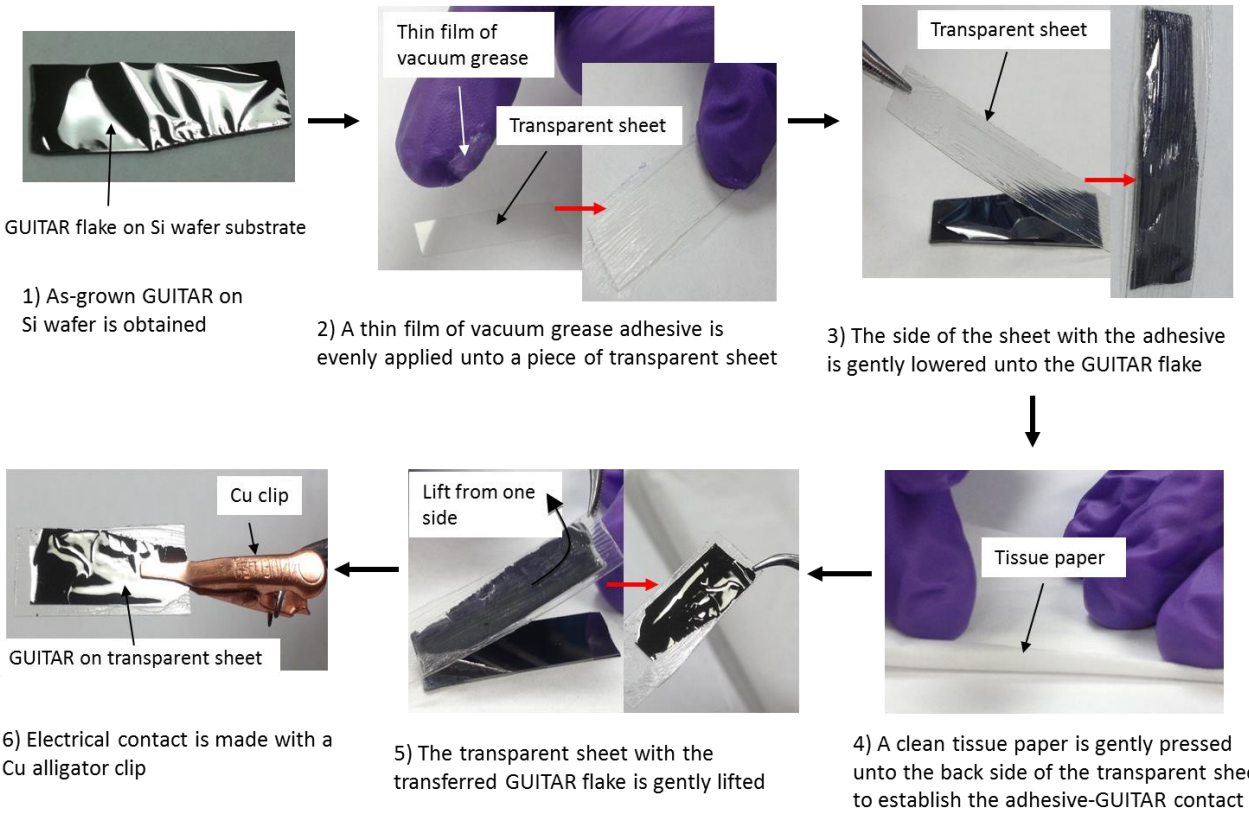

Figure 1.11. Schematic for the fabrication of GUITAR electrodes.

The projects were directed towards understanding the electrochemical properties that make GUITAR similar to or different from other carbon materials. Specific projects covered in this dissertation include;

1. Electron transfer kinetics at both edge and basal planes of GUITAR and the effect of electrode aging on these kinetics (chapter two).
2. Anodic potential limits at GUITAR electrodes in aqueous electrolytes and the factors responsible for GUITAR's relatively large overpotential performance (chapter two).

3. Cathodic potential limits at GUITAR electrodes in aqueous electrolytes and the application of GUITAR as electrode in the negative half of vanadium redox flow battery (chapters two and four).
4. Electrochemistry of biologically relevant molecules at GUITAR electrodes (chapter three).

Based on the results from these studies, further understanding of the properties of GUITAR has been gained. Despite the physical similarities outlined above, it has been established that GUITAR is neither reduced graphene oxide (r-GO) nor any of the conventional graphites reported in literature, but a disordered graphitic system with numerous advantageous properties. GUITAR has been found to be electrochemically different from especially graphite in many respects. Results from these studies have also laid significant foundations for the application of this material in various areas including; biosensing, ultracapacitors and waste water treatment (chapter 5).

1.6 References

[1] Falcao, Eduardo HL.; Wudl, Fred. Carbon allotropes: beyond graphite and diamond. *J Chem Technol Biotechnol*. **2007**, *82*, 524-531.

[2] Singh, Shiv B.; Singh, Aaditya. The Third Allotrope of Carbon: Fullerene an Update. *Int. J. ChemTech Res*. **2013**, *5*, 167-171.

[3] Wang, Jian-Tao; Chen, Changfeng; Wang, Enge; Kawazoe, Yoshiyuki. A New Carbon Allotrope with Six-Fold Helical Chains in all-sp^2 Bonding Networks. *Sci. Rep*. | 4 : 4339 | DOI: 10.1038/srep04339.

[4] Shenderova, O. A.; Zhirnov, V. V.; Brenner, D. W. Carbon Nanostructures. *Crit. Rev. Solid State Mater. Sci*. **2002**, *27*, 227–356.

[5] Chung, D. D. L. Graphite. *J Mater Sci*. **2002**, *37*, 1475-1489.

[6] McCreery, Richard L. Advanced Carbon Electrode Materials for Molecular Electrochemistry. *Chem. Rev*. **2008**, *108*, 2646–2687.

[7] McCreery, Richard L.; Cline, Kristin K. *In Laboratory techniques in electroanalytical chemistry*. Kissinger, P. T.; Heineman, W. R. eds.; 2nd ed., Marcel Dekker: New York, 1996

[8] McCreery, Richard L. Electrochemical properties of carbon surfaces. *Interfacial Electrochemistry: Theory: Experiment and Applications*. **1999**, 631-648.

[9] Pumera, Martin. Graphene-based nanomaterials and their electrochemistry. *Chem. Soc. Rev.* **2010**, DOI:10.1039/C002690P.

[10] Martín, Aida; Escarpa, Alberto. Graphene: The cutting-edge interaction between chemistry and electrochemistry. *Trends Anal. Chem*. **2014**, *56*, 13-26.

[11] Novoselov, K. S.; Geim, A. K.; Morozov, S. V.; Jiang, D.; Zhang, Y.; Dubonos, S. V.; Grigorieva, I. V.; Firsov, A. A. Electric Field Effect in Atomically Thin Carbon Films. *Science* **2004**, *306*, 666–669.

[12] Novoselov, K. S.; Jiang, D.; Schedin, F.; Booth, T. J.; Khotkevich, V. V.; Morozov, S. V.; Geim, A. K. Two-dimensional atomic crystals. *Proc. Natl. Acad. Sci*. *U.S.A*. **2005**, *102*, 10451–10453.

[13] Zhi, L.; Mullen, K. A bottom-up approach from molecular nanographenes to unconventional carbon materials. *J. Mater. Chem*. **2008**, *18*, 1472–1484.

[14] Wassei, Jonathan K.; Kaner, Richard B. Oh, the Places You'll Go with Graphene. *Acc. Chem. Res*. **2013**, *46*, 2244-2253.

[15] Eswaraiah, V.; Aravind, S. S. J.; Ramaprabhu, S. Top down method for synthesis of highly conducting graphene by exfoliation of graphite oxide using focused solar radiation. *J. Mater. Chem*. **2011**, *21*, 6800-6803.

[16] Avouris, Phaedon; Dimitrakopoulos, Christos. Graphene: synthesis and applications. *Mater. Today*, **2012**, *15*, 86-97.

[17] Lee, Seunghyun; Lee, Kyunghoon; Zhong, Zhaohui. Wafer Scale Homogeneous Bilayer Graphene Films by Chemical Vapor Deposition. *Nano Lett*. **2010**, *10*, 4702-4707.

[18] Somani, Prakash R.; Somani, Savita P.; Umeno, Masayoshi. Planer nano-graphenes from camphor by CVD. *Chem. Phys. Lett*. **2006**, *430*, 56-59.

[19] Li, Xuesong; Cai, Weiwei; An, Jinho; Kim, Seyoung; Nah, Junghyo; Yang, Dongxing; Piner, Richard; Velamakanni, Aruna; Jung, Inhwa; Tutuc, Emanuel; Banerjee, Sanjay K.; Colombo, Luigi; Ruoff, Rodney S. Large-Area Synthesis of High-Quality and Uniform Graphene Films on Copper Foils. *Science* **2009**, *324*, 1312- 1314.

[20] Diaz-Pinto, C.; De, D.; Hadjiev, V. G.; Peng, H. AB-Stacked Multilayer Graphene Synthesized via Chemical Vapor Deposition: A Characterization by Hot Carrier Transport. *ACS Nano* **2012**, *6*, 1142-1148.

[21] Brownson, Dale A. C.; Banks, Craig E. CVD graphene electrochemistry: the role of graphitic islands. *Phys. Chem. Chem. Phys.*, **2011**, *13*, 15825-15828.

[22] Brownson, D. A. C.; Kampouris, D. K.; Banks, C. E. Graphene electrochemistry: fundamental concepts through to prominent applications. *Chem Soc Rev*. **2012**, *41*, 6944-76.

[23] Lim, Chee S.; Chua, Chun K.; Pumera, Martin. Permanganate-Route-Prepared Electrochemically Reduced Graphene Oxides Exhibit Limited Anodic Potential Window. *J. Phys. Chem. C* **2014**, *118*, 23368-23375.

[24] Li, D.; Muller, M. B.; Gilje, S.; Kaner, R. B.; Wallace, G. G. Processable aqueous dispersions of graphene nanosheets. *Nat. Nanotechnol.* **2008**, *3*, 101-105.

[25] Tung, V. C.; Allen, M. J.; Yang, Y.; Kaner, R. B. High-throughput solution processing of large-scale graphene. *Nat. Nanotechnol*. **2009**, *4*, 25-29.

[26] Strong, V.; Dubin, S.; El-Kady, M. F.; Lech, A.; Wang, Y.; Weiller, B. H.; Kaner, R. B. Patterning and electronic tuning of laser scribed graphene for flexible all-carbon devices. *ACS Nano* 2012, 6, 1395-1403.

[27] Dubin, S.; Gilje, S.; Wang, K.; Tung, V. C.; Cha, K.; Hall, A. S.; Farrar, J.; Varshneya, R.; Yang, Y.; Kaner, R. B. A one-step, solvothermal reduction method for producing reduced graphene oxide dispersions in organic solvents. *ACS Nano* **2010**, *4*, 3845-3852.

[28] Poh, H. L.; Sanek, F.; Ambrosi, A.; Zhao, G.; Sofer, Z.; Pumera, M. Graphenes prepared by Staudenmaier, Hofmann and Hummers methods with consequent thermal exfoliation exhibit very different electrochemical properties. *Nanoscale* **2012**, *4*, 3515-3522.

[29] Guo, P.; Song, H.; Chen, X. Electrochemical performance of graphene nanosheets as anode material for lithium-ion batteries. *Electrochem. Commun*. **2009**, *11*, 1320-1324.

[30] Banks, C. E.; Davies, T. J.; Wildgoose, G. G.; Compton, R. G. Electrocatalysis at graphite and carbon nanotube modified electrodes: edge-plane sites and tube ends are the reactive sites. *Chem. Commun.* **2005**: 829–841.

[31] Popov, Valentin N. Carbon nanotubes: properties and application. *Mater. Sci. Eng., R* **2004**, 43, 61-102.

[32] Prasek, Jan; Drbohlavova, Jana; Chomoucka, Jana; Hubalek, Jaromir; Jasek, Ondrej; Adamc, Vojtech; Kizek, Rene. Methods for carbon nanotubes synthesis—review. *J. Mater. Chem*., **2011**, *21*, 15872-15884.

[33] Szabó, Andrea; Perri, Caterina; Csató, Anita; Giordano, Girolamo; Vuono, Danilo; Nagy, János B. Synthesis Methods of Carbon Nanotubes and Related Materials. *Materials* **2010**, *3*, 3092-3140.

[34] Dai, Hongjie. Carbon Nanotubes: Synthesis, Integration, and Properties. *Acc. Chem. Res*. **2002**, *35*, 1035-1044.

[35] Banks, Craig E.; Compton, Richard G. New electrodes for old: from carbon nanotubes to edge plane pyrolytic Graphite. *Analyst* **2006**, *131*, 15-21.

[36] Swain, Greg M.; Ramesham, Rajeshuni. The Electrochemical Activity of Boron-Doped Polycrystalline Diamond Thin Film Electrodes. *Anal. Chem*. **1993**, *65*, 345-351.

[37] Ramesham, R.; Rose, M.F. Cyclic voltammetric, a.c. and d.c. polarization behavior of boron-doped CVD diamond. *Thin Solid Films* **1997**, *300*, 144-153.

[38] Kraft, Alexander. Doped Diamond: A Compact Review on a New, Versatile Electrode Material. *Int. J. Electrochem. Sci*. **2007**, *2*, 355-385.

[39] Luong, John H. T.; Male, Keith B.; Glennon, Jeremy D. Boron-doped diamond electrode: synthesis, characterization, functionalization and analytical applications. *Analyst* **2009**, *134*, 1965-1979.

[40] Duo, I.; Levy-Clement, C.; Fujishima, A.; Comninellis, C. Electron transfer kinetics on boron-doped diamond Part I: Influence of anodic treatment. *J. Appl. Electrochem*. **2004**, *34*, 935-943.

[41] Zeng, Aiping; Neto, Victor F.; Gracio, Jose J.; Fan, Qi H. Diamond-like carbon (DLC) films as electrochemical electrodes. *Diamond Relat. Mater*. **2014**, *43*, 12-22.

[42] Cheng, I. F.; Xie, Yuqun; Gonzales, R. A.; Brejna, Przemysław R.; Sundararajan, Jency P.; Kengne, B-A. F.; Aston, D. E.; McIlroy, David N.; Foutch, Jeremy D.; Griffiths, Peter R. Synthesis of Graphene Paper from Pyrolyzed Asphalt. *Carbon* **2011**, *49*, 2852-2861.

[43] Xie, Yuqun; McAllister, Simon D.; Hyde, Seth A.; Sundararajan, Jency P.; Kengne, B-A. F.; McIlroy, David N.; Cheng, I. F. Sulfur as an important co-factor in the formation of multilayer graphene in the thermolyzed asphalt reaction. *J. Mater. Chem*. **2012**, *22*, 5723-5729.

[44] Morrison, N. J.; Porter, M. Temperature effects on the stability of intermediates and crosslinks in sulfur vulcanization. *Rubber Chem. Technol*. **1984**, *57*, 63-85.

[45] Morrison, N. J. The reactions of crosslink precursors in natural rubber. *Rubber Chem. Technol*. **1984**, *57*, 86-96

[46] Kowata, T.; Lee, S. H.; Hiratsuka, H.; Hareyama, T. Effect of sulfide shape on graphitization of flake graphite cast iron. *J. Japan Foundry Eng. Soc*. **2002**, *74*, 9578-9583.

[47] Semmelhack, H. C.; Hohne, R.; Esquinazi, P.; Wagner, G.; Rahm, A.; Hallmeier, K. H. Growth of highly oriented graphite films at room temperature by pulsed laser deposition using carbon-sulfur targets. *Carbon* **2006**, *44*, 3064-3072.

[48] Double, D. D.; Hellawell, A. The nucleation and growth of graphite- the modification of cast iron. *Acta Metall. Mater*. **1995**, *43*, 2435-2442.

[49] Cheng, I. F.; Xie, Yuqun; Gyan, Isaiah O.; Nicholas, Nolan W. Highest measured anodic stability in aqueous solutions: graphenic electrodes from the thermolyzed asphalt reaction. *RSC Adv*. **2013**, *3*, 2379-2384.

[50] Xie, Yuqun. Electrochemical studies of graphene-like materials synthesized by the thermolyzed asphalt reaction. Ph.D. Dissertation, University of Idaho, Moscow, ID., 2013.

[51] Gyan, Isaiah O.; Wojcik, Peter M.; Aston, D. E.; McIlroy, David N.; Cheng, I. F. A Study of the Electrochemical Properties of a New Graphitic Material: GUITAR. *CHEMELECTROCHEM*. **2015**, doi: 10.1002/celc.201402433.

[52] Davies, Trevor J.; Hyde, Michael E.; Compton, Richard G. Nanotrench Arrays Reveal Insight into Graphite Electrochemistry. *Angew. Chem. Int. Ed*. **2005**, *44*, 5121-5126.

[53] Patel, Anisha N.; Collignon, Manon G.; O'Connell, Michael A.; Hung, Wendy O. Y.; McKelvey, Kim; Macpherson, Julie V.; Unwin, Patrick R. A New View of Electrochemistry at Highly Oriented Pyrolytic Graphite. *J. Am. Chem. Soc*. **2012**, *134*, 20117-20130.

[54] Dikin, Dmitriy A.; Stankovich, S.; Zimney, E. J.; Piner, R. D.; Dommett, G. H. B.; Evmenenko, G.; Nguyen, S. T and Ruoff, R. S. Preparation and characterization of graphene oxide paper. *Nature* **2007**, *448*, 457-460.

[55] Wang, G.; Wang, B.; Park, J.; Wang, Y.; Sun, B.; Yao, J. Highly efficient and large-scale synthesis of graphene by electrolytic exfoliation. *Carbon,* **2009**, *47*, 3242-3246.

[56] Pan, D.; Wang, S.; Zhao, B.; Wu, M.; Zhang, H.; Wang, Y.; Jiao, Z. Li Storage Properties of Disordered Graphene Nanosheets. *Chem. Mater.* **2009**, *21*, 3136-3142.

[57] Makarov, T. L.; Han, K-H. Graphite under the magnetic force microscope. *phys. stat. sol. (b)* **2007**, *244*, 4138-4142.

[58] Ferrari, A.; Robertson, J. Interpretation of Raman spectra of disordered and amorphous carbon. *Phys. Rev. B : Condens. Matter.* **2000**, *61*,14095-14107.

[59] Matthews, M. J.; Pimenta, M. A.; Dresselhaus, G; Endo, M. Origin of dispersive effects of the Raman D band in carbon materials. *Phys. Rev. B* **1999**, *59*, R6585-R6588.

[60] Luning, Z.; Dušan A. P.; Geng, B.; Marschall, J. Surface modification of highly oriented pyrolytic graphite by reaction with atomic nitrogen at high temperatures. *Appl. Surf. Sci.* **2011**, *257*, 5647–5656.

[61] Huang, P. Y.; Ruiz-Vargas, C. S.; Zande, A. M. van der; Whitney, W. S.; Levendorf, M. P.; Kevek, J. W.; Garg., S. Grains and grain boundaries in single-layer graphene atomic patchwork quilts. *Nature* **2011**, *469*, 389-392.

[62] Brownson, D. A. C; Munro, L. J.; Kampouris, D. K; Banks, C. E. Electrochemistry of graphene: not such a beneficial electrode material? *RSC Adv.* **2011**, *1*, 978-988.

[63] Mao, Hong Y.; Laurent, Sophie; Chen, Wei; Akhavan, Omid; Imani, Mohammad; Ashkarran, Ali A.; Mahmoudi, Morteza. Graphene: Promises, Facts, Opportunities, and Challenges in Nanomedicine. *Chem. Rev*. **2013**, *113*, 3407-3424.

[64] Han, Pengxian; Yue, Yanhua; Liu, Zhihong; Xu, Wei; Zhang, Lixue; Xu, Hongxia; Donga, Shanmu; Cui, Guanglei. Graphene oxide nanosheets/multi-walled carbon nanotubes hybrid as an excellent electrocatalytic material towards VO2+/VO2+ redox couples for vanadium redox flow batteries. *Energy Environ. Sci*. **2011**, *4*, 4710-4717.

[65] Rao, Tata N.; Yagi, I.; Miwa, T.; Tryk, D. A.; Fujishima, A. Electrochemical Oxidation of NADH at Highly Boron-Doped Diamond Electrodes. *Anal. Chem*. **1999**, *71*, 2506-2511.

[66] Demarconnay, L.; Raymundo-Pinero, E.; Beguin, F. A symmetric carbon/carbon supercapacitor operating at 1.6V by using a neutral aqueous solution. *Electrochem. Commun*. **2010**, *12*, 1275-1278.

[67] Wang, Joseph. Analytical Electrochemistry. 3rd ed.; Wiley & Sons: New Jersey, 2006.

[68] Brownson, Dale A. C.; Banks, Craig E. The handbook of graphene electrochemistry. DOI: 10.1007/978-1-4471-6428-9_1, Springer-Verlag London Ltd., 2014.

[69] Bard, Allen J.; Faulkner, Larry R. Electrochemical methods. Fundamentals and applications. 2nd ed.; Wiley & Sons: New York, 2001.

[70] Nicholson, Richard S. Theory and Application of Cyclic Voltammetry from Measurement of Electrode Reaction Kinetics. *Anal. Chem*. **1965**, *37*, 1351-1355.

[71] Klingler, R. J.; Kochi, J. K. Electron-transfer kinetics from cyclic voltammetry. Quantitative description of electrochemical reversibility. *J. Phys. Chem*. **1981**, *85*, 1731-1741.

[72] Kneten, Kristin R.; McCreery, Richard L. Effects of Redox System Structure on Electron-Transfer Kinetics at Ordered Graphite and Glassy Carbon Electrodes. *Anal. Chem*. **1992**, *64*, 2518-2524.

[73] McCreery, Richard L.; McDermott, Mark T. Comment on electrochemical kinetics at ordered graphite electrodes. *Anal. Chem*. **2012**, *84*, 2602-2605.

[74] McDermott, Christie A.; Kneten, Kristin R.; McCreery, Richard L. Electron Transfer Kinetics of Aquated Fe +3/+2, Eu +3/+2 and V+3/+2 at Carbon Electrodes. Inner Sphere Catalysis by Surface Oxides. *J. Electrochem. Soc*. **1993**, *140*, 2593-2599.

[75] Cline, Kristin K.; McDermott, Mark T.; McCreery, Richard L. Anomalously Slow Electron Transfer at Ordered Graphite Electrodes: Influence of Electronic Factors and Reactive Sites. *J. Phys. Chem*. **1994**, 98, 5314-5319.

[76] Tang, Longhua; Wang, Ying; Li, Yueming; Feng, Hongbing; Lu, Jin; Li, Jinghong. Preparation, Structure, and Electrochemical Properties of Reduced Graphene Sheet Films. *Adv. Funct. Mater*. **2009**, *19*, 2782-2789.

[77] Bowling, Robert; Packard, Richard T.; McCreery, Richard L. Mechanism of Electrochemical Activation of Carbon Electrodes: Role of Graphite Lattice Defects. *Langmuir* **1989**, *5*, 683-688

[78] Rice, Ronald J.; McCreery, Richard L. Quantitative Relationship between Electron Transfer Rate and Surface Microstructure of Laser-Modified Graphite Electrodes. *Anal. Chem*. **1989**, *61*, 1637-1641.

[79] Brownson, Dale A. C.; Gómez-Mingot, Maria; Banks, Craig E. CVD graphene electrochemistry: biologically relevant molecules. *Phys. Chem. Chem. Phys*. **2011**, *13*, 20284-20288.

[80] Ambrosi, Adriano; Pumera, Martin. Amorphous Carbon Impurities Play an Active Role in Redox Processes of Carbon Nanotubes. *J. Phys. Chem. C* **2011**, *115*, 25281-25284.

[81] Pumera, Martin. Carbon Nanotubes Contain Residual Metal Catalyst Nanoparticles even after Washing with Nitric Acid at Elevated Temperature Because These Metal Nanoparticles Are Sheathed by Several Graphene Sheets. *Langmuir* **2007**, *23*, 6453-6458.

[82] Pumera, Martin. Voltammetry of Carbon Nanotubes and Graphenes: Excitement, Disappointment, and Reality. *Chem. Rec*. **2012**, *12*, 201-213.

[83] Hutton, Laura A.; Iacobini, James G.; Bitziou, Eleni; Channon, Robert B.; Newton, Mark E.; Macpherson, Julie V. Examination of the Factors Affecting the Electrochemical Performance of Oxygen-Terminated Polycrystalline Boron-Doped Diamond Electrodes. *Anal. Chem*. **2013**, *85*, 7230-7240.

[84] Zeng, Aiping; Bilek, Marcela M. M.; McKenzie, David R.; Lay, Peter A.; Fontaine, Alexandre L.; Keast, Vicki J. Correlation between film structures and potential limits for hydrogen and oxygen evolutions at a-C:N film electrochemical electrodes. *Carbon* **2008**, *46*, 663-670.

[85] Nose, Masafumi; Kinumoto, Taro; Choo, Hyun-Suk; Miyazaki, Kohei; Abe, Takeshi; Ogumi, Zempachi. Lactone Formation on Carbonaceous Materials during Electrochemical Oxidation. *Chem. Lett*. **2009**, *38*, 788-789.

[86] Rossmeisl, J.; Qu, Z.-W.; Zhu, H.; Kroes, G.-J.; Nørskov, J. K. Electrolysis of water on oxide surfaces. *J. Electroanal. Chem*. **2007**, *607*, 83-89.

[87] Das, Rajib K.; Wang, Yan; Vasilyeva, Svetlana V.; Donoghue, Evan; Pucher, Ilaria; Kamenov, George; Cheng, Hai-Ping; Rinzler, Andrew G. Extraordinary Hydrogen Evolution and Oxidation Reaction Activity from Carbon Nanotubes and Graphitic Carbons. *ACS Nano* **2014**, *8*, 8447-8456.

[88] Hu, Lianzhe; Li, Haijuan; Zhu, Shuyun; Fan, Lishuang; Shi, Lihong; Liu, Xiaoqing; Xu, Guobao. Cathodic electrochemiluminescence in aqueous solutions at bismuth electrodes. *Chem. Commun*. **2007**, 4146-4148.

[89] Chen, Fuyu; Liu, Jianguo; Chen, Hui; Yan, Chuanwei. Study on Hydrogen Evolution Reaction at a Graphite Electrode in the All-Vanadium Redox Flow Battery. *Int. J. Electrochem. Sci*. **2012**, *7*, 3750-3764.

[90] Pasta, Mauro; Mantia, Fabio La; Hu, Liangbing; Deshazer, Heather D.; Cui, Yi. Aqueous Supercapacitors on Conductive Cotton. *Nano Res* **2010**, 3, 452-458.

[91] Xia, Hui; Meng, Ying S.; Yuan, Guoliang; Cui, Chong; Lu, Li. A Symmetric RuO_2/RuO_2 Supercapacitor Operating at 1.6 V by Using a Neutral Aqueous Electrolyte. *Electrochem. Solid-State Lett*. **2012**, *15*, A60-A63.

[92] Frackowiak, Elzbieta; Béguin, Francois. Carbon materials for the electrochemical storage of energy in capacitors. *Carbon* **2001**, *39*, 937-950.

[93] Qu, Deyang; Shi, Hang. Studies of activated carbons used in double-layer capacitors. *J. Power Sources* **1998**, *74*, 99-107.

[94] Khomenko, V.; Raymundo-Pinero, E.; Béguin, F. High-energy density graphite/AC capacitor in organic electrolyte. *J. Power Sources* **2008**, *177*, 643-651.

[95] Ndlovu, T.; Arotiba, O. A.; Sampath, S.; Krause, R. W.; Mamba, B. B. Reactivities of Modified and Unmodified Exfoliated Graphite Electrodes in Selected Redox Systems. *Int. J. Electrochem. Sci*. **2012**, *7*, 9441-9453.

[96] Tanaka, Yoriko; Furuta, Masahiro; Kuriyama, Koichi; Kuwabara, Ryosuke; Katsuki, Yukiko; Kondo, Takeshi; Fujishima, Akira; Honda, Kensuke. Electrochemical properties of N-doped hydrogenated amorphous carbon films fabricated by plasma-enhanced chemical vapor deposition methods. *Electrochim. Acta* **2011**, *56*, 1172-1181.

[97] Martin, Heidi B.; Argoitia, Alberto; Landau, Uziel; Anderson, Alfred B.; Angus, John C. Hydrogen and Oxygen Evolution on Boron-Doped Diamond Electrodes. *J. Electrochem. Soc*. **1996**, 143, L133-L136.

[98] Teófilo, Reinaldo F.; Ceragioli, Helder J.; Peterlevitz, Alfredo C.; Da Silva, Leonardo M.; Damos, Flavio S.; Ferreira, Márcia M. C.; Baranauskas, Vitor; Kubota, Lauro T. Improvement of the electrochemical properties of “as-grown” boron-doped polycrystalline diamond electrodes deposited on tungsten wires using ethanol. *J Solid State Electrochem* **2007**, 11, 1449-1457.

[99] Alves, S. A; Migliorini, F. L.; Baldan, M. R.; Ferreira, N. G.; Lanza, M. R. V. Electrochemical and morphology study of the BDD/Ti electrodes with different doping levels. *ECS Trans*. **2012**, *43*, 191-197.

[100] Ferro, Sergio; De Battisti, Achille. The 5-V window of polarizability of fluorinated diamond electrodes in aqueous solutions. *Anal. Chem*. **2003**, *75*, 7040-7042.

[101] Ferro, Sergio; De Battisti, Achille. Physicochemical properties of fluorinated diamond electrodes. *J. Phys. Chem. B* **2003**, *107*, 7567-7573.

[102] Hathcock, Kevin W.; Brumfield, Jay C.; Goss, Charles A.; Irene, Eugene A.; Murray, Royce W. Incipient Electrochemical Oxidation of Highly Oriented Pyrolytic Graphite: Correlation between Surface Blistering and Electrolyte Anion Intercalation, *Anal. Chem*. **1995**, *67*, 2201-2206.

[103] Goss, C. A; Brumfield, J. C.; Irene, E. A; Murray, R W. Imaging the incipient electrochemical oxidation of highly oriented pyrolytic graphite. *Anal. Chem*. **1993**, *65*, 1378-1389.

[104] Alsmeyer, D. C.; McCreery, R L. In Situ Raman Monitoring of Electrochemical Graphite Intercalation and Lattice Damage in Mild Aqueous Acids. *Anal. Chem*. **1992**, *64*, 1528-1533.

[105] Choo, Hyun-Suk; Kinumoto, Taro; Nose, Masafumi; Miyazaki, Kohei; Abe, Takeshi; Ogumi, Zempachi. Electrochemical oxidation of highly oriented pyrolytic graphite during potential cycling in sulfuric acid solution. *J. of Power Sources* **2008**, *185*, 740-746.

[106] Toh, Her S.; Ambrosi, Adriano; Chua, Chun K.; Pumera, Martin. Graphene Oxides Exhibit Limited Cathodic Potential Window Due to Their Inherent Electroactivity. *J. Phys. Chem. C* **2011**, *115*, 17647-17650.

[107] Trevethan, T.; Dyulgerova, P.; Latham, C. D.; Heggie, M. I.; Seabourne, C. R.; Scott, A. J.; Briddon, P. R.; Rayson, M. J. Extended Interplanar Linking in Graphite Formed from Vacancy Aggregates. *Phys. Rev. Lett*. **2013**, *111*, 095501.

Chapter 2: A Study of the Electrochemical Properties of a New Graphitic Material: GUITAR[†]

Isaiah O. Gyan[a], Peter M. Wojcik[b], D. Eric Aston[c], David N. McIlroy[b] and I. Francis Cheng[a]

[a]Department of Chemistry, University of Idaho, Moscow, Idaho 83844-2343, USA
ifcheng@uidaho.edu, Tel (208) 885-6387, Fax 208-885-6173

[b]Department of Physics, University of Idaho

[c]Department of Chemical Engineering, University of Idaho

Abstract

Previous studies of Graphite from the University of Idaho Thermolyzed Asphalt Reaction (GUITAR) indicate two unique properties that distinguish it from other sp^2 hybridized carbon electrodes. In property (i), the standard heterogeneous rate constant across the basal plane (BP) of GUITAR with $Fe(CN)_6^{3-/4-}$ of 0.01 cms^{-1} was 2-7 orders of magnitude greater than BP-graphite and graphene. With (ii), the anodic potential limit exceeds other graphites by 500 mV. Two new properties are now described. In (iii), the hydrogen overpotential in 1 M H_2SO_4 exceeds other graphitic materials by 500 mV. The combination of (ii) and (iii) gives a 3 V window in 1 M H_2SO_4, the largest reported for a graphitic material and competitive with diamond electrodes. In (iv), effects of air oxidation on the edge planes (EP) is reversed by mild cathodic reduction and does not allow for electrolyte intercalation. Based on these characteristics along with atomic force micrographs, we hypothesize that GUITAR may be a

[†] Published in ChemElectroChem (ChemElectroChem **2015**, DOI: 10.1002/celc.201402433). Reproduced with permission.

new allotrope of carbon. Coupled with expected low costs, GUITAR will find a myriad of applications in electrochemical sensors, water purification, energy storage and conversion.

2.1 Introduction

Recent reports have emphasized the need for faster heterogeneous electron transfer (HET) rates of graphene electrodes in sensing, energy storage and conversion applications. [1,2] An important consideration in this need is the anisotropic behavior of HET. The basal plane (BP) is inferior to edge planes (EP) by 1-7 orders of magnitude both on graphene and crystalline graphites (Figure 2.1). [3,4] Another consideration is that exposure of the basal plane to electrolyte solution is the natural configuration for graphene and graphite electrodes. Various methods are been developed to improve HET kinetics and performance at graphene electrodes. These methods include; laser-scribing, ion irradiation, heteroatom doping and various functionalizations. [1,2,5-7] Many of these strategies appear to increase the edge exposure and/or the structural disorder within the BP of graphene and graphite electrodes. Increasing disorder increases the density of states (DOS) near the Fermi level of these zero band-gap semiconductors. [1,4,8-10] Ideally, any technique aimed at increasing HET kinetics should focus on the BP as this is the surface that will find most exposure to solution. Moreover, although increased EP exposure increases HET rates, this plane along with step defects is more susceptible to corrosion relative to the BP. [11-13]

We have recently described a graphitic material synthesized from the combination of organics with sulfur; Graphite/Graphene from the University of Idaho Thermolyzed Asphalt Reaction (GUITAR). [14-16] It is comprised of sp^2 hybridized carbon free of sulfur with minor quantities of oxygen. [14] The optical and scanning electron micrographs indicate a flat,

layered material similar to ordered graphites, including highly oriented pyrolytic graphite (HOPG) but the Raman spectrum indicates that it is nanocrystalline with 5 nm grains (L_a). [14,15] Graphene papers have similar grain sizes. [17,18] Based on a previous study that highlights two distinctive characteristics it is apparent that GUITAR stands unique from other graphitic materials.

Property (i) is based on the relative disorder of GUITAR within its planes. This gives rise to excellent rates of HET across its BP with aqueous solutions of $Fe(CN)_6^{3-/4-}$ and $Ru(NH_3)_6^{3+/2+}$. The standard heterogeneous rate constants (k^0) are 1-8 orders of magnitude faster than crystalline graphites. [16] This matches EP graphitic materials, e.g. glassy carbon (GC), edge plane pyrolytic graphite (EPPG) and edge plane highly oriented pyrolytic graphite (EP-HOPG).[8-10,19-24] The high k^o for $Fe(CN)_6^{3-/4-}$ (0.01 cms^{-1}) observed on BP-GUITAR electrodes indicates that disorder within its planes increases DOS over HOPG. Figure 2.1 illustrates these trends. Lower quality graphites such as BPPG offer k^o intermediate to HOPG and GC. [25]

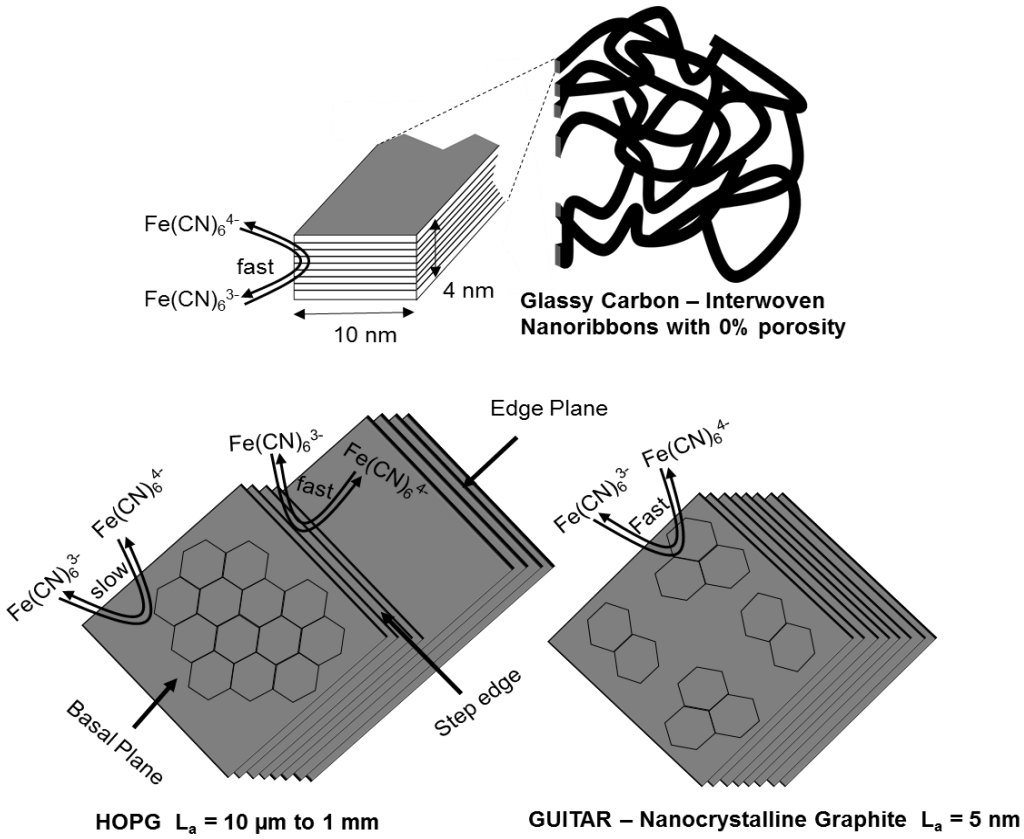

Figure 2.1. Schematic of the microstructure of glassy carbon, HOPG and GUITAR and corresponding electron transfer kinetics with potassium ferri/ferrocyanide.

Property (ii) is that the frontier planes of BP-GUITAR do not allow for electrolyte intercalation. Electrolyte intercalation through the frontier BP into subsurface layers occurs with all graphites. In these materials at high anodic potentials, CO_2 and O_2 are generated below the surface graphene planes forming blisters and corrosion pits. [26-29,32-35] Lack of intercalation gives rise to significantly higher corrosion resistance. In 1 M H_2SO_4, the 200 μAcm^{-2} limit is 2.1 V, an increase of 0.4 V over BP-HOPG. [30-35] The corrosion onset potential of BP-GUITAR is competitive with synthetic diamonds which range from 1.7 to 2.5 V. [31,36,37] The sum of all these characteristics indicate that GUITAR while having 5 nm grains does not

have physical gaps. These structurally defective BP-GUITAR planes are continuous unlike those of graphenes and HOPG which are polycrystalline, containing a multitude of step defects and grain edges. [38,39] Figure 2.2 illustrates the proposed structural differences between GUITAR and graphites.

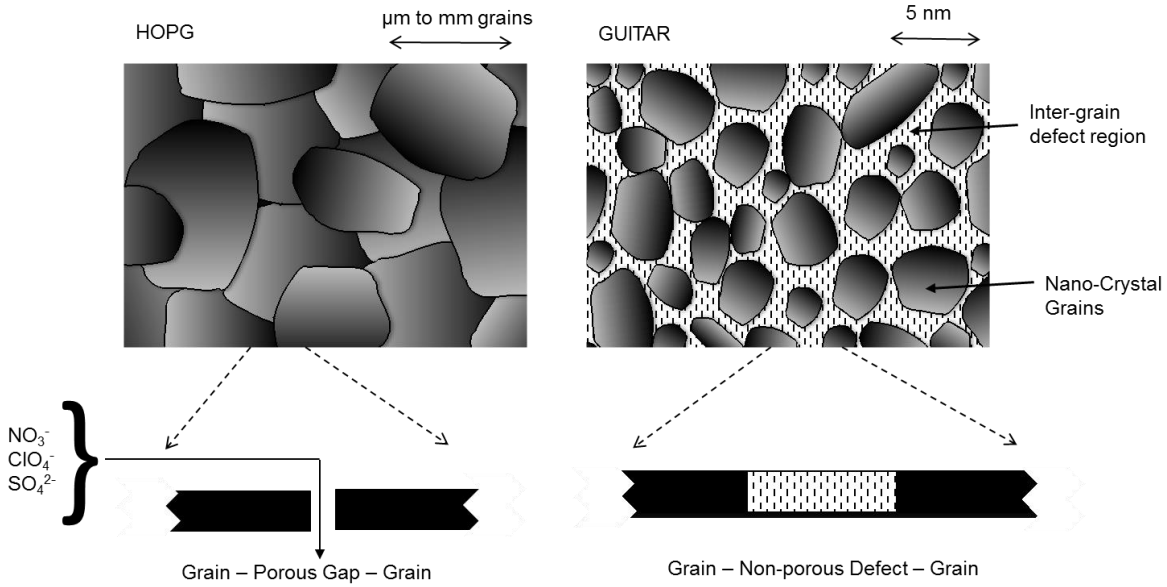

Figure 2.2. Proposed morphological differences between graphite (left) and GUITAR (right). The gaps between graphite grains allow for electrolyte intercalation. GUITAR has smaller grains and more disorder in the inter-grain regions that allow for faster heterogeneous electron transfer in property (i) and lacks porous defects that allow for electrolyte intercalation. This extends its aqueous anodic limit to 2.1 V and is property (ii).

In this investigation, we describe two more distinctive features. In property (iii), we demonstrate that GUITAR has 400-600 mV higher hydrogen overpotential compared to other sp^2 carbon materials. In property (iv), we show that the edge planes of GUITAR are more resistant to aging effects and air oxidation than other graphitic electrodes. Air

oxidation degrades k^0 performance on graphitic electrodes. [40,41] There is one report that fresh surfaces of BP-HOPG gives k^o for $Fe(CN)_6^{3-/4-}$ of 0.10 cms^{-1} or higher. [41]

However, this is lost with exposure to electrolyte solution in a few hours. These features indicate that GUITAR may have a myriad of applications in sensors, batteries, ultracapacitors and water purification where electrode durability over long time-scales is an important consideration. [42-47]

2.2 Results and Discussion

Morphologies of Edge and Basal Planes of GUITAR. Figure 2.3 shows an SEM of the edge (EP) and basal planes of GUITAR. Thickness of the edge plane vary from 0.25 to 1.5 µm depending on deposition conditions. The image and apparent morphologies are similar to those obtained for the cross-section of HOPG and graphene papers. [48,49] The basal plane appears flat to the resolution of SEM. However, the AFM image in Figure 2.3 shows that the basal plane morphology is textured with circular pits 10-50 nm in diameter and with an amplitude of 20 nm. There is no evidence of step defects with GUITAR as is apparent with AFM images of HOPG. [24,41] The hypothesis presented in Figure 2.2, where the GUITAR molecular planes are nonporous and nano-crystalline, agrees with the AFM. Future investigations will examine the interlayer spacing and crystal structure of GUITAR.

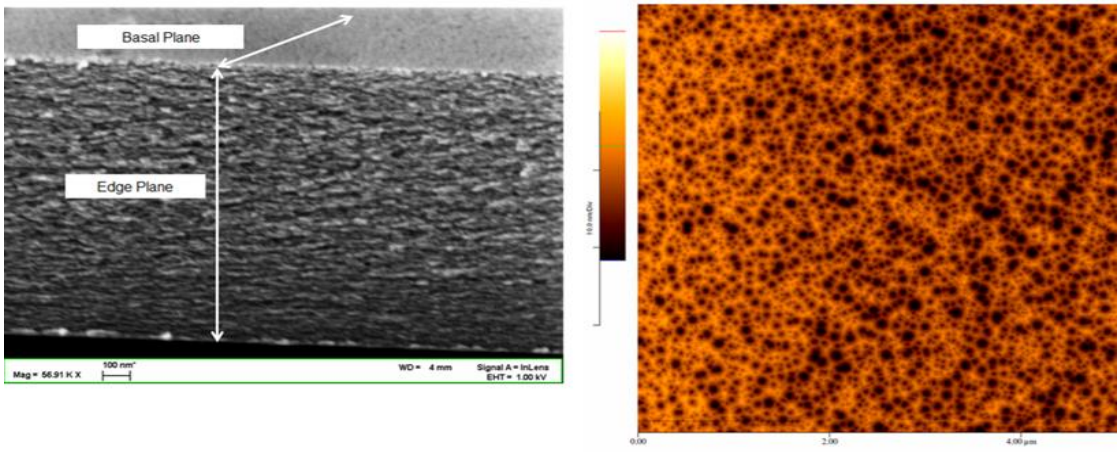

Figure 2.3. (Left) Scanning electron micrograph of GUITAR showing the basal and edge planes. (Right) Atomic forces micrograph of the GUITAR basal plane. The surface has circular pits 10-50 nm in diameter distributed in a semi-random pattern. The amplitude of the pits is about 20 nm.

Anodic Limits of Basal Plane Electrodes in 1 M H_2SO_4. Isolation of the BP through the scheme of Supporting Figure S2.1A gives the background cyclic voltammograms in Figure 2.4. In 1 M H_2SO_4, the 200 μAcm^{-2} anodic limit of BP-GUITAR is 2.09 V (or 1.88 V vs. Ag/AgCl) versus 1.45 V vs. SHE for BPPG, an increase of 0.64 V. The BP-GUITAR anodic limit is competitive with synthetic diamonds and surpasses other sp^2 hybridized carbon materials. [30,31,36,37,50] An illustration of the potential limit extrapolations at 200 μAcm^{-2} are presented in Figure S2.2 in supporting information. Table S2.1 summarizes the potential limits of GUITAR and materials from literature.

The increase in anodic limit of BP-GUITAR is attributable to the lack of electrolyte intercalation through grain boundary gaps and step defects. [26-29] A diagnostic for this characteristic is a cathodic peak (1.45 V) attributable to the deintercalation of HSO_4^- through Equation 1, where x and y are the appropriate stoichiometric coefficients. [26]

$$[C_x^+ HSO_4^-]y(H_2O) + e^- \rightarrow C_x + HSO_4^- + yH_2O \quad E_{peak} = 1.45 \text{ V vs. Ag/AgCl} \qquad (1)$$

The BP-GUITAR electrode lacks this feature that is common to BPPG and HOPG. Figure 2.4 illustrates these voltammetric characteristics and shows that GUITAR is impervious to electrolyte leakage. This increases the anodic limit in 1 M H_2SO_4 by a significant 400 to 700 mV when compared with BPPG and HOPG (see Table S2.1). The GUITAR electrodes were also found to be impervious to other electrolytes. [16,26,29,35]

Anodic Limits of Edge Plane Electrodes. The EP electrode anodic limits were examined and shown in Figure 2.4. The EPPG anodic limit of 1.58 V vs. SHE is positive (+0.13 V) of the BPPG one (Table S2.1). This is unexpected as graphitic edges are often cited as more reactive than the basal plane. [11,34] Figure 2.4 shows that HSO_4^- intercalation occurs on EPPG by the cathodic peak at ca. 1.5 V vs. Ag/AgCl. However, the current for BPPG deintercalation is larger (3100 μAcm^{-2}) over EPPG (2000 μAcm^{-2}). This result may be interpreted as the inter-grain gaps of BPPG having more ability to allow for intercalation relative to the edge planes. The EP-GUITAR electrode anodic limit of 1.71 V vs. SHE is less stable by 380 mV than the basal plane configuration (Figure 2.4 and Table S2.1). This is in agreement with the hypothesis that edge planes are more susceptible to corrosion. [11,34] However the cyclic voltammogram in Figure 2.4 of EP-GUITAR lacks an electrolyte deintercalation current peak. Ongoing investigations are aimed at developing hypotheses for this feature. It is noteworthy that the lack of intercalation between the planes of EP-GUITAR allows for a higher anodic stability than either EPPG or BPPG. This is another unique feature of GUITAR and contributes to property (ii).

Cathodic Limits of Basal and Edge Plane Electrodes. Figure 2.4 illustrates the 200 μAcm^{-2} cathodic limit of -0.89 V vs SHE on BP-GUITAR which is extended by 0.37 V when compared to the BPPG electrode of this investigation (-0.52 V vs SHE). The edge plane materials, EP-GUITAR and EPPG have onsets of -0.60 and -0.57 V vs. SHE respectively at 200 μAcm^{-2}. A *t*-test at 95% confidence with n = 3 for BPPG, EPPG and EP-GUITAR indicate that all these materials have statistically similar hydrogen overpotentials. This is an indication that the edges and the step defects of BPPG have similar reactivities in the hydrogen evolution reaction. In literature, other carbon electrodes have cathodic onset potentials of -0.3 to -0.5 V vs. SHE at this current density (Table S2.1). [30] It is important to note that the H_2 overpotential of EP-GUITAR is an estimate as the reductive current increased on the reverse scan down to sweep rates as low as 2 mVs^{-1}. In this sequence, BP-GUITAR has the highest hydrogen overpotential of the graphitic materials. Investigations are underway to develop hypotheses for this behavior. It is possible that the lack of more reactive edge and step sites is the basis for BP-GUITAR behavior as highlighted by the statistically similar hydrogen overpotentials of BPPG, EPPG and EP-GUITAR. This 300-600 mV higher hydrogen overpotential among the graphitic materials is a unique characteristic of GUITAR and is noted as property (iii) and summarized in Table S2.1.

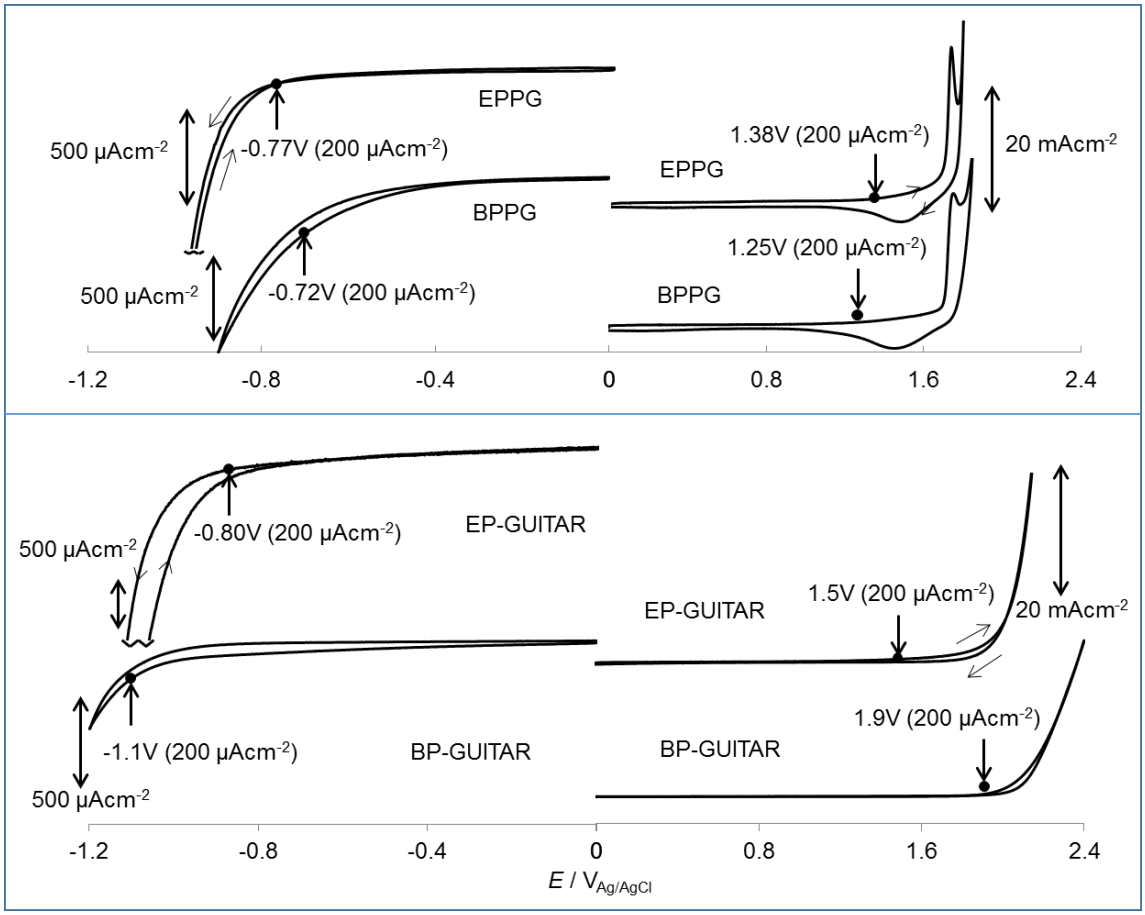

Figure 2.4. Cyclic voltammograms illustrating the cathodic and anodic limits on edge and basal plane configurations of GUITAR and pyrolytic graphite (PG) in 1M H_2SO_4 at 50 mVs^{-1}. EPPG and BPPG exhibit electrolyte intercalation, indicated by the peak on the reverse scan of the anodic voltammograms. Both EP-GUITAR and BP-GUITAR lack this feature. Onset currents of 200 μAcm^{-1} and corresponding potentials are shown. An illustration of how these limits were derived is in Figure S2.2 of supporting information.

Electrochemical Potential Window of GUITAR. At the 200 μAcm^{-2} onset limits, the entire potential window of BP-GUITAR is 3.0 V, which surpasses other sp^2 carbon electrodes that range from 2.0 to 2.2 V and is competitive with synthetic diamond electrodes that range from 2.3 to 3.5 V windows in H_2SO_4.[30,31,36,50,51] Table S2.1 summarizes these limits and windows.

Cyclic Voltammetric Behavior of $Fe(CN)_6^{3-/4-}$ and $Ru(NH_3)_6^{3+/2+}$. All electrodes of this study exhibited quasi-reversible cyclic voltammograms (Figure S2.3) with $Ru(NH_3)_6^{3+/2+}$ which is less susceptible to surface effects. [52,53] The k^o calculated from ΔE_p were 1.7×10^{-2} to 1.9×10^{-2} cms^{-1} for all electrode materials and configurations at 50 mVs^{-1}. Table 2.1 summarizes these findings. The EPPG, BPPG and GC materials of this study fall within the range of k^o values of literature. Literature values for crystalline graphites (BP-graphene and BP-HOPG) show slower heterogeneous rate constants (10^{-4} to 10^{-3} cms^{-1}), which are attributable to lower DOS. [9]

Cyclic voltammetric responses for 1 mM $Fe(CN)_6^{3-/4-}$ in 1 M KCl are shown in Figure 2.5. Relatively fast electrode kinetics are evident with BP-GUITAR with ΔE_p of 73. This matches the performance of the two edge plane materials, EPPG and GC with 69, and 72 mV, respectively. A slower response is observed with BPPG with ΔE_p of 156 mV. The voltammetric response of the EP-GUITAR electrode is indicative of a micro-band electrode with a steady-state current at 1 mVs^{-1} and mixed steady with semi-infinite linear diffusion at 50 mVs^{-1} and above**.** In Figure S2.4, the peak current of EP-GUITAR response is plotted vs. log of the potential scan rate (ν). It is apparent that radial diffusion effects predominate at sweep rates of 100 mVs^{-1} and less. At 1 mVs^{-1}, the electrode width is calculated as 0.6 µm. [54,55] This is in good agreement with thicknesses from SEM (0.25 µm to 1.5 µm). The EPPG electrode has a width of approximately 350 µm giving rise to semi-infinite linear diffusion characteristics in Figure 2.5.

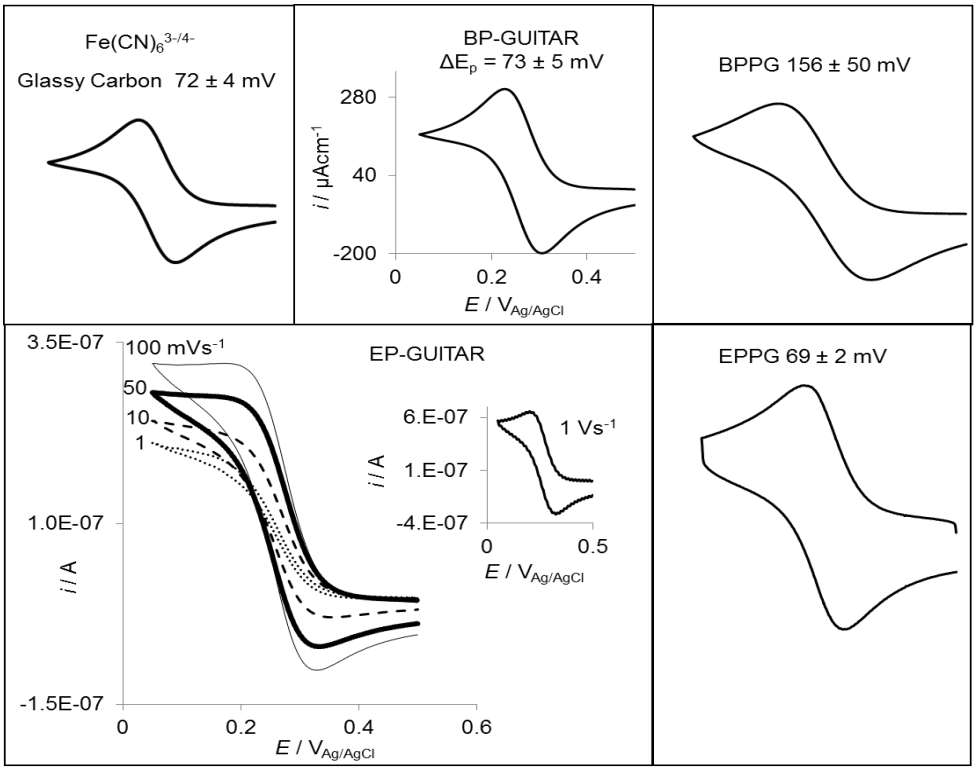

Figure 2.5. Cyclic voltammograms of $Fe(CN)_6^{3-/4-}$ in 1 M KCl on glassy carbon, BP- and EP-GUITAR, BPPG and EPPG. The current peak potential differences (ΔE_p) are indicated. EP-GUITAR has a micro-band electrode behavior indicated by the limiting current for the reduction of $Fe(CN)_6^{3-}$. See also Figure S2.4.

Table 2.1 summarizes standard heterogeneous rate constants, k^o for $Fe(CN)_6^{3-/4-}$ obtained from ΔE_p (see supporting information). Voltammetric behaviors of EPPG and of GC electrodes follow the same trends as described by previous investigators. [9,21,56,57] Fast rates of k^o for $Fe(CN)_6^{3-/4-}$ occur with materials rich in step defects and with graphitic edges as observed with EPPG (this work and literature) and with GC (~10^{-2} cms^{-1}). [58]

The literature values for reduced graphene oxide electrodes indicate k^o values up to 10^{-2} cms^{-1}. [23]

This is to be expected as the basal plane configuration of this electrode has a multitude of step defects. Recent voltammetric results on high quality graphene indicate that the EP-graphene follows this trend with fast k^o values to 10^{-2} cms^{-1}. [59]

Table 2.1. Heterogeneous electron transfer rate constants for the redox of $Fe(CN)_6^{3-/4-}$ and $Ru(NH_3)_6^{3+/2+}$ at various carbon electrodes. GUITAR has been found to exhibit comparable rates to edge plane graphite and glassy carbon.

Material	HET rate constant (k° (cm/s))		Reference
	$Fe(CN)_6^{3-/4-}$	$Ru(NH_3)_6^{3+/2+}$	
BP-GUITAR	1.2×10^{-2}	1.7×10^{-2}	This work
EPPG	1.7×10^{-2}	1.9×10^{-2}	This work
BPPG	1.4×10^{-3}	1.9×10^{-2}	This work
Glassy Carbon	1.3×10^{-2}	1.9×10^{-2}	This work
EPPG	4.3×10^{-3}, 1.5×10^{-2}	8.5×10^{-3}	[56,65]
BPPG	$5.3 \times 10^{-4} – 7 \times 10^{-3}$	6.1×10^{-3}	[25,65]
Glassy Carbon	$6.88 \times 10^{-5} – 2.9 \times 10^{-2}$	$7.4 \times 10^{-3} – 5.2 \times 10^{-2}$	[56,58,65,60,61,23]
EP-HOPG	$2.36 \times 10^{-3} – 1.8 \times 10^{-1}$	$5.6 \times 10^{-3} – 1.8 \times 10^{-1}$	[21,9,24,57,58]
BP-HOPG	$1 \times 10^{-9} – 1 \times 10^{-6}$, > 0.1	$9 \times 10^{-4} – 1.70 \times 10^{-2}$	[8-10,19,24,57,58,41]
EP-graphene	$2 \times 10^{-4} – 1 \times 10^{-2}$	---	[59,62]
BP-graphene	$2.80 \times 10^{-10} – 1 \times 10^{-9}$	$2.5 \times 10^{-3} – 5.3 \times 10^{-3}$	[9,59,63]
DLC[a]	3.2×10^{-5}, 1.02×10^{-4}	$2.6 \times 10^{-3} – 1.5 \times 10^{-2}$	[30,64]
BDD[b]	$5.42 \times 10^{-5} – 9.22 \times 10^{-4}$	$1.6 \times 10^{-3} – 4.5 \times 10^{-3}$	[30,60]

[a] DLC = Diamond-like carbon [b] = Boron-doped diamond

From literature, BP-HOPG and BP-graphene are slow with values of k^o from 10^{-10} to 10^{-6} cms^{-1}. [21,52] The BPPG material of this study and literature generally exhibit higher k^o of 10^{-5} to 10^{-3} cms^{-1}, indication of more disorder and step defects.[25,65] The BP-GUITAR electrode stands as the exception to the basal plane trend with k^0 of 1.2 x 10^{-2} cms^{-1}. In this aspect, it behaves more like the edge planes of the other graphitic materials.

Effects of Electrode Aging. Previous investigators have investigated air oxidation of graphitic electrodes in which both edge and basal planes decrease in k^0 of $Fe(CN)_6^{3-/4-}$.[40,41,66] Ji and coworkers observed that BPPG electrodes exposed in air for 2 hours increased the ΔE_p for $Fe(CN)_6^{3-/4-}$ from 227 to 596 mV while EPPG increased from 89 to 137 mV after 24 hours. [40] On HOPG, Patel et al also showed that ΔE_p increases from 58 mV to greater than 1 V in 24 hours. [41]

Both BP and EP electrodes were examined for the effects of air oxidation. Table 2.2 summarizes the results for all electrodes in this study. The ΔE_p for BP-GUITAR electrode increased from 73 to 93 mV over 3 hours and to 125 mV over 24 hours, a mild decrease in k^0 from 1.2 x 10^{-2} cms^{-1} to 2.2 x 10^{-3} cms^{-1}. The BPPG of this study increased from 145 to 298 mV, respectively or 1.6 × 10^{-3} to 3.1 × 10^{-4} cms^{-1} after 24 hours.

Edge plane materials also experienced air oxidation effects. The EPPG electrode increased from 71 to 157 mV for $Fe(CN)_6^{4-/3-}$ after 24 hours and GC increased from 68 to 142 mV during this period. Figure S2.5 shows the effects of aging on the voltammetric behavior of the micro-band EP-GUITAR electrode. The k^0 obtained from modeling of the voltammetric responses indicate that it decreased from 3 × 10^{-2} to 8 × 10^{-3} cms^{-1}. Table 2.2 shows all the k^0

calculated from ΔE_p of the macro-electrode systems. In general all electrodes experienced a 1 to 1.5 order of magnitude loss of k^0 after 24 hours of air exposure. This is in agreement with a previous study. [40]

The $Ru(NH_3)_6^{3+/2+}$ redox couple proved to be invariant to the air oxidation of GUITAR, GC and BPPG electrodes. The ΔE_p of this species was 69 mV in all cases before and after 24 hours of laboratory atmosphere exposure (see Table S2.2). This is in agreement with previous studies that found this outer-sphere couple to be insensitive to oxygenated sites. [40,41]

Electrode Regeneration. During the course of this investigation it was found that the effects of air oxidation can be reversed on the two basal plane materials, and on EP-GUITAR. The other edge plane materials, EPPG and GC suffered irreversible losses in k^0 of $Fe(CN)_6^{4-/3-}$. The restoration was conducted by voltammetrically cycling between 0 and -1.2 V in 1 M H_2SO_4 at 50 mVs^{-1}. Table 2.2 and Figure S2.5 illustrate these trends with ΔE_p and k^0. The 24-hr aged BP-GUITAR electrode was restored to the pristine value of 73 from 125 mV. The BPPG electrode followed the same trend.

Insofar as the edge plane materials, GC and EPPG could not completely be restored from the effects of 24 hours of air oxidation. The ΔE_p increased by 10 and 29 mV, respectively, after cyclic voltammetric treatment (Table 2.2). A t-test (n = 3) of the ΔE_p for GC and EPPG electrodes; the as-fabricated (t = 0) and after voltammetric cathodic treatment indicate that the values are statistically different (Table 2.2). Unlike the other edge plane materials the k^0 of the EP-GUITAR electrode was recovered after the restoration procedure (Table 2.2). Figures S2.5 A-C present the voltammetric responses of EP-GUITAR in this study. This

difference in behavior in the oxidized edges of EP-GUITAR and those of EPPG and GC is referred to as property (iv).

The lack of edge plane intercalation in Figure 2.4 and the associated discussion above indicates that the edge sites of GUITAR are in a chemically different environment than those of other graphitic materials.

Table 2.2. Effects of air exposure of carbon electrodes to $Fe(CN)_6^{3-/4-}$ voltammetry/kinetics and recoverability after cathodic treatment. Standard deviations were calculated using n = 3.

Material	ΔE_p (mV) and k^0 (cm/s) from CV peak currents of 1 mM $Fe(CN)_6^{3-/4-}$		
	As-fabricated	After 24 hrs in air	After Cathodic treatment
BP-GUITAR	73 ± 3 $k^o = 1.2 \times 10^{-2}$	125 ± 5 $k^o = 2.2 \times 10^{-3}$	73 ± 3 $k^o = 1.2 \times 10^{-2}$
EP-GUITAR[a]	Reversible $k^o = 3 \times 10^{-2}$	Irreversible $k^o = 8 \times 10^{-3}$	Reversible $k^o = 4 \times 10^{-2}$
Glassy Carbon	68 ± 2 $k^o = 1.9 \times 10^{-2}$	142 ± 27 $k^o = 1.6 \times 10^{-3}$	78 ± 4 $k^o = 9.6 \times 10^{-3}$
EPPG	71 ± 2 $k^o = 1.4 \times 10^{-2}$	157 ± 8 $k^o = 1.4 \times 10^{-3}$	100 ± 4 $k^o = 4.2 \times 10^{-3}$
BPPG	145 ± 6 $k^o = 1.6 \times 10^{-3}$	298 ± 11 $k^o = 3.1 \times 10^{-4}$	136 ± 11 $k^o = 1.8 \times 10^{-3}$

[a] = The EP-GUITAR micro-band electrode voltammetry is shown in Figure S2.5.

Aging in $Fe(CN)_6^{4-}$ Solutions. Patel et al demonstrated another aging effect through the continuous exposure of HOPG electrodes to solutions of 1 mM $Fe(CN)_6^{4-}$ in 0.1 M KCl(aq).[41] The investigators attributed a decrease in HET kinetics to an irreversible formation of

material from the adsorption of a Prussian Blue or related film. [67] In that study HOPG aged for 3 hours increased in ΔE_p from 58 mV to about 500 mV.

Using the same conditions, it was found that at BP-GUITAR, only slight loss was noted with ΔE_p increasing from 73 to 91 mV during the same time interval.

2.3 Conclusions

Where Does GUITAR fit Into the Spectrum of Graphitic Materials? The results of this investigation give further evidence that GUITAR is unlike graphitic materials. GUITAR has facile HET at its basal planes in property (i), anodic limits that rival synthetic diamonds in property (ii). [16] This was previously noted as an attribute of the lack of electrolyte intercalation through the basal plane. [16] This notable characteristic applies to the edge planes of GUITAR as it is also unable to intercalate concentrated sulfuric acid electrolyte which adds to electrode durability. In property (iii), cathodic limits in 1 M H_2SO_4 are extended by over 300 mV above the reference BPPG material of this investigation and literature graphitic materials (see Table S2.1). The total electrochemical window in 1 M H_2SO_4 is 3 volts for BP-GUITAR and places the material well beyond other sp^2-hybridized carbon materials and within the range of synthetic diamonds (Table S2.1). This high hydrogen overpotential can be linked to the lack of edge and step defects on the surface of GUITAR, an indication that the surface of the BP-GUITAR electrode is free of physical gaps. In property (iv), we show that the edge plane of GUITAR is a chemically different environment as the detrimental effects of air oxidation on k^0 of $Fe(CN)_6^{4-/3-}$ can be reversed by mild cathodic treatment and that it does not allow for electrolyte intercalation. The sum of these

features indicate that GUITAR may be a new allotrope of carbon distinct from graphitic materials. Together with the low-cost synthetic method and the combined features of properties (i-iv) indicate that GUITAR will have a myriad of applications in energy storage and conversion, water purification, and voltammetric sensors. We will report on these applications and more properties that distinguish GUITAR from other carbon electrode materials.

2.4 Experimental Section

Silicon wafers, (111) orientation and 300 nm thermal oxide layer were obtained from University Wafer (Boston, MA). Paraffin wax and high vacuum grease were from Royal Oak Enterprises (Georgia, USA) and Dow Corning (Midland, MI), respectively. Pyrolytic graphite blocks (1" x 1" x 3/16“) and glassy carbon electrode were obtained from Emovendo magnets and elements, (West Virginia, USA) and Bioanalytical Systems, (West Lafayette, IN, USA). Alumina powder was obtained from Pace Technologies, (AZ, USA). Sulfuric acid (96.3%) was purchased from J.T Baker Chemical Co. (Phillipsburg, N.J, USA). Potassium chloride was obtained from Fisher Scientific (N.J, USA), potassium ferricyanide was obtained from Acros Organics (N.J, USA) and hexaammine ruthenium (III) chloride was obtained from Strem Chemicals Inc. (Newburyport, MA, USA). All chemicals were used as received and all aqueous solutions were prepared with deionized water purified by passage through an activated carbon purification cartridge (Barnstead, model D8922, Dubuque, IA). Electrode fabrication, electrochemical setup, and modelling are described in the Supporting Information section (appendix one of this dissertation).

Keywords: cyclic voltammetry • electrochemistry • electron transfer • graphitic electrodes • kinetics

2.5 References

[1] J-H. Zhong, J. Zhang, X. Jin, J-Y. Liu, Q. Li, M-H. Li, W. Cai, D-Y. Wu, D. Zhan, B. Ren, *J. Am. Chem. Soc*. **2014**, *136*, 16609 – 16617.

[2] S. Boopathi, T. N. Narayanan, S. S. Kumar, *Nanoscale*, **2014**, *6*, 10140 – 10146.

[3] R. J. Bowling, R.T. Packard, R. L. McCreery, *J. Am. Chem. Soc.* **1989**, *111*, 1217 – 1223.

[4] C. Tan, J. Rodríguez-López, J. J. Parks, N. L. Ritzert, D. C. Ralph, H. D. Abruňa, *ACS Nano* **2012**, *6*, 3070 – 3079.

[5] K. Griffiths, C. Dale, J. Hedley, M. D. Kowal, R. B. Kaner, Neil Keegan, *Nanoscale* **2014**, *6*, 13613 – 13622.

[6] L. Yan, Y. B. Zheng, F. Zhao, S. Li, X. Gao, B. Xu, P. S. Weiss, Y. Zhao, *Chem. Soc. Rev*. **2012**, *41*, 97 – 114.

[7] X. Chia, A. Ambrosi, M. Otyepka, R. Zbořil, M. Pumera, *Chem. Eur. J.* **2014**, *20*, 6665 – 6671.

[8] K. K. Cline, M. T. McDermott, R. L. McCreery, *J. Phys. Chem.* **1994**, *98*, 5314 – 5319.

[9] A. Ambrosi, M. Pumera, *J. Phys. Chem. C* **2013**, *117*, 2053 – 2058.

[10] K. R. Kneten, R. L. McCreery, *Anal. Chem*. **1992**, *64*, 2518 – 2524.

[11] L. Wei, F. Wu, D. Shi, C. Hu, X. Li, W. Yuan, J. Wang, J. Zhao, H. Geng, H. Wei, Y. Wang, N. Hu, Y. Zhang, *Sci. Rep.*, DOI: 10.1038/srep02636.

[12] L. Rodríguez-Pérez, M. Á. Herranz, N. Martín, *Chem. Commun*. **2013**, *49*, 3721 – 3735.

[13] S. Pan, I. A. Aksay, *ACS Nano* **2011**, *5*, 4073 – 4083.

[14] I. F. Cheng, Y. Xie, R. A. Gonzales, P. R. Brejna, J. P. Sundararajan, B. A. Fouetio Kengne, D. E. Aston, D. N. McIlroy, J. E. Foutch, P. R. Griffiths, *Carbon* **2011**, *49*, 2852 – 2861.

[15] Y. Xie, S. D. McAllister, S. A. Hyde, J. P. Sundararajan, B. A. Fouetio Kengne, D. N. McIlroy, I. F. Cheng, *J. Mater. Chem*. **2012**, *22*, 5723 – 5729.

[16] I. F. Cheng, Y. Xie, I. O. Gyan, N. W. Nicholas, *RSC Adv*. **2013**, *3*, 2379 – 2384.

[17] C. Gómez-Navarro, R. T. Weitz, A. M. Bittner, M. Scolari, A. Mews, M. Burghard, K. Kern, *Nano Lett*. **2007**, *7*, 3499 – 3503.

[18] S. Stankovich, D. A. Dikin, R. D. Piner, K. A. Kohlhaas, A. Kleinhammes, Y. Jia, Y. Wu, S. T. Nguyen, R. S. Ruoff, *Carbon* **2007**, *45*, 1558 – 1565.

[19] C. E. Banks, T. J. Davies, G. G. Wildgoose, R. G. Compton, *Chem. Commun.* **2005**, 829 – 841.

[20] C. E. Banks, R. G. Compton, *Analyst* **2006**, *131*, 15 – 21.

[21] D. A. C. Brownson, L. J. Munro, D. K. Kampouris, C. E. Banks, *RSC Adv.* **2011**, *1*, 978 – 988.

[22] F. Wantz, C. E. Banks, R. G. Compton, *Electroanalysis* **2005**, *17*, 1529 – 1533.

[23] L. Tang, Y. Wang, Y. Li, H. Feng, J. Lu, J. Li, *Adv. Funct. Mater*. **2009**, *19*, 2782 – 2789.

[24] T. J. Davies, M. E. Hyde, R. G. Compton, *Angew. Chem. Int. Ed.* **2005**, *44*, 5121 – 5126; *Angew. Chem.* **2005**, *117*, 5251 – 5256.

[25] R. L. McCreery, K. K. Cline in *Laboratory techniques in electroanalytical chemistry*, 2nd Ed. (Eds.: P. T. Kissinger, W. R. Heineman), Marcel Dekker, New York, **1996**, pp. 293 – 332.

[26] C. A. Goss, J. C. Brumfield, E. A. Irene, R. W. Murray, *Anal. Chem.* **1993**, *65*, 1378 – 1389.

[27] D. C. Alsmeyer, R. L. McCreery, *Anal. Chem.* **1992**, *64*, 1528 – 1533.

[28] D. Alliata, R. Kötz, O. Hass, H. Siegenthaler, *Langmuir* **1999**, *15*, 8483 – 8489.

[29] D. Alliata, P. Häring, O. Haas, R. Kötz, H. Siegenthaler, *Electrochem. Commun.* **1998**, *1998* 1998 – 1998.

[30] Y. Tanaka, M. Furuta, K. Kuriyama, R. Kuwabara, Y. Katsuki, T. Kondo, A. Fujishima, K. Honda, *Electrochim. Acta* **2011**, *56*, 1172 – 1181.

[31] H. B. Martin, A. Argoitia, U. Landau, A. B. Anderson, J. C. Angus, *Electrochem. Soc.* **1996**, *143*, L133 – L136.

[32] M. S. Dresselhaus, G. Dresselhaus, *Advances in Physics* **2002**, *51*, 1 – 186.

[33] K. Persson, V. A. Sethuraman, L. J. Hardwick, Y. Hinuma, Y. S. Meng, A. van der Ven, V. Srinivasan, R. Kostecki, G. Ceder, *J. Phys. Chem. Lett.* **2010**, *1*, 1176 – 1180.

[34] M. Matsumoto, T. Manako, H. Imai, *J. Electrochem. Soc.* **2009**, *156*, B1208 – B1211.

[35] K. W. Hathcock, J. C. Brumfield, C. A. Goss, E. A. Irene, R. W. Murray, *Anal. Chem.* **1995**, *67,* 2201 – 2206.

[36] R. F. Teófilo, H. J. Ceragioli, A. C. Peterlevitz, L. M. Da Silva, F. S. Damos, M. M. C. Ferreira, V. Baranauskas, L. T. Kubota, *J. Solid State Electrochem.* **2007,** *11*, 1449 – 1457.

[37] S. A. Alves, F. L. Migliorini, M. R. Baldan, N. G. Ferreira, M. R. V. Lanza, *ECS Transactions* **2012**, *43*, 191 – 197.

[38] X. Lu, H. Huang, N. Nemchuk, R. S. Ruoff, *Appl. Phys. Lett.* **1999**, *75*, 193 – 195.

[39] K. Kim, Z. Lee, W. Regan, C. Kisielowski, M. F. Crommie, A. Zettl, *ACS Nano* **2011**, *5*, 2142 – 2146.

[40] X. Ji, C. E. Banks, A. Crossley, R. G. Compton, *ChemPhysChem* **2006**, *7*, 1337 – 1344.

[41] A. N. Patel, M. G. Collignon, M. A. O'Connell, W. O. Y. Hung, K. McKelvey, J. V. Macpherson, P. R. Unwin, *J. Am. Chem. Soc*. **2012**, *134*, 20117 – 20130.

[42] W. Yang, K. R. Ratinac, S. P. Ringer, P. Thordarson, J. J. Gooding, F. Braet, *Angew. Chem. Int. Ed.* **2010**, *49*, 2114 – 2138; *Angew. Chem*. **2010**, *122*, 2160 – 2185.

[43] Y. Wang, Y. Li, L. Tang, J. Lu, J. Li, *Electrochem. Commun*. **2009**, *11*, 889 – 892.

[44] J. Wang, S. Yang, D. Guo, P. Yu, D. Li, J. Ye, L. Mao, *Electrochem. Commun.* **2009**, *11*, 1892 – 1895.

[45] S. N. Patankar, S. D. McAllister, I. F. Cheng, D. B. Edwards, *J. Power Sources* **2010**, *195*, 362 – 366.

[46] R. Ponraj, S. D. McAllister, I. F. Cheng, D. B. Edwards, *J. Power Sources* **2009**, *189*, 1199 – 1203.

[47] S. D. McAllister, S. N. Patankar, I. F. Cheng, D. B. Edwards, *Scr. Mater*. **2009**, *61*, 375 – 378.

[48] A. N. Patel, S-Y. Tan, T. S. Miller, J. V. Macpherson, P. R. Unwin, *Anal. Chem.* **2013**, *85*, 11755 – 11764.

[49] I. K. Moon, J. Lee, R. S. Ruoff, H. Lee, *Nat. commun.*, DOI: 10.1038/ncomms1067

[50] T. Ndlovu, O. A. Arotiba, S. Sampath, R. W. Krause, B. B. Mamba, *Int. J. Electrochem. Sci.* **2012**, *7*, 9441 – 9453.

[51] G. R. Salazar-Banda, A. E. de Carvalho, L. S. Andrade, R. C. Rocha-Filho, L. A. Avaca, *J Appl Electrochem.* **2010**, *40*, 1817 – 1827.

[52] R. L. McCreery, M. T. McDermott, *Anal. Chem.* **2012**, *84*, 2602 – 2605.

[53] G. P. Keeley, N. McEvoy, H. Nolan, M. Holzinger, S. Cosnier, G. S. Duesberg, *Chem. Mater.* **2014**, *26*, 1807 – 1812.

[54] W. Yuan, Y. Zhou, Y. Li, C. Li, H. Peng, J. Zhang, Z. Liu, L. Dai, G. Shi, *Sci. Rep.*, DOI: 10.1038/srep02248

[55] K. R. Wehmeyer, M. R. Deakin, R. M. Wightman, *Anal. Chem.* **1985**, *57*, 1913 – 1916.

[56] D. S. Shishmarev, N. V. Rees, R. G. Compton, *Electroanalysis* **2010**, *22*, 31 – 34.

[57] E. P. Randviir, D. A. C. Brownson, M. Gomez-Mingot, D. K. Kampouris, J. Iniesta, C. E. Banks, *Nanoscale* **2012**, *4*, 6470 – 6480.

[58] R. L. McCreery, *Chem. Rev.* **2008**, *108*, 2646 – 2687.

[59] M. Pumera, *Chem. Soc. Rev*. **2010**, *39*, 4146 – 4157.

[60] C. X. Lim, H. Y. Hoh, P. K. Ang, K. P. Loh, *Anal. Chem.* **2010**, *82*, 7387 – 7393.

[61] H. L. Poh, F. Šaněk, A. Ambrosi, G. Zhao, Z. Sofer, M. Pumera, *Nanoscale* **2012**, *4*, 3515 – 3522.

[62] A. Ambrosi, A. Bonanni, M. Pumera, *Nanoscale* **2011**, *3*, 2256 – 2260.

[63] D. A. C. Brownson, C. E. Banks, *Phys. Chem. Chem. Phys.* **2011**, *13*, 15825 – 15828.

[64] N. Menegazzo, M. Kahn, R. Berghauser, W. Waldhauser, B. Mizaikoff, *Analyst* **2011**, *136*, 1831–1839.

[65] M. C. Henstridge, L. Shao, G. G. Wildgoose, R. G. Compton, G. Tobias, M. L. H. Green, *Electroanalysis* **2008**, *20*, 498 – 506.

[66] S. C. S. Lai, A. N. Patel, K. M^{c}Kelvey, P. R. Unwin, *Angew. Chem. Int. Ed.* **2012**, *51*, 5405 – 5408; *Angew. Chem.* **2012**, *124*, 5501 – 5504.

[67] C. M. Pharr, P. R. Griffiths, *Anal. Chem.* **1997**, *69*, 4665 – 4672.

Chapter 3: Electrochemical Study of Biologically Relevant Molecules at Electrodes Constructed from GUITAR, a New Carbon Allotrope[‡]

Isaiah O. Gyan and I. Francis Cheng*

Department of Chemistry, University of Idaho, Moscow, ID 83844-2343, Tel. (208) 885-6387
ifcheng@uidaho.edu

Abstract

Graphite has a well-known anisotropic behavior where heterogeneous electron transfer (HET) is much faster on its edge (EP) versus basal plane (BP). This is problematic in bioanalytical applications where the BP exposure is the most convenient configuration in sensors. We have reported earlier on a new carbon allotrope, GUITAR that exhibits near equal facile HET on its apparent EP and BP. In this contribution we report on three biologically significant analytes, ascorbic acid, dopamine and NADH. The BP-GUITAR surface has electrochemical overpotentials (ca. 100-200 mV) lower than other BP materials and equal to EP graphitic electrodes. All electrodes in this study (GUITAR, graphite, and glassy carbon (GC)) suffer from eventual signal losses due to irreversible adsorption from repeated electro-oxidation of either ascorbic acid, NADH or dopamine. Of these materials only GUITAR could be regenerated by pulsing the electrode surface to 2.2 volts in pH 7.2 phosphate buffer. Graphite and GC suffered oxidative damage by the procedure. Furthermore, the GUITAR electrode was able to undergo four regeneration cycles with reproducible dopamine cyclic voltammetric characteristics. More cycles are possible. The ascorbate detection limit and linear range of 0.15 μM and 0.05-6250 μM respectively on GUITAR are at 2 orders of

[‡] Published in Microchemical Journal (*Microchem. J.* **2015**, *122*, 39-44). Reproduced with permission

magnitude or more better in each category than other systems. Again this can be attributed to the facile HET rates on GUITAR. These features indicate that GUITAR will be advantageous for enclosed sensor applications where surface renewal can be difficult, e.g., *in vivo* implants, liquid chromatography and microfluidics.

Keywords: Electrochemistry, Carbon Electrodes, Biosensing, Electrode Regeneration, Electron Transfer, Voltammetry.

3.1 Introduction

We have recently reported on the electrochemical properties of a new allotrope of carbon, GUITAR (graphite from the University of Idaho Thermolyzed Asphalt Reaction). While having the appearance of a crystalline graphite or graphene, the atomic forces micrograph of GUITAR indicates that is has pits 10-20 nm in diameter and lacks crystal grain boundaries and steps common with graphites and graphene [2]. Four chemical properties distinguish GUITAR from other sp^2 carbon electrodes. These are (i) the anisotropic characteristics of graphite, where the heterogeneous electron transfer (HET) rates are much faster by several orders of magnitude on the edge (EP) versus basal planes (BP) are not observed with GUITAR. The EP and BP-GUITAR electrodes have nearly equal standard HET rates (k^0) of c.a. 10^{-2} cm/s for $Fe(CN)_6^{3-/4-}$ and $Ru(NH_3)_6^{3+/2+}$. These rates are the same as other EP graphite electrodes [1,2]. This implies an increased density of electronic states (DOS) in GUITAR relative to crystalline graphites [2,3]. In (ii) the anodic limits of GUITAR exceed other graphites by 500 mV in 1 M H_2SO_4. With (iii) the cathodic limits are increased by 500 mV in 1 M H_2SO_4. The combination of (ii) and (iii) gives a potential window of 3 V, the largest

reported for a graphitic material and competitive with boron-doped diamond electrodes [2,4]. Finally, GUITAR was found to be less susceptible to air oxidation which forms Property (iv). Anodic stability of GUITAR over graphite was found to be due to lack of electrolyte intercalation through both basal and edge planes of GUITAR, unlike graphite electrodes [1,2]. The combination of i-iv indicates a myriad of applications for GUITAR. Among the proposed applications of GUITAR, we report on electrochemical sensing of biologically relevant molecules. In the current study, we examine three common analytes, ascorbic acid (AA), β-nicotinamide adenine dinucleotide (NADH) and dopamine (DA). AA is an antioxidant and is also essential for cartilage, bones and tendon developments [5,6]. DA is a neurotransmitter that plays an essential role in the function of the central nervous system. Its deficiency or excess has been linked to Parkinson's disease and schizophrenia [7,8]. NADH is an electron and proton carrier in living organisms. It participates in many biosynthetic reactions and is a cofactor of several enzymatic reactions [9,10]. Due to the biological relevance of these molecules, accurate and facile detection of their concentrations both *in vivo* and *in vitro* is crucial [8,11]. Results from this study highlights remarkable performances at GUITAR electrodes and adds to the uniqueness of this material when compared with other carbon materials.

3.2 Experimental Section

3.2.1 Chemicals and Materials

Silicon wafers, (111) orientation and 300 nm thermal oxide layer were obtained from University Wafer (Boston, MA). Paraffin wax and high vacuum grease were obtained from Royal Oak Enterprises (Georgia, USA) and Dow Corning (Midland, MI), respectively. Pyrolytic

graphite sheet (90 x 115 mm) and glassy carbon electrode were obtained from Allied Electronics Inc. (Fort Worth, TX, USA) and Bioanalytical Systems, (West Lafayette, IN, USA) respectively. Alumina powder was obtained from Pace Technologies, (AZ, USA). Ascorbic acid was purchased from J.T Baker Chemical Co. (Phillipsburg, N.J, USA). Potassium hydroxide, potassium chloride and sodium phosphate monobasic salt were obtained from Fisher Chemicals (Fair Lawn, NJ, USA). Sodium phosphate dibasic salt was purchased from EMD Chemicals Inc. (Gibbstown, NJ, USA). Dopamine hydrochloride and β-NADH (reduced sodium salt trihydrate) were obtained from Sigma-Aldrich and goldbio.com respectively, (both in St. Louis, MO, USA). All chemicals were used as received and all aqueous solutions were prepared with deionized water purified by passage through an activated carbon purification cartridge (Barnstead, model D8922, Dubuque, IA).

3.2.2 Electrode fabrication and electrochemical setup

GUITAR was synthesized as described in previous publications [12,13]. Electrode fabrication and geometric area isolation were performed as described previously [2]. Glassy carbon was polished with 1-micron alumina powder and sonicated in DI water prior to use. Unless otherwise noted, the setup used for all electrochemical studies was a three-electrode undivided cell with graphite rod counter electrode, Ag/AgCl/3M NaCl(aq) (0.209V vs. SHE) reference electrode. Ascorbic acid, dopamine and NADH were prepared in 0.1 M phosphate buffer (pH 7.2) and studied with cyclic voltammetry at 0.1 V/s. Electrode regeneration was achieved by applying +2.2 V vs Ag/AgCl for 5 minutes in 0.1 M PBS (pH 7.2). Electrochemical studies were carried out using a Bioanalytical Systems Epsilon potentiostat (West Lafayette, IN).

3.3 Results and Discussion

3.3.1 Cyclic voltammetry of AA

Ascorbic acid undergoes a 2-proton, 2-electron transfer according to equation 1 [14].

$$AA + H_2O = \text{dehydro-AA} + 2H^+ + 2e^- \qquad E^{0\prime}_{red} = -0.036 \text{ V vs SHE (pH 7.2)} \quad (1)$$

This electro-oxidation process is chemically irreversible at electrodes. The dehydro-AA reacts to form hydrated bicyclic species [15,16]. Compared to the redox potential for this process, most electrodes exhibit high overpotentials for its determination (Table 3.2), however, at BP-GUITAR electrodes, this overpotential is lower by 100-200 mV than at other BP-materials and comparable to EP ones. This observation is attributed to faster HET rates across BP-GUITAR. Limit of detection based on 3σ at BP-GUITAR electrodes was found to be 0.15 ± 0.01 µM (n = 5) with a linear range of 0.05 µM – 6250 µM (Figure 3.1). The latter was the highest AA concentration studied and may not represent the upper limit. Detection limit at BP-GUITAR is found to be ca. 500 times lower than EPPG (71 µM) and 800 times lower than reported for graphene nano-sheets (120 µM) [17,34]. Comparison of these limits at planar, non-planar and carbon composite electrodes is presented in Table 3.1, along with linear ranges. We hypothesize that faster HET kinetics across BP-GUITAR is responsible for the low detection limit [47]. In Table 3.1, GUITAR possesses the widest linear range for ascorbic acid detection. This is also attributed to the low fouling rate and fast HET across BP-GUITAR.

At GUITAR electrodes, the linear range is a combination from separate electrodes, whose calibration plots produce an average slope of $1.1 \times 10^{-2} \pm 3.9 \times 10^{-3}$ µA/µM (n = 5).

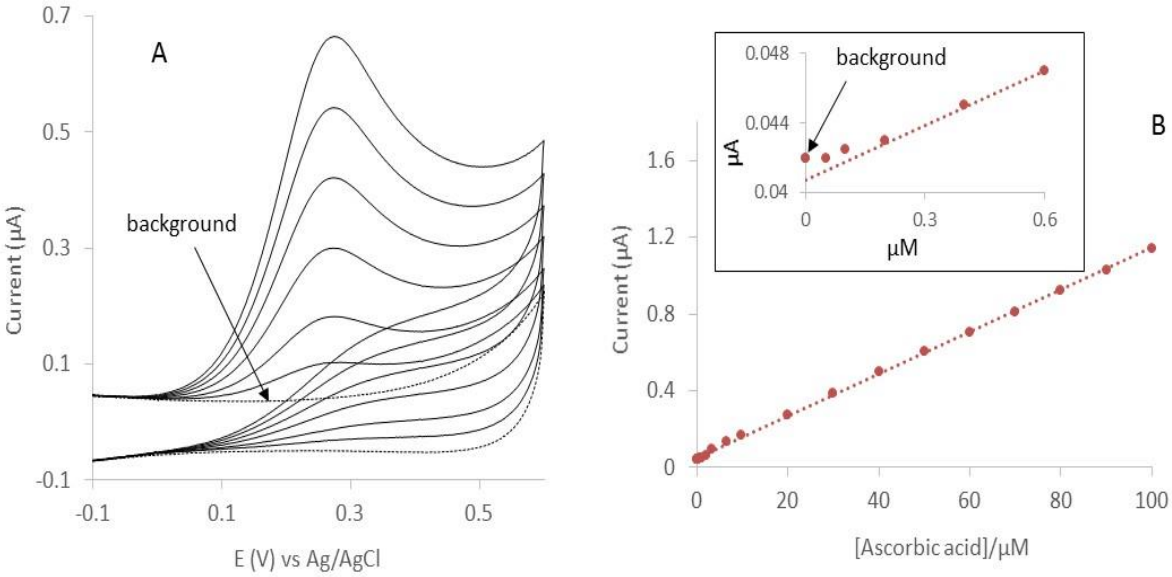

Figure 3.1. A – Cyclic voltammetric response of increasing AA concentration; bottom to top: 0, 3, 10, 20, 30, 40 and 50 μM and B – corresponding plot of the oxidation peak current vs AA concentration. In B, a plot of the lower concentration region is shown as inset. Ascorbic acid was added to 0.1 M phosphate buffer (pH 7.2). Scan rate was 0.1 V/s. Limit of detection was calculated as 0.15 ± 0.01 μM (n = 5) by the 3σ method. The best fit line by least squares analysis has a slope of 1.1×10^{-2} μA/μM with an intercept of 0.047 μA and $r^2 = 0.999$.

Material	Detection limit (µM)	Linear range (µM)	Reference
BP-GUITAR	0.15 ± 0.01 (n = 5)	0.05 – 6250	This work
BPPG*	13	25 – 500	[18]
EPPG	71	200 – 2200	[34]
Nitrogen doped graphene	2.2	5 – 1300	[6]
Graphene nano-sheets	120	400 – 6000	[17]
Carbon nanotube composite electrodes	0.03 – 7.71	0.1 – 800	[19 -24]
Sol-gel carbon ceramic composite	0.10	0.5 – 20	[25]
Carbon nanofiber	2	2 – 64	[26]
Ordered mesoporous carbon	20	40 – 800	[27]
Chitosan-graphene	50	50 – 1200	[28]
Nitrogen-doped carbon nanofiber	50	50 – 3000	[29]

Table 3.1. Comparison of ascorbic acid limit of detection and linear range at various planar, non-planar and carbon composite electrodes. Linear range at GUITAR is a combination from separate electrodes, whose plots produce an average slope of $1.1 \times 10^{-2} \pm 3.9 \times 10^{-3}$ µA/µM (n = 5). *Electrochemically activated.

3.3.2 Overall behavior with AA, DA and NADH

Cyclic voltammetric performances of BP-GUITAR, BPPG and GC with 1 mM of either AA, DA or NADH in 0.1 M PBS at pH 7.2 are presented in Figure 3.2 and Table 3.2. In general BP-GUITAR electrode exhibited superior performance relative to BPPG of this investigation and other BP materials from literature (Table 3.2). This is based on CV current peak potential which indicate lower overpotentials for all three analytes. The peak positions of BP-GUITAR are within the range of literature edge plane materials in Table 3.2. This is similar to a previous investigation with $Fe(CN)_6^{3-/4-}$ and $Ru(NH_3)_6^{3+/2+}$ [2]. In general BP-GUITAR has a 100-200 mV lower overpotential when compared to literature BP materials. It is also important to note that GC is an edge-plane material.

The facile HET rates of BP-GUITAR is attributed to increased density of electronic states (DOS) from the structural defects within its molecular planes [1,2]. An important note is that the natural configuration of layered graphitic materials is basal plane towards to the sample which outlines advantage of BP-GUITAR over edge plane materials [30,31]. Glassy carbon of this investigation had excellent CV characteristics for AA and DA, better than literature edge plane materials in terms of CV peak potentials (Table 3.2). The BP-GUITAR surpassed GC with NADH current response (Figure 3.2).

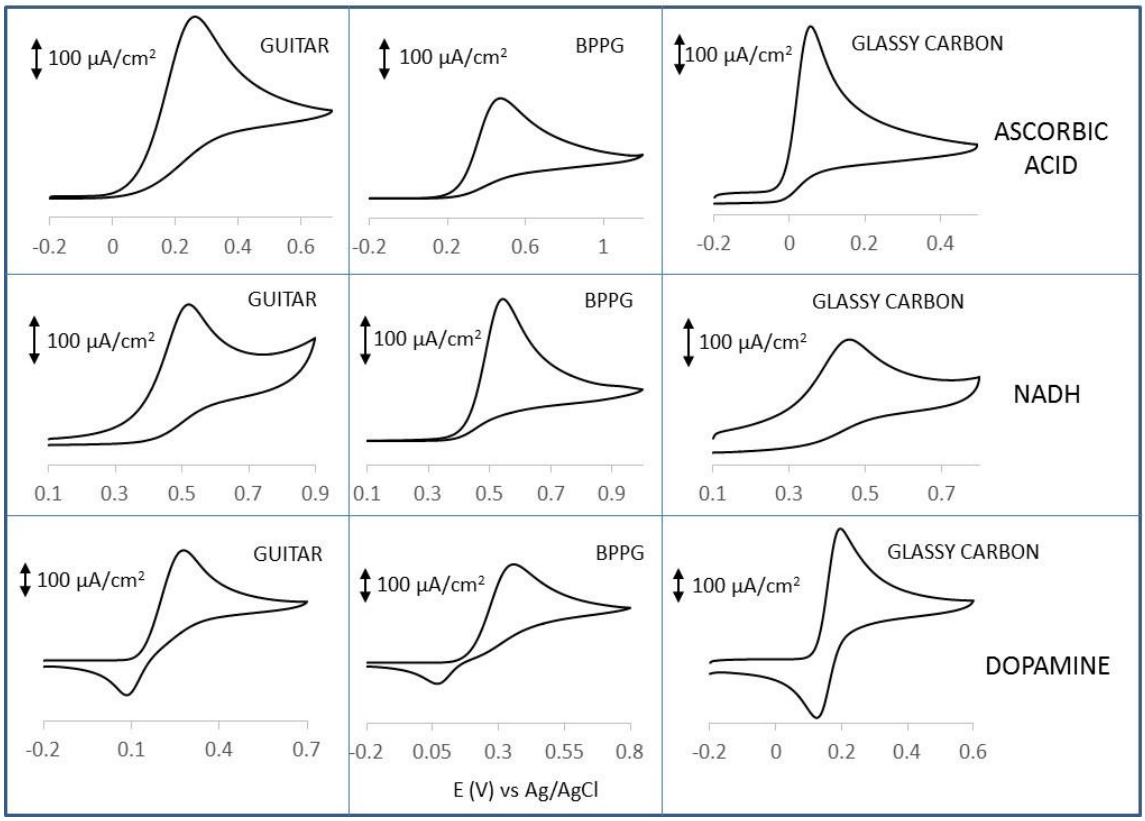

Figure 3.2. Cyclic voltammogram of ascorbic acid, NADH and dopamine at BP-GUITAR, BPPG and glassy carbon. Test solutions were at 1 mM concentration in 0.1 M phosphate buffer (pH 7.2) and scan rate was 0.1 V/s. Performance of BP-GUITAR was found to be intermediate between BPPG and glassy carbon electrodes. See also Table 3.2.

Material	Cyclic voltammetric oxidation peak potential (V vs SHE)			
	Ascorbic acid	NADH	Dopamine	Reference
BP-GUITAR	0.45 ± 0.02 (3)	0.73 ± 0.01 (4)	0.47 ± 0.03 (10)	This work
BPPG	0.68 ± 0.02 (3)	0.78 ± 0.04 (4)	0.54 ± 0.03 (6)	This work
GC	0.28 ± 0.03 (3)	0.67 ± 0.01 (4)	0.39 ± 0.01 (7)	This work
Basal plane materials				
BPPG	0.64 – 0.91	0.90 – 1.06	0.61 – 0.7	[33 – 39]
CVD graphene (single and multilayer)	0.58 – 1.25	0.72 – 1.28	0.50 – 0.73	[33,37,39]
Single layer graphene (basal)	0.65	0.88	---	[32]
Edge plane materials				
EPPG	0.44 – 0.60	0.64 – 0.85	0.48 – 0.5	[33 – 39]
Reduced graphene oxide (r-GO)	0.37, 0.41	0.62, 0.76	0.45	[40,41*,38,42]
Single layer graphene (edge)	0.54	0.68	---	[32]
Stacked graphene nanofibers (open edge)	0.41	0.70	0.40	[43]
GC	0.69, 0.70	0.79, 0.95	---	[34,35,40,41*]
Others				
Stacked graphene nanofibers (folded edge)	0.61	0.77	0.51	[43]
BDD	0.78, 0.66	0.77	0.44, 0.56	[35,44]

Table 3.2. Comparison of electrode performance from the voltammetric determination of Ascorbic acid, NADH and dopamine. Experimental condition for all entries include phosphate buffer (pH 7 to 7.4) and scan rate of 0.05 V/s or 0.1 V/s unless otherwise stated. For materials studied in this work, averages and standard deviations were calculated with number of electrodes in parenthesis. Oxidation peak potentials at BP-GUITAR is competitive with edge plane materials. *NADH was dissolved in pH 6.8 phosphate buffer

3.3.3 Electrode passivation and regeneration

Electro-polymerization products from AA, DA and NADH are often reported to passivate electrodes [7,8,45]. The resistance of GUITAR, BPPG and GC to this effect was studied by obtaining ten consecutive CV cycles at 5 sec interval in either 1 mM AA, DA or NADH at pH 7.2 PBS. Results are presented in Figure 3.3. The peak current for each CV is normalized against the value of the first run ($I_{p(n)}/I_{p(1)}$, n = cycle number (1 to 10)) and plotted versus the number of cycles. For dopamine, potential peak separation (ΔE_p) is also plotted versus number of cycles. GUITAR demonstrates highest resistance to fouling in both AA and DA and compares with GC in NADH. This is evident in Figure 3.3. Almost In all cases, BPPG exhibited the least resistance to passivation. For the CV cycling of AA, GUITAR retains 90% of its activity after 10 runs and 80% for the other species. Only GC in NADH approached GUITAR in performance in this aspect. We hypothesize that the GUITAR surface offers fewer sites for surface passivation. It is notable that while GUITAR is rich in structural defects it lacks grain boundaries as observed with graphene and graphites [46]. The extent of passivation of GUITAR in dopamine is similar to boron doped diamond (BDD), which experienced the lowest passivation in literature [47]. However, BDD has slower HET kinetics relative to GUITAR which is important for sensor applications [47].

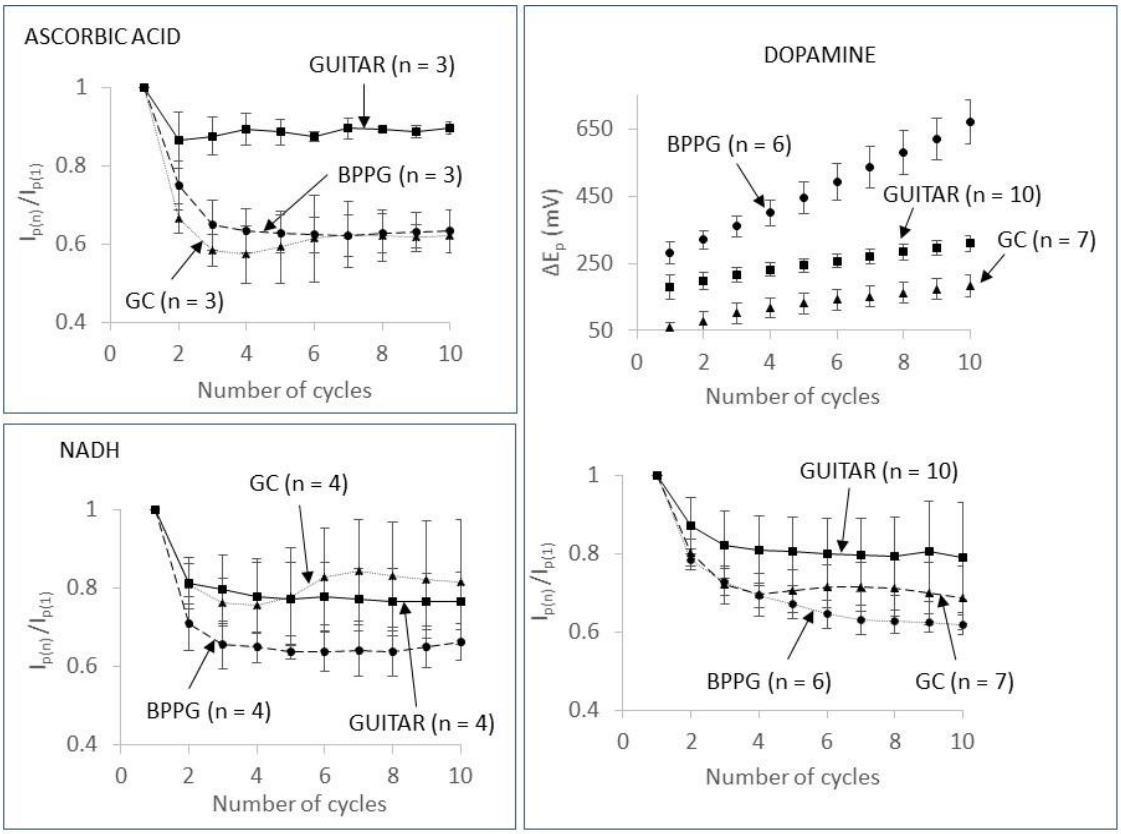

Figure 3.3. Plots of normalized oxidation peak current and peak separation (dopamine only) versus number of voltammetric cycles at BP-GUITAR, BPPG and glassy carbon (GC). Ten voltammetric cycles with 5 sec interval were recorded at each electrode and in each solution. Experimental conditions are as in Figure 3.2. $I_{p(n)}/I_{p(1)}$ is the oxidation peak current for the n^{th} cycle (n = 1 to 10) normalized against the peak current for the first cycle. GUITAR electrodes are found to exhibit the highest resistance to passivation in ascorbic acid and dopamine, and compares with glassy carbon in NADH.

Regeneration of passivated electrodes was studied with dopamine as fouling medium. Regeneration was performed by applying +2.2 V vs Ag/AgCl for 5 minutes in 0.1 M PBS (pH 7.2). This potential allows for the electro-oxidation of organics [48]. Before treatment, 20 CV cycles in dopamine were observed to decrease the initial peak current by 35% (Figure 3.5B).

After regeneration the BP-GUITAR electrode had a peak current that was 30% greater than the initial pristine surface (Figure 3.5B). In this study, BP-GUITAR electrode was regenerated four times. In Figure 3.5A, voltammograms of the first cycles at pristine and multi-regenerated BP-GUITAR are shown. It is notable that the first CV after the regeneration improved with each regeneration. Studies are underway to determine if this feature maximizes after more regeneration cycles and the maximum number of cycles GUITAR can sustain.

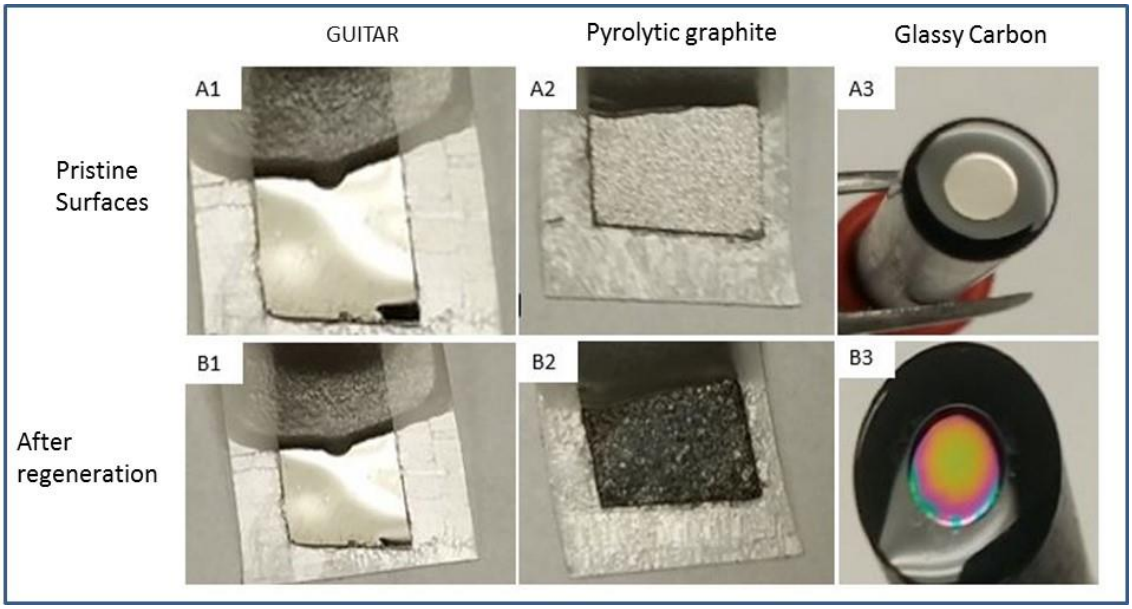

Figure 3.4. Effect of electrode regeneration treatment on GUITAR, BPPG and glassy carbon. Pristine surfaces (A1 – A3) were passivated from cyclic voltammetry of dopamine after which a regeneration treatment; +2.2 V vs Ag/AgCl, 5 minutes in 0.1 M PBS (pH 7.2) was applied. Effect of this treatment is shown as B1 – B3. PG and GC undergo morphological changes whereas GUITAR lacks visible changes to its surface.

Regeneration of electrodes is important for biosensing [49], and ability to regenerate GUITAR electrodes show promise for applications in closed systems such as enclosed microfluidics, where electrode regeneration is essential but challenging [49, 50]. Under the conditions of regeneration, significant corrosion was evident for both BPPG and GC which inhibited their continual use. Figure 3.4, presents images of the electrodes before and after regeneration and shows corrosion of both BPPG and GC, whereas GUITAR electrodes do not undergo any visible morphological changes. These results corroborate relative stability of GUITAR over other graphitic electrodes and will offer advantages in long term use of GUITAR electrodes [1,2].

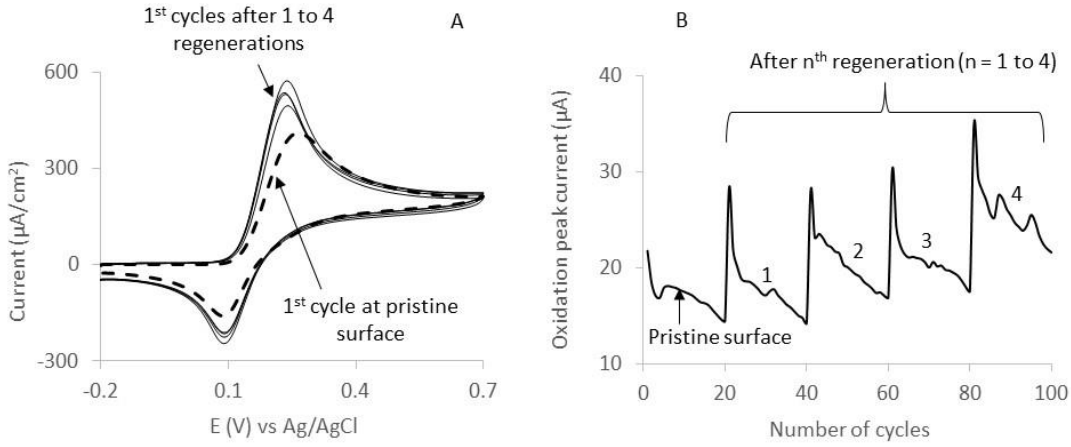

Figure 3.5. A – Cyclic voltammograms showing the first cycles of dopamine redox and B – Corresponding plots of the oxidation peak current vs number of voltammetric cycles at pristine and regenerated electrodes. Multiple regeneration of GUITAR (four regenerations) were performed, each by applying +2.2 V vs Ag/AgCl for 5 minutes in 0.1 M PBS (pH 7.2). Before and after each treatment, twenty voltammetric cycles with 5 sec interval between cycles were recorded in 1 mM dopamine/0.1 M phosphate buffer (pH 7.2). Scan rate was 0.1 V/s.

3.4 Conclusions

In this contribution we demonstrated that BP-GUITAR has HET rates comparable to other EP graphitic materials with three biologically significant analytes. Furthermore, with ascorbate, BP-GUITAR has a significantly lower limit of detection (0.15 μM) than other electrodes in literature. The observed linear range spanned 5 orders of magnitude (0.05 μM to 6250 μM). In general this surpassed literature reports with carbon electrodes by 2 orders of magnitude (Table 3.1). The fouling and passivation of the electrode surface was also found to be less with GUITAR (Figure 3.3). Another significant feature of the GUITAR electrode is its ability to withstand electrode regeneration by pulsing to +2.2 V vs. Ag/AgCl. Polymeric coatings are expected to electro-oxidize off at that potential. Both GC and BPPG underwent significant corrosion with attempts at regeneration (Figure 3.4). This property has implications for closed systems, where *in situ* electrode surface renewal is essential.

3.5 References

[1] I. F. Cheng, Y. Xie, I. O. Gyan, N. W. Nicholas, Highest measured anodic stability in aqueous solutions: graphenic electrodes from the thermolyzed asphalt reaction, RSC Adv. 3 (2013) 2379 – 2384.

[2] I. O. Gyan, P. M. Wojcik, D. E. Aston, D. N. McIlroy, I. F. Cheng, A Study of the Electrochemical Properties of a New Graphitic Material: GUITAR. CHEMELECTROCHEM, 2015, doi: 10.1002/celc.201402433

[3] K. K. Cline, M. T. McDermott, R. L. McCreery, Anomalously Slow Electron Transfer at Ordered Graphite Electrodes: Influence of Electronic Factors and Reactive Sites, J. Phys. Chem. 98 (1994) 5314-5319.

[4] Y. Tanaka, M. Furuta, K. Kuriyama, R. Kuwabara, Y. Katsuki, T. Kondo, A. Fujishima, K. Honda, Electrochemical properties of N-doped hydrogenated amorphous carbon films fabricated by plasma-enhanced chemical vapor deposition methods, Electrochim. Acta, 56 (2011) 1172–1181.

[5] G-H. Wu, Y-F. Wu, X-W. Liu, M-C. Rong, X-M. Chen, X. Chen, An electrochemical ascorbic acid sensor based on palladium nanoparticles supported on graphene oxide, Anal. Chim. Acta 745 (2012) 33-37.

[6] Z-H. Sheng, X-Q. Zheng, J-Y. Xu, W-J. Bao, F-B. Wang, X-H. Xia, Electrochemical sensor based on nitrogen doped graphene: Simultaneous determination of ascorbic acid, dopamine and uric acid, Biosens. Bioelectron. 34 (2012) 125-131.

[7] S. Hou, N. Zheng, H. Feng, X. Li, Z. Yuan, Determination of dopamine in the presence of ascorbic acid using poly(3,5-dihydroxy benzoic acid) film modified electrode, Anal. Biochem. 179 (2008) 179-184.

[8] R. F. Lane, A. T. Hubbard, Differential Double Pulse Voltammetry at Chemically Modified Platinum Electrodes for in vivo Determination of Catecholamines, Anal. Chem. 48 (1976) 1287-1293.

[9] M. Musameh, J. Wang, A. Merkoci, Y. Lin, Low-potential stable NADH detection at carbon-nanotube-modified glassy carbon electrodes, Electrochem. Commun. 4 (2002) 743-746.

[10] F. Valentini, A. Salis, A. Curulli, G. Palleschi, Chemical Reversibility and Stable Low-Potential NADH Detection with Nonconventional Conducting Polymer Nanotubule Modified Glassy Carbon Electrodes, Anal. Chem. 76 (2004) 3244-3248.

[11] S. S. L. Castro, R. J. Mortimer, M. F. de Oliveira, N. R. Stradiotto, Electrooxidation and Determination of Dopamine Using a Nafion®-Cobalt Hexacyanoferrate Film Modified Electrode, Sensors 8 (2008) 1950-1959.

[12] I. F. Cheng, Y. Xie, R. A. Gonzales, P. R. Brejna, J. P. Sundararajan, B-A. F. Kengne, D. E. Aston, D. N. McIlroy, J. E. Foutch, P. R. Griffiths, Synthesis of graphene paper from pyrolyzed asphalt, Carbon 49 (2011) 2852-2861.

[13] Y. Xie, S. D. McAllister, S. A. Hyde, J. P. Sundararajan, B-A. F. Kengne, D. N. McIlroy, I. F. Cheng, Sulfur as an important co-factor in the formation of multilayer graphene in the thermolyzed asphalt reaction, J. Mater. Chem. 22 (2012) 5723-5729.

[14] D. C. Harris, Quantitative Chemical Analysis, eighth ed., 2010, W. H. Freeman and Co., New York, 2010.

[15] C. R. Raj, K. Tokuda, T. Ohsaka, Electroanalytical applications of cationic self-assembled monolayers: square-wave voltammetric determination of dopamine and ascorbate, Bioelectrochemistry 53 (2001) 183-191.

[16] R. G. Compton, F-M. Matysik, Sonovoltammetric Behavior of Ascorbic Acid and Dehydroascorbic Acid at Glassy Carbon Electrodes: Analysis Using Pulsed Sonovoltammetry, Electroan. 8 (1998) 218-222.

[17] G. P. Keeley, A. O'Neill, N. McEvoy, N. Peltekis, J. N. Colemanac, G. S. Duesberg, Electrochemical ascorbic acid sensor based on DMF-exfoliated graphene, J. Mater. Chem. 20 (2010) 7864-7869.

[18] R. P. da Silva, A. W. O. Lima, S. H.P. Serrano, Simultaneous voltammetric detection of ascorbic acid, dopamine and uric acid using a pyrolytic graphite electrode modified into dopamine solution, Anal. Chim. Acta 612 (2008) 89-98.

[19] B. B. Xu, Q. J. Song, H. H. Wang, Simultaneous determination of ascorbic acid, dopamine, and uric acid based on double-walled carbon nanotubes/choline-modified electrode, Anal. Methods 5 (2013) 2335-2342.

[20] Y-T. Shieh, H-F. Jiang, Graphene oxide-assisted dispersion of carbon nanotubes in sulfonated chitosan-modified electrode for selective detections of dopamine, uric acid, and ascorbic acid J. Electroanal. Chem. 736 (2015) 132-138.

[21] V. Vinoth, J. J. Wu, A. M. Asiri, S. Anandan, Simultaneous detection of dopamine and ascorbic acid using silicate network interlinked gold nanoparticles and multi-walled carbon nanotubes Sensor Actuat B 210 (2015) 731-741.

[22] Y. Peng, D. Zhang, C. Zhang, Simultaneous voltammetric determination of ascorbic acid and uric acid using a seven-hole carbon nanotube paste multielectrode array, Anal. Methods 6 (2014) 8965-8972.

[23] J. Balamurugan, S. M. S. Kumar, R. Thangamuthu, A. Pandurangan, Facile and controlled growth of SWCNT on well-dispersed Ni-SBA-15 for an efficient electro-catalytic oxidation of ascorbic acid, dopamine and uric acid, J. Mol. Catal. A: Chem. 372 (2013) 13-22.

[24] B. Habibia, M. H. Pournaghi-Azar, Simultaneous determination of ascorbic acid, dopamine and uric acid by use of a MWCNT modified carbon-ceramic electrode and differential pulse voltammetry, Electrochim. Acta 55 (2010) 5492-5498.

[25] A. Salimi, H. MamKhezri, R. Hallaj, Simultaneous determination of ascorbic acid, uric acid and neurotransmitters with a carbon ceramic electrode prepared by sol–gel technique, Talanta 70 (2006) 823-832.

[26] Y. Liu, J. Huang, H. Hou, T. You, Simultaneous determination of dopamine, ascorbic acid and uric acid with electrospun carbon nanofibers modified electrode, Electrochem. Commun. 10 (2008) 1431–1434

[27] D. Zheng, J. Ye, L. Zhou, Y. Zhang, C. Yu, Simultaneous determination of dopamine, ascorbic acid and uric acid on ordered mesoporous carbon/Nafion composite film, J. Electroanal. Chem. 625, (2009) 82-87.

[28] D. X. Han, T. T. Han, C. S Shan, A. Ivaska, L. Niu, Simultaneous Determination of Ascorbic Acid, Dopamine and Uric Acid with Chitosan-Graphene Modified Electrode, Electroanal. 22 (2010) 2001-2008.

[29] J. Sun, L. Li, X. Zhang, D. Liu, S. Lv, D. Zhu, T. Wu, T. You, Simultaneous determination of ascorbic acid, dopamine and uric acid at a nitrogen-doped carbon nanofiber modified electrode, RSC Adv. 5 (2015) 11925-11932.

[30] K. R. Ratinac, W. Yang, J. J. Gooding, P. Thordarson, F. Braet, Graphene and Related Materials in Electrochemical Sensing. Electroanal. 23 (2011) 803-826.

[31] C. E. Banks, R. G. Compton, New electrodes for old: from carbon nanotubes to edge plane pyrolytic Graphite, Analyst 131 (2006) 15-21.

[32] W. Yuan, Y. Zhou, Y. Li, C. Li, H. Peng, J. Zhang, Z. Liu, L. Dai, G. Shi, The edge- and basal-plane-specific electrochemistry of a single-layer graphene sheet, SCIENTIFIC REPORTS | 3 : 2248 | DOI: 10.1038/srep02248.

[33] D. A. C. Brownson, M. Gómez-Mingot, C. E. Banks, CVD graphene electrochemistry: biologically relevant molecules. Phys. Chem. Chem. Phys. 13 (2011) 20284-20288.

[34] F. Wantz, C. E. Banks, R. G. Compton, Direct Oxidation of Ascorbic Acid at an Edge Plane Pyrolytic Graphite Electrode: A Comparison of the Electroanalytical Response with Other Carbon Electrodes, Electroanal. 17 (2005) 1529-1533.

[35] C. E. Banks, R. G. Compton, Exploring the electrocatalytic sites of carbon nanotubes for NADH detection: an edge plane pyrolytic graphite electrode study, Analyst 130 (2005) 1232-1239.

[36] E. P. Randviir, D. A. C. Brownson, M. Gomez-Mingot, D. K. Kampouris, J. Iniesta, C. E. Banks, Electrochemistry of Q-Graphene, Nanoscale 4 (2012) 6470-6480.

[37] A. Ambrosi, M. Pumera, Electrochemistry at CVD grown multilayer graphene transferred onto flexible substrates, J. Phys. Chem. C 117 (2013) 2053-2058.

[38] W-J. Lin, C-S. Liao, J-H. Jhang, Y-C. Tsai, Graphene modified basal and edge plane pyrolytic graphite electrodes for electrocatalytic oxidation of hydrogen peroxide and β-nicotinamide adenine dinucleotide, Electrochem. Commun. 11 (2009) 2153-2156.

[39] G. P. Keeley, N. McEvoy, H. Nolan, M. Holzinger, S. Cosnier, G. S. Duesberg, Electroanalytical Sensing Properties of Pristine and Functionalized Multilayer Graphene, Chem. Mater. 26 (2014) 1807-1812.

[40] H. L. Poh, F. Šaněk, A. Ambrosi, G. Zhao, Z. Sofer, M. Pumera, Graphenes prepared by Staudenmaier, Hofmann and Hummers methods with consequent thermal exfoliation exhibit very different electrochemical properties, Nanoscale 4 (2012) 3515-3522.

[41] L. Tang, Y. Wang, Y. Li, H. Feng, J. Lu, J. Li, Preparation, Structure, and Electrochemical Properties of Reduced Graphene Sheet Films, Adv. Funct. Mater. 19 (2009) 2782-2789.

[42] S. Alwarappan, A. Erdem, C. Liu, C-Z. Li, Probing the Electrochemical Properties of Graphene Nanosheets for Biosensing Applications, J. Phys. Chem. C 113 (2009) 8853-8857.

[43] A. Ambrosi, A. Bonanni, M. Pumera, Electrochemistry of folded graphene edges, Nanoscale 3 (2011) 2256-2260.

[44] W. C. Poh, K. P. Loh, W. D. Zhang, S. Triparthy, J-S. Ye, F-S. Sheu, Biosensing Properties of Diamond and Carbon Nanotubes, Langmuir 20 (2004) 5484-5492.

[45] M. Pumera, R. Scipioni, H. Iwai, T. Ohno, Y. Miyahara, M. Boero, A Mechanism of Adsorption of β-Nicotinamide Adenine Dinucleotide on Graphene Sheets: Experiment and Theory, Chem. Eur. J. 15 (2009) 10851-10856.

[46] P. Simonis, C. Goffaux, P. A. Thiry, L. P. Biro, Ph. Lambin, V. Meunier, STM study of a grain boundary in graphite, Surf. Sci. 511 (2002) 319-322.

[47] A. N. Patel, S-Y Tan, T. S. Miller, J. V. Macpherson, P. R. Unwin, Comparison and Reappraisal of Carbon Electrodes for the Voltammetric Detection of Dopamine, Anal. Chem. 85 (2013) 11755−11764.

[48] M. Panizza, G. Cerisola, Direct And Mediated Anodic Oxidation of Organic Pollutants, Chem. Rev. 109 (2009) 6541-6569.

[49] K. Sun, B. Jiang, X. Jiang, Electrochemical desorption of self-assembled monolayers and its applications in surface chemistry and cell biology, J. Electroanal. Chem. 656 (2011) 223-230.

[50] S. Choi, J. Chae. Reusable biosensors via in situ electrochemical surface regeneration in microfluidic applications, Biosens. Bioelectron. 25 (2009) 527-531.

Chapter 4: Cathodic Potential Limits at GUITAR Electrodes and Application as Negative Electrode in the Vanadium Redox Flow Battery[§]

Isaiah O. Gyan, Md. Kabir, Haoyu Zhu, I. Francis Cheng*

Department of Chemistry, University of Idaho, Moscow, ID 83844-2343, Tel. (208) 885-6387
ifcheng@uidaho.edu

Abstract

The negative half of the vanadium redox flow battery (VRB) is currently plagued with hydrogen evolution at the carbon electrodes that are commonly used. This undesired reaction results in reduced coulombic efficiency and poor performance of the battery. Current research is aimed at finding materials with wide cathodic potential limits for use in the VRB. In this work, we have studied cathodic potential limits at GUITAR electrodes in aqueous electrolytes and application of this material as a negative electrode in the VRB. In sulfuric acid, which is the electrolyte used in the VRB, we have discovered that GUITAR electrodes demonstrate at least 400 mV more negative cathodic limit than typical graphitic carbon materials, including graphite felt which is a common negative electrode in the VRB. The wide cathodic limits at GUITAR translates into 2.7 % of hydrogen evolution current at the peak potential during reduction of V^{3+}. At graphite felt control electrodes, this was found to be 25 %. We have also discovered that heterogeneous standard electron transfer rate constant for the redox of V^{3+}/V^{2+} at GUITAR electrodes, is within an order of magnitude of that of edge plane and textured carbon materials, and is improved by a factor of 6.6 by

[§] This chapter is been developed for publication.

electrochemical pretreatment. Together with the possibility of fabricating high-surface composite GUITAR-based electrodes, GUITAR is presented as the most suitable carbon material for high coulombic efficiency in the negative half of the vanadium redox flow battery.

4.1 Introduction

In previous reports following the discovery of a unique carbon material from the thermolyzed asphalt reaction, [1,2] we described electrochemical properties that distinguish this material from other graphite and graphene-based electrode materials. [3,4] These are (i), fast heterogeneous electron transfer across its basal plane (BP). [3] Crystalline graphites and graphenes have a barrier to electron transfer due to the low density of electronic states (DOS) near their Fermi level. [5,6] The GUITAR electrode is a disordered graphitic system which increases DOS. [4] The standard rate constant for the $Fe(CN)_6^{3-/4-}$ system is 10^{-2} cm/s on GUITAR which is 2-7 orders of magnitude greater than other crystalline graphites. [4] (ii), in 1 M H_2SO_4 GUITAR has anodic limit greater than other graphitic electrodes by 400 mV. The frontier plane of GUITAR is nonporous; other graphitic electrodes allow for electrolyte intercalation which results in blisters and pit corrosion. [3,4] (iii), the H_2 overpotential that is ca. 400 mV larger than graphitic electrodes in 1 M H_2SO_4. [4] Taken together, the aqueous potential window of GUITAR is 3 V as compared to 2.2 V for other sp^2 carbon electrodes. [4] This performance is competitive with synthetic diamonds which have a window of 2.2 to 3.5 V in this electrolyte. [35,37,38] (iv), the edge plane (EP) of GUITAR electrode is more resistant to the effects of air oxidation relative to EP-HOPG and EP pyrolytic graphite (EPPG). [4] Furthermore, EP-GUITAR, like BP-GUITAR does not allow for electrolyte intercalation

observed with other edge plane graphites. This behavior contributes to the improved anodic stability described in property (iv). [4]

We have also reported on application of GUITAR electrodes in biosensing, with exceptional performance indicators such as; (i), facile kinetics for the oxidation of ascorbic acid, dopamine and NADH, (ii), extremely low detection limit and wide linear range for ascorbic acid, (iii), relatively high resistance to passivation and (iv), ability to regenerate GUITAR electrodes for repetitive use, without any visible microstructural changes to the electrode as was observed for pyrolytic graphite and glassy carbon. [7]

In this contribution, we examine GUITAR's unusually high hydrogen evolution potentials in aqueous electrolytes as well the application of this material as a negative electrode in the vanadium redox flow battery (VRB). The aqueous electrochemical window encompasses the reduction of water to hydrogen at the cathodic end (Reaction 1) and both oxygen evolution and corrosion at the anodic limits (Reactions 2 and 3).

$2H^+ + 2e^- = H_2$ $E^0 = 0.00$ V (1)

$2H_2O = O_2 + 4H^+ + 4e^-$ $E^0 = 1.23$ V (2)

$C + 2H_2O = CO_2 + 4H^+ + 4e^-$ $E^0 = 0.207$ V (3)

The potential limits are of fundamental and applied importance when considering water splitting, anodic stripping voltammetry, cathodic electrochemiluminescence, and aqueous ultracapacitors where cell voltages are limited to 1.0 to 2.0 V. [8-12] The latter is based on the 1.23 V required for decomposition of water (Reaction 1 and 2). The advantages of aqueous

electrolytes in this application are superior ionic conductivity, nonflammability, lower costs and green solvent considerations. On the other hand, organic solvents can achieve 5 V of cell potential. [13-15] Of keen interest is the importance of potential limits to vanadium redox flow battery, where mostly, the evolution of hydrogen gas at negative electrodes limit coulombic efficiency and leads to poor battery performance. [16,17]

The vanadium redox flow battery (VRB) is one kind of energy source that has gained a lot of attention due to advantages that include; ability to independently control power and storage capacity, long cycle life and little or no cross contamination effects. [16,18-20] Operation of this type of battery is based on the oxidation and reduction reactions of V^{5+}/V^{4+} at the positive half cell (equation 4) and V^{3+}/V^{2+} at the negative half cell (equation 5) both in sulfuric acid. [21]

$$VO_2^+ + 2H^+ + e^- = VO^{2+} + H_2O \qquad E^o = +1.00 \text{ V vs SHE} \quad (4)$$

$$V^{3+} + e^- = V^{2+} \qquad E^o = -0.26 \text{ V vs SHE} \quad (5)$$

The negative half reaction (equation 5) is reported to be the limiting half in the VRB. At this half, two major issues are of great concern; (i), slow exchange of electrons between the electrode and V^{3+}/V^{2+} redox couple and (ii), hydrogen evolution. [17] A consequence of the former, is low power density whereas the latter results in a reduction in both coulombic and energy efficiency of the battery. [16]

Electrode materials that are applicable for both equations 4 & 5 above are expected to have high overpotentials for undesired competing electrochemical reactions including oxygen and hydrogen evolution in the medium of the battery's applicability. The ideal material should

also have a high surface area, be mechanically & chemically stable and should exhibit high conductivity for the redox processes in equations 4 & 5. [22-24] Active research is on-going to identify electrodes with high overpotentials for hydrogen evolution and fast electron transfer kinetics to support efficient application in the VRB. Currently, various carbon materials are applied as electrodes in the VRB given the cost of using metal electrodes. [25-29] The likes of carbon/graphite felt offer the advantage of high surface area and cost effectiveness but these electrodes (including all graphitic materials), have very low overpotentials for hydrogen evolution and slow kinetics for vanadium redox. [16,30]

In this work, we have studied cathodic potential limits in aqueous electrolytes at GUITAR electrodes. Together with preliminary studies towards the application of GUITAR electrodes in the negative half of vanadium redox flow batteries, we show; (i), GUITAR exhibits high overpotentials for hydrogen evolution in aqueous electrolytes. These overpotentials are wider than reported for typical graphitic materials. (ii), kinetics of V^{3+}/V^{2+} at GUITAR is comparable to other carbon materials, and could be improved by anodic treatment, (iii), the possibility of fabricating a GUITAR-graphite felt composite electrodes. The sum of these is that, high surface area GUITAR-based composite electrodes can be fabricated with high overpotential for hydrogen evolution and improved electron transfer kinetics towards the V^{3+}/V^{2+} redox couple. This electrode is expected to achieve high energy and coulombic efficiencies when used in the VRB.

4.2 Experimental methods

Materials and chemicals: Silicon wafer of 111 orientation, 300nm layer of thermal oxide, and resistivity of 0.001 – 0.002 ohm cm were obtained from University Wafer (Boston, MA). Graphite felt (KFD 2.5 EA type) was donated by SGL Carbon Company (PA, USA). High vacuum grease was obtained from Dow Corning (Midland, MI). Sulfuric (96.3%) and phosphoric (85.3%) acids were obtained from J.T Baker chemical Co. (Phillipsburg, N.J, USA). Potassium and sodium nitrates, ammonium sulfate (99.9%) were obtained from Fisher Scientific (Fair Lawn, N.J, USA), lithium perchlorate (95.0%) was obtained from Alfa Aesar (Ward hill, MA). Vanadium (III) chloride (97%) was obtained from Sigma-Aldrich (St. Louis, MO). All aqueous solutions were prepared with deionized water purified by passage through an activated carbon purification cartridge (Barnstead, model D8922, Dubuque IA).

Electrolyte preparation: Vanadium solution (0.05 M V^{3+}) was prepared from VCl_3 salt in 1 M H_2SO_4, under conditions that prevented possible oxidation to V^{4+} by atmospheric oxygen. To do this, the salt was dissolved in a N_2-saturated solution of the acid and kept under N_2 purge throughout the period of the experiment. This solution was freshly prepared prior to each experiment. During the voltammetric studies, N_2 gas was kept as blanket over the solution.

Electrode fabrication and electrochemical cell setup: GUITAR was synthesized as described by previous procedures. [1] Flakes of GUITAR, pyrolytic graphite and graphite felt were manipulated onto a microscope slide using a thin layer of high vacuum grease as an adhesive. Unless otherwise noted, setup used for all electrochemical studies consisted of GUITAR, pyrolytic graphite or graphite felt, graphite rod and Ag/AgCl/3M NaCl(aq) (0.209V

vs. SHE) as working, counter/auxiliary and reference electrodes respectively in a three-electrode undivided cell. All potentials are with respect to this reference electrode.

Cyclic voltammetry and electrochemical treatment: Cyclic voltammetry was carried out using a Bioanalytical Systems Epsilon potentiostat (West Lafayette, IN). Measurements were conducted at a scan rate of 50 mV/s. Electrochemical treatment of GUITAR electrodes were performed by applying a potential of +2.0 V vs Ag/AgCl for 30 seconds in 1 M H_2SO_4.

4.3 Results

Cyclic Voltammetric Behavior. In Figure 4.1, cyclic voltammograms at GUITAR electrodes in 1 M aqueous solutions of KNO_3, H_3PO_4, H_2SO_4, $LiClO_4$, and $(NH_4)_2SO_4$ and at pyrolytic graphite (PG) in 1 M H_2SO_4 are presented. Corresponding cathodic limits are presented in Table 4.1, along with anodic limits. Potential limits were estimated from voltammograms at 200 μA/cm^2 according to a method illustrated previously. [4] Studies in these electrolytes are important because of their use in regular electrochemistry, battery and fuel cell systems and GUITAR extends to higher potential limits than other materials reported in literature. [31-33] Cathodic limits in H_2SO_4 at various carbon materials have been compared in Table 4.2. GUITAR has been found to exhibit wider limits than the PG and graphite felt of this investigation as well as all graphites cited and is also competitive with synthetic diamond electrodes.

Cyclic voltammograms of the V^{3+}/V^{2+} redox couple at GUITAR electrode is shown in Figure 4.2, along with a background cycle. (1 M H_2SO_4). Observation of the voltammograms show that there is very little contribution of hydrogen evolution current to the total reduction

current at GUITAR. The effect of anodic treatment on the performance of GUITAR electrodes for the V^{3+}/V^{2+} redox is shown in Figure 4.3. The optimal treatment condition was found to be application of +2.0 V vs Ag/AgCl for 30 seconds in 1 M H_2SO_4. Figure 4.3 shows that anodic treatment improves electron transfer kinetics for V^{3+}/V^{2+} redox at GUITAR electrodes.

GUITAR-Graphite felt composite electrodes. The possibility of fabricating composite electrodes from GUITAR and carbon/graphite felt is demonstrated in Figure 4.4. The figure shows that graphite felt can be applied to the TAR process as a substrate for the deposition of GUITAR. Such composite electrodes is expected to possess a high surface area, faster electron transfer kinetics and exhibit low hydrogen evolution activity when applied in the VRB.

4.4 Discussion of Results

Potential Limits at GUITAR electrodes. Cathodic and anodic potential limits at GUITAR electrodes have been studied in 1 M aqueous solutions of KNO_3, H_3PO_4, H_2SO_4, $LiClO_4$, and $(NH_4)_2SO_4$. Cathodic voltammograms at GUITAR electrodes are shown in Figure 4.1 along with pyrolytic graphite in 1 M H_2SO_4. Potential limits in the range of -0.90 V to -1.44 V vs SHE and 1.93 V to 2.10 V vs SHE for cathodic and anodic limits respectively have been discovered in this study (Table 4.1). These limits amount to total potential windows between 3.0 V and 3.5 V at GUITAR electrodes. In a previous paper, we reported that in 1 M H_2SO_4, GUITAR has the highest anodic limit over sp^2 carbon materials. This property was attributed to the lack of electrolyte intercalation in GUITAR. [4]

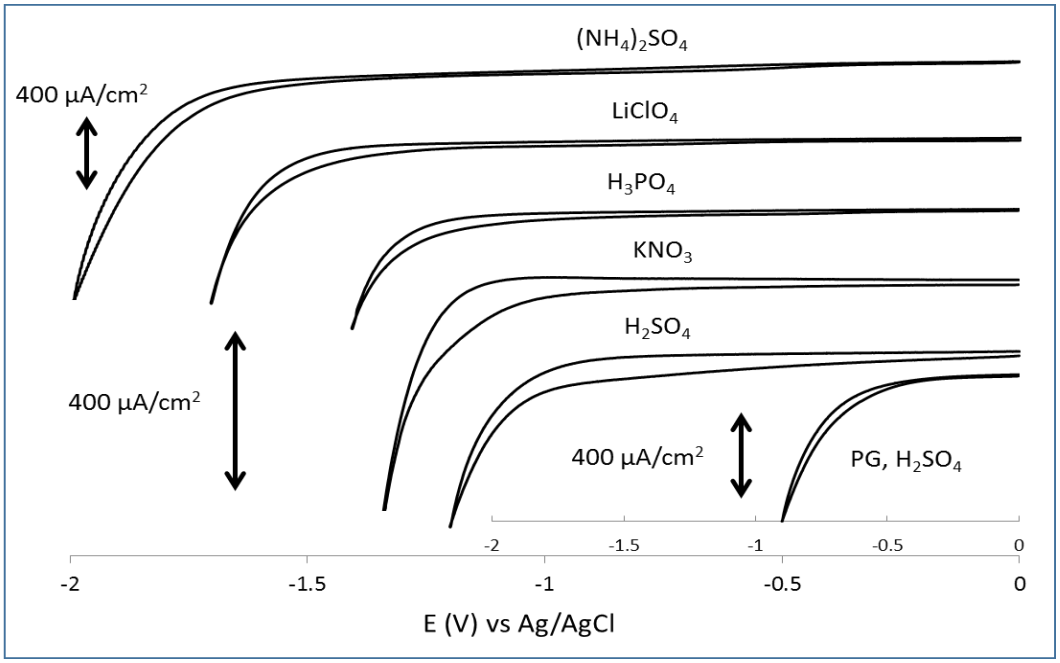

Figure 4.1. Cyclic voltammograms at GUITAR in the indicated electrolytes (1 M) and at Pyrolytic Graphite (inset, PG in 1 M H_2SO_4). Starting potential was zero and scan direction was towards more negative potentials at 50 mV/s. Potentials for hydrogen evolution were extrapolated at 200 µA/cm^2 from these voltammograms.

In H_2SO_4 cathodic potential limits are reported for graphite to be in the range of -0.30 V to -0.5 V vs SHE (Table 4.2). [34-36] In the same medium synthetic diamond extends from -0.40 V to -1.25 V vs SHE (Table 4.2). [34,35,37,38] GUITAR extends to 400 - 600 mV more negative than graphitic materials, and compares with synthetic diamond electrodes (Table 4.2). These properties of GUITAR electrodes are indications of this material's wide-potential applicability in aqueous media without interference from gas evolution.

Table 4.1. Cathodic and anodic potential limits at GUITAR in various aqueous electrolytes and at pyrolytic graphite (PG, 1 M H_2SO_4). Potentials were extrapolated at a current density of 200 μA/cm^2. Standard deviations were calculated from n = 5.

1 M Aqueous Electrolyte	GUITAR potential limits vs SHE		
	Anodic (V)	Cathodic (V)	Total Window (V)
KNO_3	1.93 ± 0.02	-1.18 ± 0.04	3.11
$LiClO_4$	1.96 ± 0.05	-1.41 ± 0.16	3.37
$(NH_4)_2SO_4$	1.95 ± 0.02	-1.44 ± 0.10	3.39
H_3PO_4	2.03 ± 0.03	-1.24 ± 0.13	3.27
H_2SO_4	2.10 ± 0.03	-0.90 ± 0.07	3.00
PG, H_2SO_4	1.45 ± 0.03	-0.52 ± 0.06	1.97

Together with facile electron transfer at GUITAR, a direct implication for the wide potential limits is the suitability of this material for applications such as sensing and vanadium redox batteries. [16] Another application is the development of GUITAR based ultracapacitors with wider potential windows than observed with conventional materials. [11,12]

Table 4.2. Cathodic potential limits (vs SHE) for various carbon materials in H_2SO_4 media. GUITAR extends to wider potential limits than all graphites studied/cited and is within those for synthetic diamonds.		
Material	Cathodic limit (V)	Reference
GUITAR	-0.90 ± 0.07 (n = 5)	This work
Pyrolytic Graphite	-0.52 ± 0.06 (n = 5)	
Graphite felt	-0.50 ± 0.05 (n = 5)	
Literature Comparison		
Graphite*	-0.4 to -0.5	34-36
Glassy carbon	-0.3 to -0.5	34-36
Synthetic diamond†	-0.4 to -1.25	34,35,37,38
*Graphite includes; HOPG and exfoliated graphite, †Synthetic Diamonds include; boron doped diamond, low and high sp^2 diamond and diamond-like-carbon.		

Hydrogen evolution at GUITAR electrodes. The high cathodic limits (overpotentials) recorded at GUITAR electrodes in this work (-0.90 V to -1.44 V), places this material over most carbon materials in this property. [33] This feature is unique and shows significant differences between GUITAR and especially graphitic (sp^2) materials. Analyses of the X-ray photoelectron spectroscopy (XPS) and Raman spectra of GUITAR indicate nearly sp^2 carbon, [1] which makes the current observations of high potential limits inconsistent with low sp^2 carbon content. [39] The high cathodic potentials observed may suggest that (i), adsorption of protons or hydronium ions on GUITAR is low, given that, the mechanism of hydrogen evolution involves adsorption of protons to the surface of the electrode [34] and (ii), there is a

barrier to electron exchange between GUITAR electrodes and protons, as a result of weak proton adsorption and/or low density of electronic states for proton reduction. In this work, we attribute the weak adsorption of protons to the hydrophobic nature of GUITAR electrode surface. Goniometric studies presents GUITAR to be hydrophobic, with water contact angle of 106 ± 13° (n = 5). Literature values ranging from 90°- 98° is reported for graphite and HOPG, 67.4° and 127° for graphene oxide and reduced graphene oxide respectively and 91°-100° is reported for single to multilayer graphene. [40-42] Comparison of these goniometric results indicates that GUITAR's surface is more hydrophobic than most graphite and graphene materials and this property may be responsible for the weak adsorption of protons, subsequently lowering hydrogen evolution activity at GUITAR electrodes.

At diamond and modified diamond electrodes, studies that compared H_2 evolution at as-grown and fluorinated diamonds demonstrate significant shifts (even up to 1.5 V) of the cathodic limit to more negative potentials after fluorination. [43-45] The shift has been reported to be due to; (i), the ability of the hydrophobic fluorinated surface to reduce the adsorption strength of both water molecules and atomic hydrogen [44] and (ii), the lack of interactions between the fluorinated surfaces and the intermediates of the cathodic reaction. [46] It is worth noting that, the surface of diamond has been shown to be hydrophobic as a result of surface hydrogenation and fluorination has been reported to impart hydrophobicity and superhydrophobicity to carbon surfaces including diamond and doped diamond. [47-51] The sum of these suggest a possible relationship between surface hydrophobicity and hydrogen evolution activity at carbon surfaces. This hypothesis agrees with discussions on hydration of hydrophilic and hydrophobic surfaces which have shown that water molecules interact

strongly with hydrophilic surfaces [52] whereas a repulsive force exists between water and hydrophobic surfaces. [53] The difference in interaction strength is due to possible differences in organization of water molecules when in contact with either a hydrophilic or hydrophobic surface. [54]

Kinetics of V^{3+}/V^{2+} redox. Performance of GUITAR and graphite felt electrodes were evaluated for the redox of V^{3+}/V^{2+} using cyclic voltammetry. Figure 4.2 presents voltammograms in the bare supporting electrolyte (1 M H_2SO_4), as well as in the presence of 0.05 M V^{3+} at GUITAR.

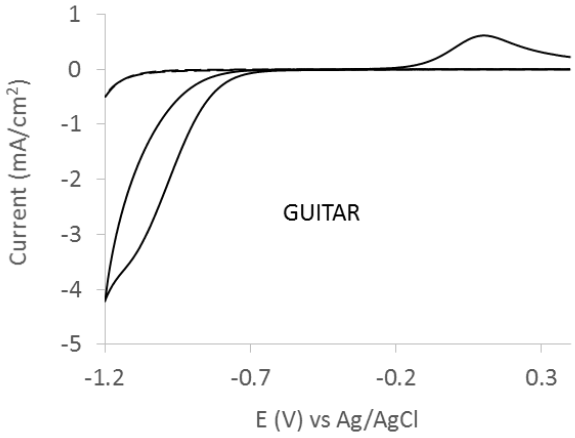

Figure 4.2. Cyclic voltammogram of 0.05 M VCl_3 + 1 M H_2SO_4 (solid line) and also in 1 M H_2SO_4 (broken line) at GUITAR. Voltammograms were acquired at 50 mV/s scan rate.

Simulation of the voltammograms gave the standard heterogeneous rate constants (k^o) reported in Table 4.3. At unmodified GUITAR electrodes, these rate constants are found to be at least an order of magnitude lower than other electrodes, including the graphite felt of this study (Table 4.3). Generally, electron exchange with the V^{3+}/V^{2+} redox couple has been reported to be slow at especially pristine carbon electrodes. [55,56] This is due to solvation of

the metal ion and low homogeneous self-exchange rate.[56] The mechanism of V^{3+}/V^{2+} electron exchange is currently not fully understood, however, the redox has been reported to involve an outer sphere mechanism.[56,57] Considering the outer sphere mechanism, the kinetics of the electron transfer is highly dependent on the electronic structure of the electrode, specifically density of electronic states at the formal potential of the redox couple.[6,58] The implication of the relatively slow kinetics recorded at GUITAR electrodes (Table 4.3), is likely, low density of states at the formal potential of V^{3+}/V^{2+}. Together with the slow kinetics for proton reduction (wider cathodic limits), there is a possibility that density of states at GUITAR electrodes is low at negative potentials or there is a barrier to electron exchange with solvated dissolved species whose redox potentials are on the negative side of the potential scale. From Table 4.3, both GUITAR and HOPG, which are basal plane materials with low surface areas, have rate constants within an order of magnitude of edge plane and high-surface area materials.

Table 4.3. Comparison of standard heterogeneous electron transfer rate constants for V^{3+}/V^{2+} redox at various carbon materials. GUITAR and HOPG are flat basal plane electrodes whereas the other entries are edge and/or textured materials.

Material	k^o (cm/s) for V^{3+}/V^{2+}	Reference
As-grown GUITAR	0.12×10^{-5}	This work
o-GUITAR†	0.79×10^{-5}	This work
Graphite felt	0.14×10^{-4}	This work
HOPG	$< 0.3 \times 10^{-5}$	56
EPPG	$3.5 \times 10^{-5} – 5.5 \times 10^{-4}$	59,60
Glassy carbon	$0.1 \times 10^{-5} – 8.7 \times 10^{-4}$	59-62
Plastic formed carbon	5.3×10^{-4}	59
Graphite reinforced carbon	$5.2 \times 10^{-4} – 9.7 \times 10^{-3}$	59
Carbon paper	$1.07 \times 10^{-3} – 3.28 \times 10^{-3}$	60

† = GUITAR that has been treated at +2.0 V for 30 sec in 1 M H_2SO_4

Pretreatment of carbon electrodes, including electrochemical pretreatment (ECP), has been reported to increase electron transfer rates by increasing the density of states and/or increasing active sites for attachment to dissolved redox species. [63-66] At graphitic materials, the former is as a result of creation of edge plane sites, which also act as active sites. [63,65,66] Specifically, surface oxides have been shown to enhance kinetics of electron transfer with V^{3+}/V^{2+} for reasons including; (i), changes in hydrophobicity or adsorption and (ii), a change of mechanism to an inner sphere one. [56,66]

Effect of electrochemical pretreatment on the kinetics of V^{3+}/V^{2+} redox was examined at GUITAR electrodes. Various potential waveforms were applied however, the optimal treatment condition was found to involve application of +2.0 V vs Ag/AgCl for 30 seconds in 1 M H_2SO_4. The treatment resulted in a well-defined wave for the reduction of V^{3+} (Figure 4.3) and also increased the electron transfer rate constant by a factor of 6.6 (Table 4.3).

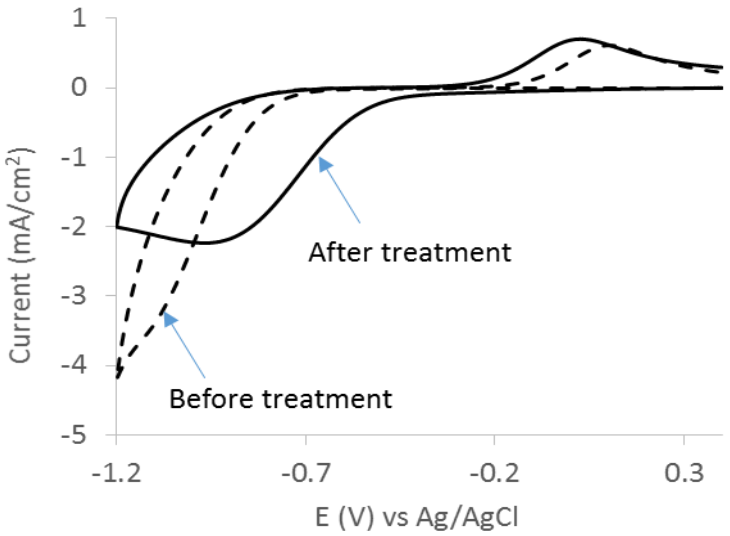

Figure 4.3. Effect of electrochemical treatment on the cyclic voltammogram of 0.05 M VCl_3 + 1 M H_2SO_4 at GUITAR. The optimal treatment was found to be application of +2.0 V for 30 sec in 1 M H_2SO_4. Voltammograms were acquired at 50 mV/s scan rate.

We argue that the ECP applied here, both decreased the hydrophobicity of the GUITAR surface and also provided active oxygen-containing sites for inner sphere electron exchange with vanadium. [56,66] Compared with ECP of HOPG and fractured glassy carbon from literature, the rate enhancement at GUITAR electrodes is less because, unlike HOPG, the treatment does not produce edges on the surface of GUITAR but only oxidizes the surface. [56] There is also the possibility of not enough active sites created, even under optimum conditions, due to the unique microstructure of GUITAR.

Hydrogen evolution contribution to V^{3+} reduction. Analyses of the background voltammogram in Figure 4.2 reveals that, at GUITAR electrodes, current corresponding to the evolution of hydrogen does not evolve until around -1.1 V vs Ag/AgCl. At this potential, about 100 μA/cm^2 of current is evolved. This observation is consistent with the slow kinetics for proton reduction (wide cathodic limits) at GUITAR electrodes. [4] From Figure 4.2, even though reduction of V^{3+} commences at around -0.7 V vs Ag/AgCl at GUITAR electrodes, the peak of the reduction wave is located around -1.05 V vs Ag/AgCl. At this potential, the proportion of the total reduction current due to the background (proton reduction), is calculated as 2.7 ± 1.3 % (n = 21 GUITAR electrodes). Similar analyses for graphite felt shows that, this value is 25 ± 4% (n = 2). The latter agrees with deductions from literature studies at graphite and graphite felt electrodes. [16,17] The high hydrogen evolution activity at graphitic electrodes is responsible for reduced coulombic efficiency and poor performance of VRBs. [16,17] The low hydrogen evolution current contribution is unique to GUITAR electrodes and will offer significant advantages with respect to coulombic efficiency and improve the performance of the VRB, especially at charging potentials below -1.05 V vs Ag/AgCl. [16,17] GUITAR-based vanadium redox flow batteries can be charged at relatively high potentials (negative) in order to increase kinetics of the V^{3+} reduction whiles maintaining low proton reduction activity.

Fabrication of GUITAR-Carbon felt composite electrodes. Literature reports show that, the most common carbon material used as electrodes in the VRB is carbon/graphite felt. [24,67] As advantages, these electrodes have high surface areas and large sizes are readily obtained,

however, the problem of hydrogen evolution is reported to inhibit the performance of these electrodes. [17,68]

It is apparent that the performance of carbon/graphite felt can be enhanced by extending its cathodic potential limit to reduce hydrogen evolution, while maintaining other properties such as surface area and electrical conductivity. [68] We have demonstrated the possibility of fabricating GUITAR-carbon felt composite electrodes for applications in the VRB. Preliminary studies utilizing graphite tape show that, GUITAR can successfully be deposited on such interwoven carbon structures. Figure 4.4 shows the successful application of the TAR process to coating carbon tape.

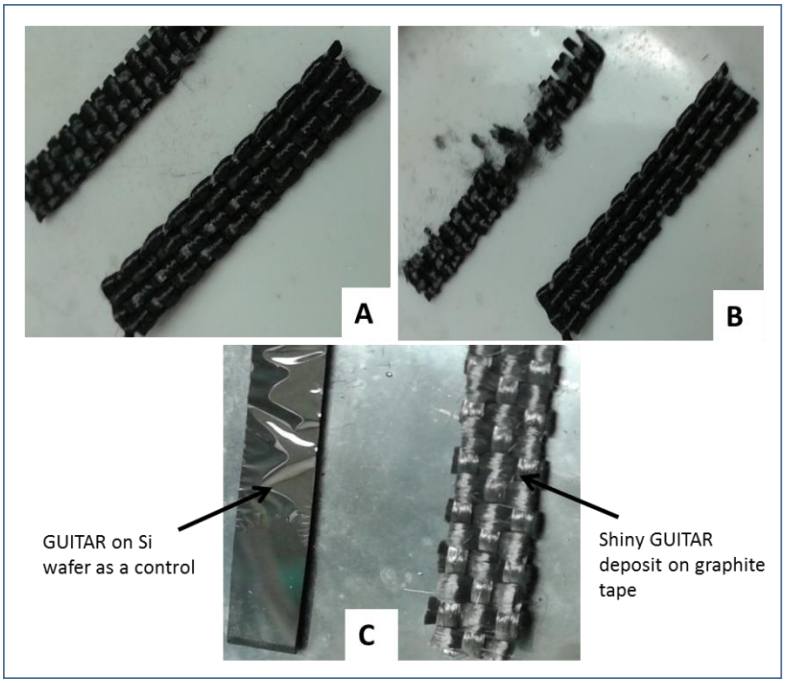

Figure 4.4. Fabrication of GUITAR-graphite tape composite. Bare graphite tape (A), graphite tape taken through the TAR process without a carbon precursor (B) and graphite tape used in the TAR process in the presence of asphalt (C). In (C), both Si wafer (control) and graphite tape were used as substrates for GUITAR deposition. Shiny nature of graphite tape in C, is indicative of the successful deposition of GUITAR flakes.

When the bare tape only is taken through the TAR process without any carbon precursor, the tape remains black and occasionally softened by the heat treatment (Figure 4.4B). However, in the presence of a carbon precursor (starting material for the TAR process), shiny deposits are discovered on the graphite tape (Figure 4.4C). The latter is an indication of the formation of GUITAR on the graphite tape substrate. It was also discovered that, the resultant GUITAR-graphite tape composite electrode is much robust, unlike the control in Figure 4.4B.

Future studies will examine application of this and other composite electrodes to the vanadium redox flow battery. It is expected that, these electrodes will offer a high surface area, wide cathodic potential limit and facile kinetics towards the V^{3+}/V^{2+} redox couple.

Conclusion. In this work, cathodic potential limits in connection with hydrogen evolution at GUITAR electrodes in various aqueous electrolytes have been studied. This material has demonstrated wider potential limits; at least 400 mV more negative than typical graphitic carbon materials in sulfuric acid medium. The implication is the suitable application of GUITAR electrodes for more-negative electrochemical processes without interference from gas evolution. As an application of the wide cathodic potential limits, performance of GUITAR electrodes for the negative half of vanadium redox flow battery was also examined. It was discovered that, whiles the wide cathodic limit translates well in this application, kinetic facility with the dissolved species (V^{3+}/V^{2+}) was found to be similar to literature HOPG and within an order of magnitude of edge plane and/or high surface-area carbon materials. The relatively slow proton and vanadium reductions at GUITAR electrodes were

explained to possibly involve the high hydrophobicity and/or electronic barriers at negative potentials, especially under conditions where the dissolved species is solvated and/or has low homogeneous self-exchange rate. Electrochemical pretreatment involving the application of anodic potentials were found to improve the heterogeneous standard electron transfer rate constant for V^{3+}/V^{2+} by a factor of 6.6 at GUITAR electrodes. This improvement in rate is explained to possibly involve a change in hydrophobicity and/or creation of oxide-containing active sites that changes the erstwhile outer sphere to an inner sphere electron transfer mechanism.

We have also demonstrated the possibility of fabricating GUITAR-carbon/graphite felt composite electrodes for application in the VRB. These electrodes are expected to have high surface areas, wide potential limits and improved kinetics towards dissolved redox couples. Findings from this work open up insights into application of GUITAR in vanadium redox flow batteries. GUITAR is presented as the most suitable carbon material for high coulombic efficiency in the negative half of the vanadium redox flow battery, with the possibility of fabricating high-surface GUITAR based composite electrodes.

4.5 References

[1] Cheng, I. F.; Xie, Yuqun; Gonzales, R. A.; Brejna, Przemysław R.; Sundararajan, Jency P.; Kengne, B-A. F.; Aston, D. E.; McIlroy, David N.; Foutch, Jeremy D.; Griffiths, Peter R. Synthesis of Graphene Paper from Pyrolyzed Asphalt. *Carbon* **2011**, *49*, 2852-2861.

[2] Xie, Yuqun; McAllister, Simon D.; Hyde, Seth A.; Sundararajan, Jency P.; Kengne, B-A. F.; McIlroy, David N.; Cheng, I. F. Sulfur as an important co-factor in the formation of multilayer graphene in the thermolyzed asphalt reaction. *J. Mater. Chem*. **2012**, *22*, 5723-5729.

[3] Cheng, I. F.; Xie, Yuqun; Gyan, Isaiah O.; Nicholas, Nolan W. Highest measured anodic stability in aqueous solutions: graphenic electrodes from the thermolyzed asphalt reaction. *RSC Adv*. **2013**, *3*, 2379-2384.

[4] Gyan, Isaiah O.; Wojcik, Peter M.; Aston, D. E.; McIlroy, David N.; Cheng, I. F. A Study of the Electrochemical Properties of a New Graphitic Material: GUITAR. *CHEMELECTROCHEM*. **2015**, doi: 10.1002/celc.201402433.

[5] Cline, Kristin K.; McDermott, Mark T.; McCreery, Richard L. Anomalously Slow Electron Transfer at Ordered Graphite Electrodes: Influence of Electronic Factors and Reactive Sites. *J. Phys. Chem*. **1994**, 98, 5314-5319.

[6] Ambrosi, Adriano; Pumera, Martin. Electrochemistry at CVD grown multilayer graphene transferred onto flexible substrates. *J. Phys. Chem. C* **2013**, *117*, 2053-2058.

[7] Gyan, Isaiah O.; Cheng, I. F. Electrochemical study of biologically relevant molecules at GUITAR electrodes. *Microchem. J.* (submitted).

[8] Rossmeisl, J.; Qu, Z.-W.; Zhu, H.; Kroes, G.-J.; Nørskov, J. K. Electrolysis of water on oxide surfaces. *J. Electroanal. Chem*. **2007**, *607*, 83-89.

[9] Hu, Lianzhe; Li, Haijuan; Zhu, Shuyun; Fan, Lishuang; Shi, Lihong; Liu, Xiaoqing; Xu, Guobao. Cathodic electrochemiluminescence in aqueous solutions at bismuth electrodes. *Chem. Commun*. **2007**, 4146-4148.

[10] Pasta, Mauro; Mantia, Fabio La; Hu, Liangbing; Deshazer, Heather D.; Cui, Yi. Aqueous Supercapacitors on Conductive Cotton. *Nano Res* **2010**, 3, 452-458.

[11] Xia, Hui; Meng, Ying S.; Yuan, Guoliang; Cui, Chong; Lu, Li. A Symmetric RuO_2/RuO_2 Supercapacitor Operating at 1.6 V by Using a Neutral Aqueous Electrolyte. *Electrochem. Solid-State Lett*. **2012**, *15*, A60-A63.

[12] Demarconnay, L.; Raymundo-Pinero, E.; Beguin, F. A symmetric carbon/carbon supercapacitor operating at 1.6V by using a neutral aqueous solution. *Electrochem. Commun.* **2010**, *12*, 1275-1278.

[13] Frackowiak, Elzbieta; Béguin, Francois. Carbon materials for the electrochemical storage of energy in capacitors. *Carbon* **2001**, *39*, 937-950.

[14] Qu, Deyang; Shi, Hang. Studies of activated carbons used in double-layer capacitors. *J. Power Sources* **1998**, *74*, 99-107.

[15] Khomenko, V.; Raymundo-Pinero, E.; Béguin, F. High-energy density graphite/AC capacitor in organic electrolyte. *J. Power Sources* **2008**, *177*, 643-651.

[16] Chen, Fuyu; Liu, Jianguo; Chen, Hui; Yan, Chuanwei. Study on Hydrogen Evolution Reaction at a Graphite Electrode in the All-Vanadium Redox Flow Battery. *Int. J. Electrochem. Sci*. **2012**, *7*, 3750-3764.

[17] Agar, Ertan; Dennison, C. R.; Knehr, K. W.; Kumbur, E. C. Identification of performance limiting electrode using asymmetric cell configuration in vanadium redox flow batteries. *J. Power Sources* **2013**, *225*, 89-94.

[18] Weber, Adam Z.; Mench, Matthew M.; Meyers, Jeremy P.; Ross, Philip N.; Gostick, Jeffrey T.; Liu, Qinghua. Redox flow batteries: a review. *J Appl Electrochem*. **2011**, *41*, 1137-1164.

[19] Yang, Zhenguo; Zhang, Jianlu; Kintner-Meyer, Michael C. W.; Lu, Xiaochuan; Choi, Daiwon; Lemmon, John P.; Liu, Jun. Electrochemical Energy Storage for Green Grid. *Chem. Rev*. **2011**, *111*, 3577-3613.

[20] Kim, Soowhan; Yan, Jingling; Schwenzer, Birgit; Zhang, Jianlu; Li, Liyu; Liu, Jun; Yang, Zhenguo; Hickner, Michael A. Cycling performance and efficiency of sulfonated poly(sulfone) membranes in vanadium redox flow batteries. *Electrochem. Commun*. **2010**, *12*, 1650-1653.

[21] Xi, Jingyu; Wu, Zenghua; Teng, Xiangguo; Zhao, Yongtao; Chen, Liquan; Qiu, Xinping. Self-assembled polyelectrolyte multilayer modified Nafion membrane with suppressed vanadium ion crossover for vanadium redox flow batteries. *J. Mater. Chem*. **2008**, *18*, 1232-1238.

[22] Li, Xianfeng; Zhang, Huamin; Mai, Zhensheng; Zhang, Hongzhang; Vankelecom, Ivo. Ion exchange membranes for vanadium redox flow battery (VRB) applications. *Energy Environ. Sci*. **2011**, *4*, 1147.

[23] Huanga, Ke-Long; Lia, Xiao-gang; Liu, Su-qin; Tan, Ning; Chen, Li-quan. Research progress of vanadium redox flow battery for energy storage in China. *Renew. Energ*. **2008**, *33*, 186-192.

[24] Parasuraman, Aishwarya; Lima, Tuti M.; Menictas, Chris; Skyllas-Kazacos, Maria. Review of material research and development for vanadium redox flow battery applications. *Electrochim. Acta* **2013**, *101*, 27-40.

[25] Zhong, S.; Padeste, C.; Kazacos, M.; Skyllas-Kazacos, M. Comparison of the physical, chemical and electrochemical properties of rayon- and polyacrylonitrile-based graphite felt electrodes. *J. Power Sources*, **1993**, *45*, 29-41

[26] Kaneko, Hiroko; Nozaki, Ken; Wada, Yutaka; Aoki, Takamichi; Negishi, Akira; Kamimoto, Masayuki. Vanadium redox reactions and carbon electrodes for vanadium redox flow battery. *Electrochim. Acta* **1991**, *36*, 1191-1196.

[27] Sun, Bianting; Skyllas-Kazakos, M. Chemical modification and electrochemical behaviour of graphite fibre in acidic vanadium solution. *Electrochim. Acta* **1991**, *36*, 513-517.

[28] Lee, Hokyun; Kim, Hansung. Development of nitrogen-doped carbons using the hydrothermal method as electrode materials for vanadium redox flow batteries. *J. Appl. Electrochem* **2013**, *43*, 553-557.

[29] Gonzalez, Zoraida; Vizireanu, Sorin; Dinescu, Gheorghe; Blanco, Clara; Santamaria, Ricardo. Carbon nanowalls thin films as nanostructured electrode materials in vanadium redox flow batteries. *Nano Energy* **2012**, *1*, 833-839.

[30] Han, Pengxian; Yue, Yanhua; Liu, Zhihong; Xu, Wei; Zhang, Lixue; Xu, Hongxia; Dong, Shanmu, Cui, Guanglei. Graphene oxide nanosheets/multi-walled carbon nanotubes hybrid as an excellent electrocatalytic material towards VO^{2+}/VO_2^+ redox couples for vanadium redox flow batteries. *Energy Environ. Sci*. **2011**, *4*, 4710.

[31] Steele, Brian C. H.; Heinzel, Angelika. Materials for fuel-cell technologies. *NATURE* **2001**, *414*.

[32] Engstrom, Royce C.; Strasser, Vernon A. Characterization of Electrochemically Pretreated Glassy Carbon Electrodes. *Anal. Chem*. **1984**, *56*, 136-141.

[33] Zittel, H. E.; Miller, F. J. A Glassy-Carbon Electrode for Voltammetry. *Anal. Chem*. **1965**, 37, 200-203.

[34] Martin, Heidi B.; Argoitia, Alberto; Landau, Uziel; Anderson, Alfred B.; Angus, John C. Hydrogen and Oxygen Evolution on Boron-Doped Diamond Electrodes. *J. Electrochem. Soc*. **1996**, 143, L133-L136.

[35] Tanaka, Yoriko; Furuta, Masahiro; Kuriyama, Koichi; Kuwabara, Ryosuke; Katsuki, Yukiko; Kondo, Takeshi; Fujishima, Akira; Honda, Kensuke. Electrochemical properties of N-doped

hydrogenated amorphous carbon films fabricated by plasma-enhanced chemical vapor deposition methods. *Electrochim. Acta* **2011**, *56*, 1172-1181.

[36] Ndlovu, T.; Arotiba, O. A.; Sampath, S.; Krause, R. W.; Mamba, B. B. Reactivities of Modified and Unmodified Exfoliated Graphite Electrodes in Selected Redox Systems. *Int. J. Electrochem. Sci*. **2012**, *7*, 9441-9453.

[37] Teófilo, Reinaldo F.; Ceragioli, Helder J.; Peterlevitz, Alfredo C.; Da Silva, Leonardo M.; Damos, Flavio S.; Ferreira, Márcia M. C.; Baranauskas, Vitor; Kubota, Lauro T. Improvement of the electrochemical properties of "as-grown" boron-doped polycrystalline diamond electrodes deposited on tungsten wires using ethanol. *J Solid State Electrochem* **2007**, 11, 1449-1457.

[38] Alves, S. A; Migliorini, F. L.; Baldan, M. R.; Ferreira, N. G.; Lanza, M. R. V. Electrochemical and morphology study of the BDD/Ti electrodes with different doping levels. *ECS Trans*. **2012**, *43*, 191-197.

[39] Menegazzo, Nicola; Kahn, Markus; Berghauser, Roswitha; Waldhauser, Wolfgang; Mizaikoff, Boris. Nitrogen-doped diamond-like carbon as optically transparent electrode for infrared attenuated total reflection spectroelectrochemistry. *Analyst* **2011**, *136*, 1831.

[40] Wang, Shiren; Yue, Zhang, Abidi, Noureddine; Cabrales, Luis. Wettability and surface free energy of graphene films. *Langmuir* **2009**, *25*, 11078-11081.

[41] Shin, Young J.; Wang, Yingying; Huang, Han; Kalon, Gopinadhan; Wee, Andrew T. S.; Shen, Zexiang; Bhatia, Charanjit S.; Yang, Hyunsoo. Surface-Energy Engineering of Graphene. *Langmuir* **2010**, *26*, 3798-3802.

[42] Taherian, Fereshte; Marcon, Valentina; van der Vegt, Nico F. A.; Leroy, Frédéric. What is the contact angle of water on graphene? *Langmuir* **2013**, *29*, 1457-1465.

[43] Ferro, Sergio; De Battisti, Achille. Physicochemical properties of fluorinated diamond electrodes. *J. Phys. Chem. B* **2003**, *107*, 7567-7573.

[44] Siné, G.; Ouattara, L.; Panizza, M.; Comninellis, C. Electrochemical behavior of fluorinated boron-doped diamond. *Electrochem. Solid-State Lett*. **2003**, *6*, D9-D11.

[45] Kondo, Takeshi; Ito, Hiroyuki; Kusakabe, Kazuhide; Ohkawa, Kazuhiro; Honda, Kensuke; Einaga, Yasuaki; Fujishima, Akira; Kawai, Takeshi. Characterization and electrochemical properties of CF_4 plasma-treated boron-doped diamond surfaces. *Diam. & Relat. Mater*. **2008**, *17*, 48-54.

[46] Ferro, Sergio; De Battisti, Achille. The 5-V window of polarizability of fluorinated diamond electrodes in aqueous solutions. *Anal. Chem*. **2003**, *75*, 7040-7042.

[47] Ostrovskaya, L. Y.; Ral'chenko, V. G.; Vlasov, I. I.; Khomich, A. A.; Bol'shakov, A. P. Hydrophobic Diamond Films. *Protection of Metals & Physical Chemistry of Surfaces* **2013**, *49*, 325-331.

[48] Boukherroub, Rabah; Wallart, Xavier; Szunerits, Sabine; Marcus, Bernadette; Bouvier, Pierre; Mermoux, Michel. Photochemical oxidation of hydrogenated boron-doped diamond surfaces. *Electrochem. Commun*. **2005**, *7*, 937-940.

[49] Biffinger, Justin C.; Kim, Hong W.; DiMagno, Stephen G. The Polar Hydrophobicity of Fluorinated Compounds. *ChemBioChem* **2004**, *5*, 622-627.

[50] Guan, Bo; Zhi, Jinfang; Zhang, Xintong; Murakami, Taketoshi; Fujishima, Akira. Electrochemical route for fluorinated modification of boron-doped diamond surface with perfluorooctanoic acid. *Electrochem. Commun*. **2007**, *9*, 2817-2821.

[51] Hsieh, Chien-Te; Chen, Jin-Ming; Huang, Yu-Hao; Kuo, Rong-Rong; Li, Chung-Tien; Shih, Han-Chang; Lin, Ta-Sen; Wu, Chu-Fu. Influence of fluorine/carbon atomic ratio on superhydrophobic behavior of carbon nanofiber arrays. *J. Vac. Sci. Technol. B* **2006**, *24*, 113-117.

[52] Li, Tai-De; Gao, Jianping; Szoszkiewicz, Robert; Landman, Uzi; Riedo, Elisa. Structured and viscous water in subnanometer gaps. *PHYS. REV. B* **2007**, *75*, 115415.

[53] Hiratsuka, K.; Bohno, A.; Endo, H. Water droplet lubrication between hydrophilic and hydrophobic surfaces. *J. Phys. Conf. Ser*. **2007**, *89*, 012012.

[54] Kim, Doo Y.; Wang, Jian; Yang, Juchan; Kim, Hyoun W.; Swain, Greg M. Electrolyte and Temperature Effects on the Electron Transfer Kinetics of $Fe(CN)_6^{-3/-4}$ at Boron-Doped Diamond Thin Film Electrodes. *J. Phys. Chem. C* **2011**, *115*, 10026-10032.

[55] Bourke, A.; Gao, X.; Lynch, R. P.; Buckley, D. N. Kinetics of the Redox Reactions in the Vanadium Redox Flow Battery. *Abstract #142, 223rd ECS Meeting*, **2013**.

[56] McDermott, Christie A.; Kneten, Kristin R.; McCreery, Richard L. Electron Transfer Kinetics of Aquated Fe +3/+2, Eu +3/+2 and V+3/+2 at Carbon Electrodes. Inner Sphere Catalysis by Surface Oxides. *J. Electrochem. Soc*. **1993**, *140*, 2593-2599.

[57] Ding, Cong; Zhang, Huamin; Li, Xianfeng; Liu, Tao; Xing, Feng. Vanadium Flow Battery for Energy Storage: Prospects and Challenges. *J. Phys. Chem. Lett*. **2013**, *4*, 1281-1294.

[58] Tang, Longhua; Wang, Ying; Li, Yueming; Feng, Hongbing; Lu, Jin; Li, Jinghong. Preparation, Structure, and Electrochemical Properties of Reduced Graphene Sheet Films. *Adv. Funct. Mater*. **2009**, *19*, 2782-2789.

[59] Yamamura, Tomoo; Watanabe, Nobutaka; Yano, Takashi; Shiokawa, Yoshinobu. Electron-Transfer Kinetics of Np^{3+}/Np^{4+}, NpO_2^+/NpO_2^{2+}, V^{2+}/V^{3+}, and VO^{2+}/VO_2^+ at Carbon Electrodes. *J. Electrochem. Soc*. **2005**, *152*, A830-A836.

[60] Wu, Xiong W.; Yamamura, Tomoo; Ohta, Suguru; Zhang, Qi X.; Lv, Fu C.; Liu, Can M.; Shirasaki, Kenji; Satoh, Isamu; Shikama, Tatsuo; Lu, Dan; Liu, Su Qin. Acceleration of the redox kinetics of VO^{2+}/VO_2^+ and V^{3+}/V^{2+} couples on carbon paper. *J Appl Electrochem*. **2011**, *41*, 1183-1190.

[61] Sum, E.; Skyllas-Kazacos, M. A study of the V(II)/V(III) redox couple for redox flow cell applications. *J. Power Sources* **1985**, *15*, 179-190.

[62] Oriji, Gaku; Katayama, Yasushi; Miura, Takashi. Investigations on V(IV)/V(V) and V(II)/V(III) redox reactions by various electrochemical methods. *J. Power Sources* **2005**, *139*, 321-324.

[63] Pumera, Martin; Sasaki, Toshio; Iwai, Hideo. Relationship between Carbon Nanotube Structure and Electrochemical Behavior: Heterogeneous Electron Transfer at Electrochemically Activated Carbon Nanotubes. *Chem. Asian J*. **2008**, *3*, 2046-2055.

[64] Bowling, Robert J.; Packard, Richard T.; McCreery, Richard L. Activation of Highly Ordered Pyrolytic Graphite for Heterogeneous Electron Transfer: Relationship between Electrochemical Performance and Carbon Microstructure. *J. Am. Chem. Soc.* **1989**, *111*, 1217-1223.

[65] Bowling, Robert; Packard, Richard T.; McCreery, Richard L. Mechanism of Electrochemical Activation of Carbon Electrodes: Role of Graphite Lattice Defects. *Langmuir* **1989**, *5*, 683-688.

[66] Hadi, M.; Rouhollahi, A.; Yousefi, M.; Taidy, F.; Malekfar, R. Electrochemical Characterization of a Pyrolytic Carbon Film Electrode and the Effect of Anodization. *Electroanal*. **2006**, *18*, 787-792.

[67] Chakrabarti, M. H.; Brandon, N. P.; Hajimolana, S. A.; Tariq, F.; Yufit, V.; Hashim, M. A.; Hussain, M. A.; Lowd, C. T. J.; Aravind, P. V. Application of carbon materials in redox flow batteries. *J. of Power Sources* **2014**, *253*, 150-166.

[68] Suárez, David J.; González, Zoraida; Blanco, Clara; Granda, Marcos; Menéndez, Rosa; Santamaría, Ricardo. Graphite Felt Modified with Bismuth Nanoparticles as Negative Electrode in a Vanadium Redox Flow Battery. *ChemSusChem* **2014**, *7*, 914-918.

Chapter 5: Conclusions, Current and Future Studies

5.1 Summary

This dissertation has presented studies on the electrochemical characterization of a unique carbon material; Graphite from the University of Idaho Thermolyzed Asphalt Reaction (GUITAR). Results from various studies, intended to identify the place of GUITAR within carbon allotropes is presented in the various chapters of this dissertation. Similarities, as well as significant differences have been discovered when GUITAR is compared to graphite, graphene, glassy carbon and even boron doped diamond (BDD). Outlined below is a summary of the findings presented in this dissertation;

1. GUITAR affords fast heterogeneous electron transfer kinetics across its basal plane (chapter two) unlike graphite and graphene, whose low density of electronic states results in low electron transfer kinetics with dissolved redox couples such as ferri/ferrocyanide.
2. GUITAR (BP-GUITAR and EP-GUITAR), graphite (BPPG and EPPG) and glassy carbon (GC) were all found to be subject to aging in air effects. This effect has also been reported for HOPG in literature. The air aging deteriorates electron transfer kinetics with the ferri/ferrocyanide redox couple. However, it was discovered that, at GUITAR (both BP and EP) and BPPG, cathodic treatment resulted in restoration of pristine kinetics, unlike EPPG and GC. The deduction is that, the edge plane of GUITAR is in a chemically different environment compared to edge plane materials (EPPG and GC).

3. In aqueous electrolytes, GUITAR possesses the largest potential window recorded at a graphitic electrode (chapters two and four). In sulfuric acid medium, the potential window at GUITAR electrode is about 1 V wider than typical graphite electrodes and compares well with synthetic diamond electrodes.
4. At GUITAR electrodes, lack of the intercalation effect which is typical at graphite electrodes, is invoked to explain the extended anodic limit over sp^2 carbon materials. The same phenomenon explains GUITAR's anodic stability over graphite (chapters two and three). Concerning the extended cathodic limit at GUITAR; electrodes, we hypothesize the surface hydrophobicity of GUITAR to retard close approach and electron transfer to protons. Low density of states at negative potentials and/or electronic barriers to electron exchange with hydrated inner sphere species, could also contribute to this finding.
5. GUITAR electrodes exhibit facile electron transfer with biologically relevant molecules; ascorbic acid (AA), dopamine (DA) and NADH. The low overpotentials for the oxidation of these molecules at BP-GUITAR electrodes were found to be on the order of edge plane materials. This feature also supports increased density of states that increases electron transfer rates across BP-GUITAR.
6. Limit of detection and linear range for the detection of AA was found to be at least two orders of magnitude better at BP-GUITAR than literature materials (specially EPPG and graphene nano flakes).
7. At GUITAR electrodes, passivation from the electro-polymerization products of AA, DA were found to be lower than BPPG ad GC and comparable with GC in NADH.

Also, once passivated, GUITAR electrodes could be regenerated by anodic potential pulse, unlike BPPG and GC, which corroded under same conditions. Stability of GUITAR to regeneration permitted reuse of the same surface without any deterioration in performance.

8. The wide cathodic limit at GUITAR electrodes translate into 2.7 % of hydrogen evolution current during the reduction of V^{3+} in the negative half of the vanadium redox flow battery (VRB). At graphite felt control electrodes, this was found to 25 %.
9. Kinetics of V^{3+}/V^{2+} redox at flat GUITAR electrodes was found to be within an order of magnitude of edge and textured high-surface carbon materials. The heterogeneous rate constants at GUITAR electrodes could be improved by a factor of 6.6 with anodic pretreatment.
10. The possibility of fabricating composite electrodes based on GUITAR and carbon felt has been demonstrated. GUITAR was successfully deposited unto carbon tape. Future experiments will examine this and other GUITAR based composite electrodes for applications in the vanadium redox flow battery.

The sum of these is that, GUITAR behaves differently from typical graphitic materials (especially pyrolytic graphite and graphene) and is currently considered to be a new allotrope of carbon. Based on the findings from the studies presented in this dissertation, GUITAR has been found ideal for a plethora of applications. A few of these applications are, at the time of this dissertation, ongoing in our research laboratory and include;

5.2 Ultracapacitors

Exploiting the wide potential window in aqueous electrolytes together with the ability to deposit unto large-surface-area materials like silica nanosprings, development of aqueous ultracapacitors based on GUITAR is an application under study. Preliminary results in aqueous 1 M H_2SO_4 indicate that, GUITAR electrodes can achieve up to 2.3 V of capacitive window. Activated carbon, which is the most common material for commercial ultracapacitors, has a capacitive window of 0.8 V. [1] Capacitance at GUITAR electrodes are in the range of 50 – 100 μF/cm^2 and can be raised to at least 500 μF/cm^2 with anodic pretreatment. The capacitive window at GUITAR electrodes is unlike typical ultracapacitor materials that are limited to 1.0 to 2.0 V, due to water breakdown reactions (oxygen and hydrogen evolution) which are easily accessible at these electrodes. [2-4] GUITAR's capacitance in 1 M H_2SO_4 far exceeds literature values of activated carbon (10 - 20 μF/cm^2). [5] With a combination of the wide window and large capacitance, energy density of > 1000 μJ/cm^2 is expected at GUITAR capacitors. Current studies are on-going to fabricate GUITAR-based working capacitors.

5.3 Water Purification

Results from the electrochemical characterization indicates GUITAR's ability as a dimensionally stable anode for water purification. This application is necessary due to the inability of conventional methods and electrodes to meet treatment demands of growing global water pollution. [6] Chlorination, filtration and advanced oxidation either results in hazardous by-products, are always not able to achieve discharge limits, generates large amount of sludge or are costly. [7-9]

$$C_xH_yO_z + (2x - z)H_2O \rightarrow xCO_2 + (4x + y - 2z)H^+ + (4x + y - 2z)e^- \quad (1)$$

Electrooxidation (Equation 1) involves the application of positive (anodic) potentials to electrodes which ideally should degrade target pollutants ($C_xH_yO_z$) completely (equation 1), but in reality, results in various stable low molecular weight compounds. This method has been proven to be effective in degrading refractory pollutants [10] but rely on electrodes (RuO_2, IrO_2, Platinum and graphite) that are either not stable, have low potentials for oxygen evolution (1.47 – 1.7 V vs SHE in H_2SO_4), exhibits poor performance or are too expensive. [11,12] Boron-doped diamond (BDD) electrodes are recognized to have good anodic stability with high oxygen evolution potential (2.3 V vs SHE, in H_2SO_4), but are expensive and difficult to synthesize into a high surface material. [13-15]

Anodic limit at GUITAR electrodes (2.1 V vs SHE in H_2SO_4) is comparable to BDD. However, GUITAR exhibits the following added advantages over BDD; (i), faster electron transfer characteristics. This will speed up the rate of pollutant removal. (ii), the TAR process is a low cost one that allows for conformable deposition of GUITAR onto a variety of surfaces, due to its low temperature requirements. This property will allow for high-surface GUITAR-based composite electrodes.

On-going investigations are applying GUITAR electrodes to degrade methylene blue, which is been used as a surrogate pollutant. The wide cathodic limits at GUITAR electrodes will also be useful for reductive purification of water. Furthermore, as-grown GUITAR has proven to be highly hydrophobic. Preliminary studies that utilize this property, has shown that, this material is able to adsorb organics, specifically crude oil.

Altogether, various properties of GUITAR make it possible to design a water treatment reactor system that incorporates adsorption/separation and degradation (anodic and cathodic).

5.4 Future studies

1. **Vanadium redox flow batteries:** further studies will explore GUITAR-graphite felt composite electrodes for the negative half of the vanadium redox flow battery. These composite electrodes are expected to be high-surface area and benefit from the wide potential limits at GUITAR for improved performance. The redox chemistry of the V^{4+}/V^{5+} will also be explored for application of GUITAR in the positive half of the VRB. Altogether, a complete VRB assembly based on GUITAR electrodes is expected to be achieved.
2. **Biosensors:** studies on GUITAR electrodes for electrochemical detection will be extended to other biologically relevant molecules. It is expected that, GUITAR-based working biosensors will be fabricated.
3. **Electronic Properties:** in order to fully understand the electron transfer abilities of GUITAR electrodes, spectroscopic and microscopic techniques will be used to examine its electron properties, specifically density of electronic states and band structure.
4. **Defects:** future studies will look into understanding the nature of defects in this material and how they are propagated across and along its graphitic planes.

5. **More Applications:** the properties of GUITAR gives it wide applicability. These properties will be exploited for applications such as fuel cells and dye-sensitized solar cells (DSSC). [16]

5.5 References

[1] Frackowiak, Elzbieta. Carbon materials for supercapacitor application. *Phys. Chem. Chem. Phys*. **2007**, *9*, 1774-1785.

[2] Pasta, Mauro; Mantia, Fabio L.; Hu, Liangbing; Deshazer, Heather D.; Cui, Yi. Aqueous Supercapacitors on Conductive Cotton. *Nano Res.* **2010**, *3*, 452-458.

[3] Xia, Hui; Meng, Ying S.; Yuan, Guoliang; Cui, Chong; Lu, Li. A Symmetric RuO_2/RuO_2 Supercapacitor Operating at 1.6 V by Using a Neutral Aqueous Electrolyte. *Electrochem. Solid-State Lett*. **2012**, *15*, A60-A63.

[4] Li, W., Chen, D.; Li, Z.; Shi, S.; Wan, Y.; Wang, G.; Jiang, Z. Nitrogen-containing carbon spheres with very large uniform mesopores: The superior electrode materials for EDLC in organic electrolyte. *Carbon* **2007**, *45*, 1757-1763.

[5] Zhang, L. L.; Zhou, Rui; Zhao, X. S. Graphene-based materials as supercapacitor electrodes. *J. Mater. Chem*. **2010**, 20, 5983–5992.

[6] Schwarzenbach, René P.; Egli, Thomas; Hofstetter, Thomas B.; von Gunten, Urs; Wehrli, Bernhard. Global Water Pollution and Human Health. *Annu. Rev. Environ. Resour*. **2010**, *35*, 109-36.

[7] United States Environmental Protection Agency. Wastewater technology fact sheet: chlorine disinfection. *EPA 832-F-99-062*, September **1999**.

[8] Bousher, A.; Shen, X.; Edyvean, R. G. J. Removal of coloured organic matter by adsorption onto low-cost waste materials. *Wat. Res.* **1997**, *31*, 2084-2092.

[9] Panizza, Marco; Cerisola, Giacomo. Direct And Mediated Anodic Oxidation of Organic Pollutants. *Chem. Rev.* **2009**, *109,* 6541-6569.

[10] Chen, Guohua. Electrochemical technologies in wastewater treatment. *Sep. Purif. Technol*. **2004**, *38*, 11-41.

[11] Zanta, C. L. P. S.; De Andrade, A. R.; Boodts, J. F. C. Electrochemical behaviour of olefins: oxidation at ruthenium-titanium dioxide and iridium-titanium dioxide coated electrodes. *J. Appl. Electrochem*. **2000**, *30*, 467-474.

[12] Comninellis, C.; Pulgarin, C. Anodic oxidation of phenol for waste water treatment. *J. Appl. Electrochem*. **1991**, *21*, 703-708.

[13] Panizza, Marco; Cerisola, Giacomo. Direct And Mediated Anodic Oxidation of Organic Pollutants. *Chem. Rev.* **2009**, *109,* 6541-6569.

[14] Fujishima, A.; Einaga, Y.; Rao, T. N.; Tryk, D. A. Diamond Electrochemistry; Elsevier: Amsterdam, The Netherlands, 2005.

[15] Pleskov, Y. V. Synthetic diamond in electrochemistry. *Russ. J. Electrochem*. **1999**, *68*, 381-392.

[16] Hasché, Frédéric; Oezaslana, Mehtap; Strasser, Peter. Activity, stability and degradation of multi walled carbon nanotube (MWCNT) supported Pt fuel cell electrocatalysts. *Phys. Chem. Chem. Phys*. **2010**, 12, 15251-15258.

Appendix 1: Supporting Information for Chapter Two

Abstract

A schematic of the isolation of edge and basal planes of GUITAR and pyrolytic graphite is shown in Figure S2.1. Figure S2.3 shows that all electrodes used in this study exhibited reversible cyclic voltammograms with the outer sphere $Ru(NH_3)_6^{3+/2+}$ redox couple. Exposure of these electrodes to laboratory air did not affect their electron transfer characteristics with this redox couple, as is also shown in Table S2.2. An illustration of how potential limits were calculated in this work is shown in Figure S2.2 and a summary of these limits from this work and literature is presented in Table S2.1. In Figures S2.4 & S2.5, data from cyclic voltammetric studies at edge-plane GUITAR (EP-GUITAR) in $Fe(CN)_6^{3-/4-}$ are shown. From Figure S2.4, it is apparent that radial diffusion effects predominate at lower scan rates, whereas a combination of radial and linear diffusion is apparent at higher scan rates. Figure S2.5 shows the aging of the micro-band EP-GUITAR electrode which is qualitatively irreversible after 24 hours in air (B) and regains reversibility (C) after potential cycling (0 to -1.2V vs Ag/AgCl, 50 mVs^{-1}) in 1 M H_2SO_4. This reversal behavior was unlike other edge electrodes (EPPG and GC).

Experimental Methods

GUITAR was synthesized as described in previous publications. [1-3] Flakes of GUITAR and pyrolytic graphite were manipulated onto a microscope slide using a thin layer of high vacuum grease as an adhesive. This design keeps the flake intact, giving it support for

electrical contacts and was used as a working electrode for all electrochemical tests. Electrical contact was achieved with copper clips.

Edge or basal plane GUITAR graphite was fabricated by sealing appropriate planes with molten paraffin wax (Figure S2.1). This method was also used to isolate the geometric areas used for the studies. In the case of EPPG, a fresh edge was obtained by cutting along the c–axis of the mounted flake and immediately using this electrode. [4] Glassy carbon was polished with 1-micron alumina powder and sonicated in DI water prior to use. Unless otherwise noted, the setup used for all electrochemical studies was a three-electrode undivided cell with graphite rod counter electrode, Ag/AgCl/3M $NaCl_{(aq)}$ (0.209 V vs. SHE) reference electrode. Scanning electron microscope (SEM) Images of GUITAR were acquired with a Zeiss Supra 35 SEM (Carl Zeiss, Germany) with in-lens detector. The AFM image was obtained with a Veeco DI CP-II atomic force microscope operating in non-contact mode (effectively, intermittent-contact under ambient atmosphere) scanning at 1 Hz.

Cyclic voltammetric, electrode aging and cathodic regeneration studies. Electrodes were either aged in test solution or in air at room temperature. For the former, electrodes were left in contact with potassium ferrocyanide/KCl test solution and voltammograms were recorded at 5-min intervals over a 4-hr period. [5] For the latter, electrodes were exposed to air at room temperature and voltammograms were recorded at predetermined time intervals. After 24 hours in air, electrodes were cathodically cycled in 1 M H_2SO_4 (0 to -1.2V vs Ag/AgCl, 50 mVs^{-1}) and voltammetry in ferricyanide was performed immediately after treatment. Cyclic voltammetry was carried out using a Bioanalytical Systems Epsilon

potentiostat (West Lafayette, IN) at 50 mVs^{-1}. All experiments were repeated in triplicate for each electrode.

Heterogeneous electron transfer rate constants (k^o cms^{-1}) were calculated from the relationship between k^o and the voltammetric peak separation, according to the method of Nicholson, assuming $\alpha = 0.5$ and using the following diffusion coefficients $Fe(CN)_6^{3-/4-}$; D_O = 7.32 x 10^{-6} cm^2s^{-1}, D_R = 6.67 x 10^{-6} cm^2s^{-1}. $Ru(NH_3)_6^{3+/2+}$; $D_O = D_R$ = 6.5 x 10^{-6} cm^2s^{-1}. [6-8] In the case of the EP-GUITAR ultramicroband electrode (L = 3.0 mm, r = 3.3 µm), k^0 was obtained by modeling with Digisim version 3.03b software (Bioanalytical Systems West Lafayette, IN).

Table S2.1. Anodic and cathodic potential limits (vs SHE) for various carbon materials in H_2SO_4 media. GUITAR extends to wider potential limits than all graphites studied/cited and is within those for synthetic diamonds. Standard deviations were calculated with n = 3 in all cases.

Material	Cathodic limit (V)	Anodic limit (V)	Total Window (V)	Reference
BP-GUITAR	-0.89 ± 0.07	2.09 ± 0.03	3.0	This work
EP-GUITAR	-0.60 ± 0.03	1.71 ± 0.03	2.3	This work
BPPG	-0.52 ± 0.06	1.45 ± 0.03	1.97	This work
EPPG	-0.57 ± 0.05	1.58 ± 0.03	2.15	This work
Graphite[a]	-0.4 to -0.5	1.6 to 1.7	2.0 to 2.2	[9-11]
Glassy Carbon	-0.3 to -0.5	1.5 to 1.8	2.0 to 2.1	[9-11]
Synthetic Diamonds[b]	-0.4 to -1.25	1.7 to 2.4	2.3 to 3.5	[9,10,12,13]

[a] Graphite includes; HOPG and exfoliated graphite. [b] Synthetic Diamonds include; boron doped diamond, low and high sp^2 diamond and diamond-like-carbon.

Table S2.2. Effect of room temperature air exposure of electrode on voltammetric performance. Electrodes were exposed to air at room temperature and voltammograms were recorded before and after 24 hours of exposure. Test solution was 1 mM $Ru(NH_3)_6^{3+/2+}$ in 1 M KCl and scan rate was 50 mVs^{-1}. Graphite rod and Ag/AgCl were used as counter and reference electrodes respectively.

Material	t = 0hrs (ΔE_p (mV) and k°(cm^{-1}))	t = 24hrs (ΔE_p (mV) and k°(cm^{-1}))
GUITAR	69 (k° = 1.7 x 10^{-2})	69 (k° = 1.7 x 10^{-2})
Glassy Carbon	68 (k° = 1.9 x 10^{-2})	68 (k° = 1.9 x 10^{-2})
BPPG	68 (k° = 1.9 x 10^{-2})	69 (k° = 1.7 x 10^{-2})

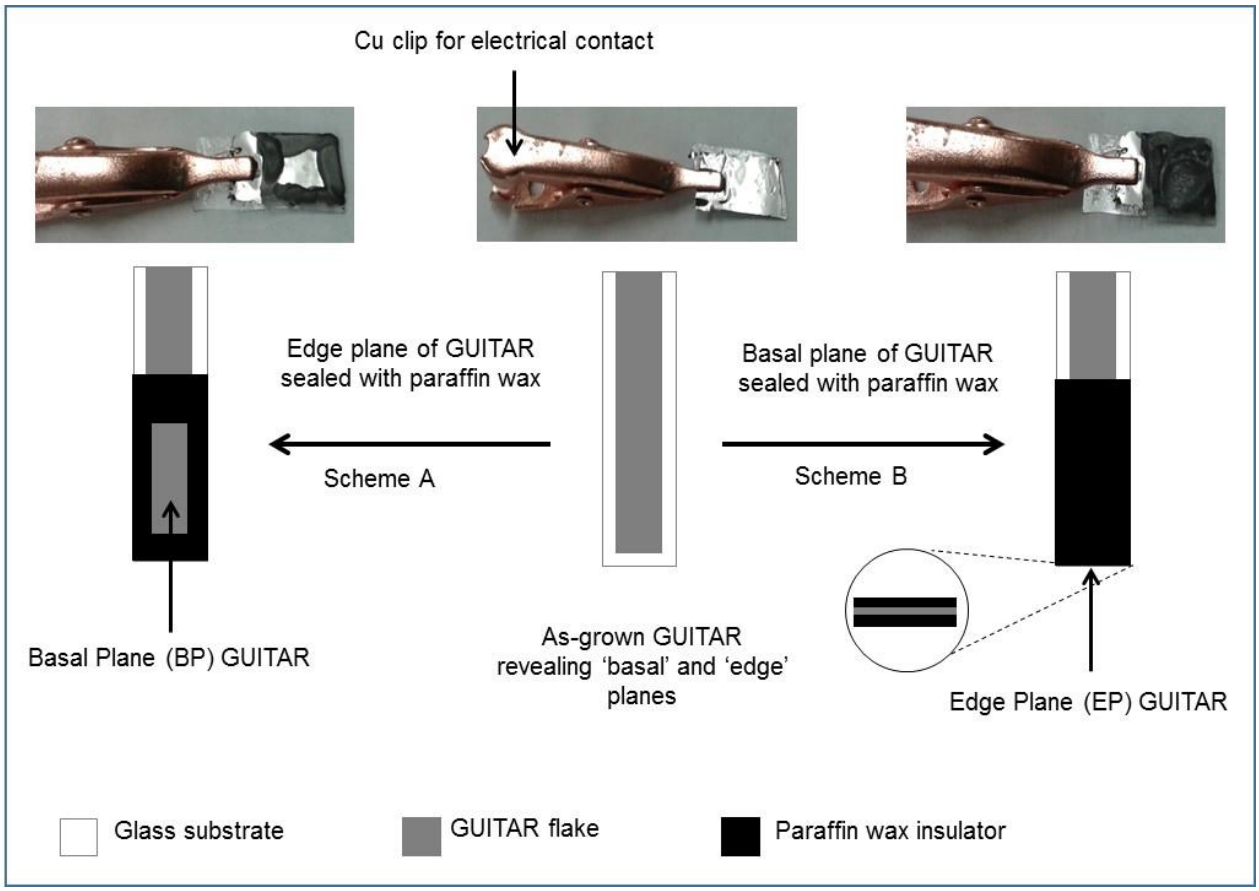

Figure S2.1. Schematic for the fabrication of basal and edge plane GUITAR. As-grown GUITAR is mounted onto a microscope glass slide with vacuum grease as adhesive. Molten paraffin wax was applied as desired to isolate the planes used for electrochemical studies. In A, wax is used to exclude edge planes. In B, the basal of the GUITAR flake is insulated with the edge plane exposed.

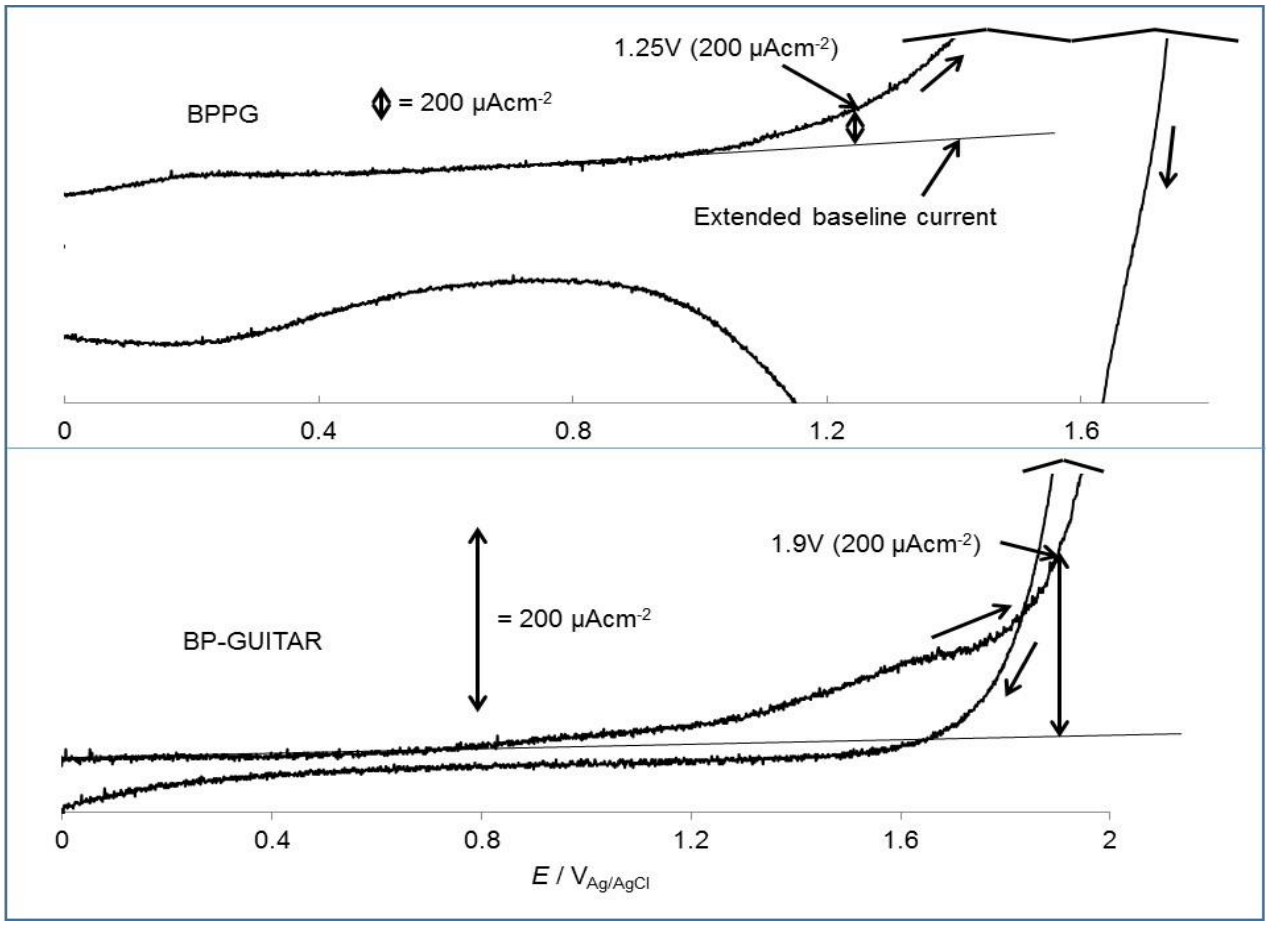

Figure S2.2. Illustration of how potential limits were obtained in this work. Voltage corresponding to the portion of the forward scan that is 200 µAcm^{-2} (double arrow bar) relative to the extended baseline current was used as the potential limit. Shown in this figure, are examples for anodic voltammograms at basal planes of pyrolytic graphite (BPPG) and GUITAR (BP-GUITAR).

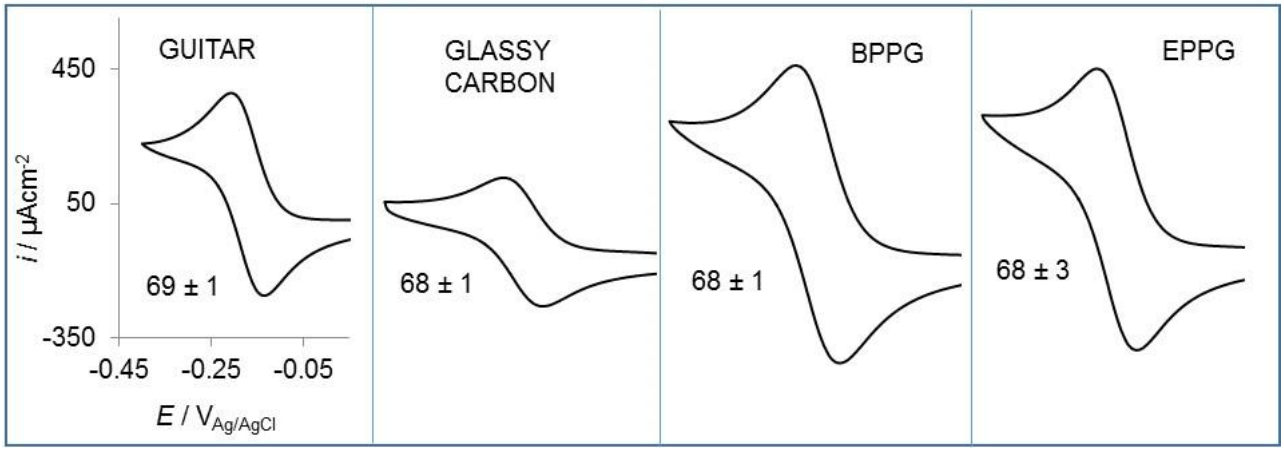

Figure S2.3. Cyclic voltammetry at various Carbon materials in 1mM $Ru(NH_3)_6^{3+/2+}$/1M KCl. Separation of anodic and cathodic peaks (ΔE_p, mV) are also shown with standard deviations from n = 3. Voltammograms were performed at 50 mVs^{-1} with graphite rod and Ag/AgCl as counter and reference electrodes respectively.

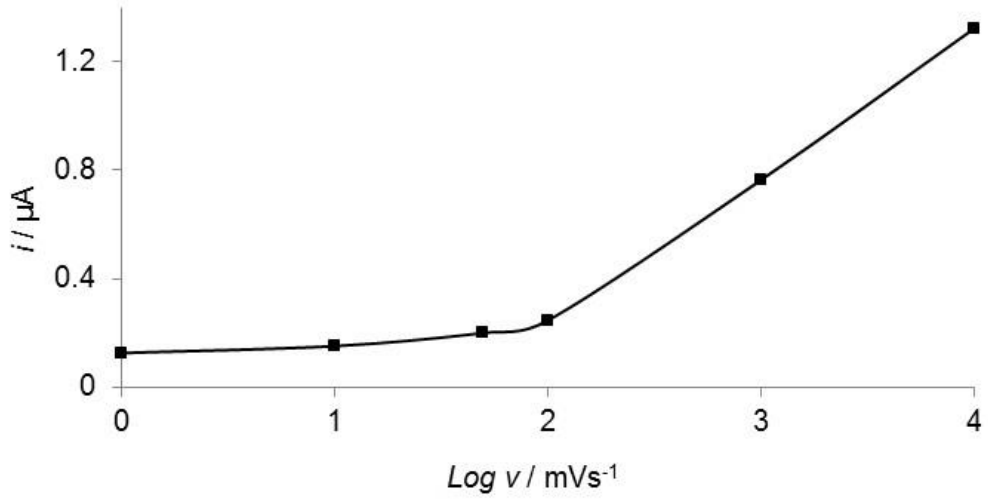

Figure S2.4. Plot of the limiting cathodic current vs. log of scan rate for the cyclic voltammetry at edge plane GUITAR in 1 mM $Fe(CN)_6^{3-/4-}$/1M KCl. See also Figure 2.5 in article (chapter two of this dissertation). At slower scan rates, diffusion is radial whereas a combination of radial and linear diffusion is seen at faster scan rates. Width of the band microelectrode was calculated as 0.6 µm with data from slower rates. This is in agreement with the 0.25 µm to 1.5 µm calculated from SEM.

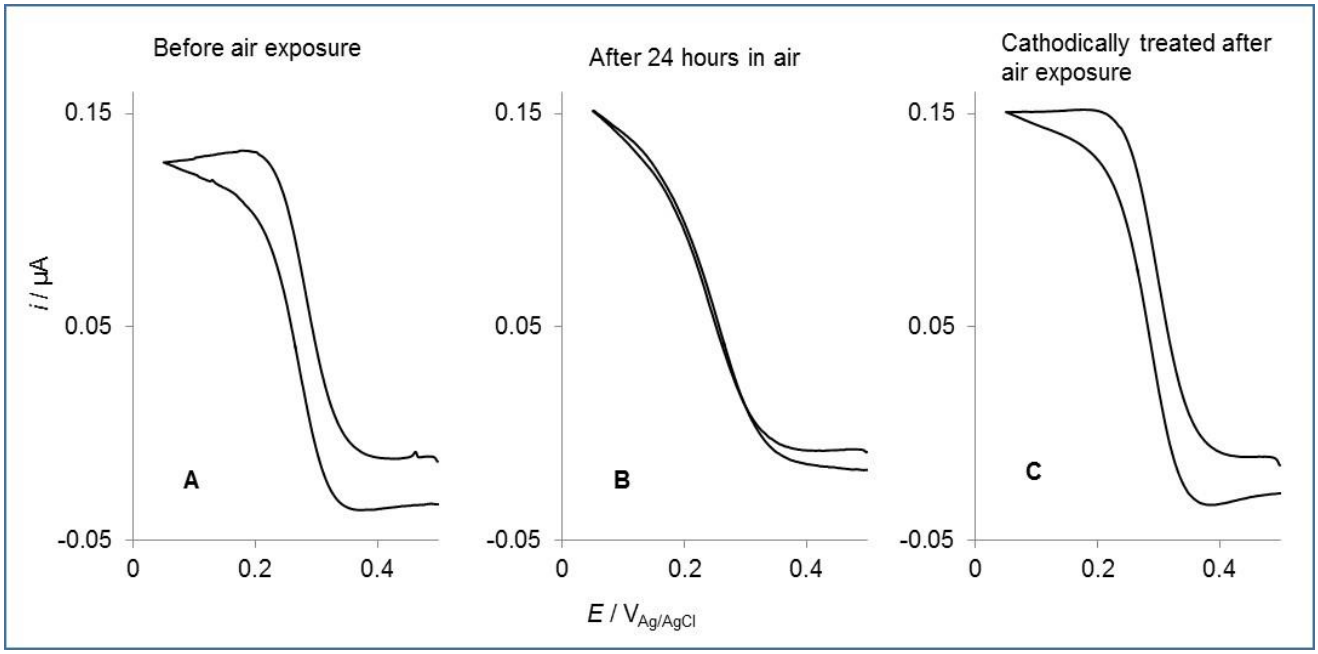

Figure S2.5. Effects of air oxidation and cathodic restoration on the voltammetric responses of 1 mM $Fe(CN)_6^{3-/4-}$ in 1 M KCl on edge-plane GUITAR. (A) EP-GUITAR before air exposure. (B) After 24 hours of air exposure the response becomes irreversible. (C) Cathodic treatment after 24 hours of air exposure restores electrochemical reversibility.

References

[1] I. F. Cheng, Y. Xie, R. A. Gonzales, P. R. Brejna, J. P. Sundararajan, B. A. Fouetio Kengne, D. E. Aston, D. N. McIlroy, J. E. Foutch, P. R. Griffiths, *Carbon* **2011**, *49*, 2852 – 2861.

[2] Y. Xie, S. D. McAllister, S. A. Hyde, J. P. Sundararajan, B. A. Fouetio Kengne, D. N. McIlroy, I. F. Cheng, *J. Mater. Chem*. **2012**, *22*, 5723 – 5729.

[3] I. F. Cheng, Y. Xie, I. O. Gyan, N. W. Nicholas, *RSC Adv*. **2013**, *3*, 2379 – 2384.

[4] C. E. Banks, R. G. Compton, *Analyst* **2006**, *131*, 15 – 21.

[5] A. N. Patel, M. G. Collignon, M. A. O'Connell, W. O. Y. Hung, K. McKelvey, J. V. Macpherson, P. R. Unwin, *J. Am. Chem. Soc*. **2012**, *134*, 20117 – 20130.

[6] A. Ambrosi, M. Pumera, *J. Phys. Chem. C* **2013**, *117*, 2053 – 2058.

[7] R. S. Nicholson, *Anal. Chem*. **1965**, *37*, 1351 – 1355.

[8] S. J. Konopka, B. McDuffie, *Anal. Chem.* **1970**, *42*, 1741 – 1746.

[9] Y. Tanaka, M. Furuta, K. Kuriyama, R. Kuwabara, Y. Katsuki, T. Kondo, A. Fujishima, K. Honda, *Electrochim. Acta* **2011**, *56*, 1172 – 1181.

[10] H. B. Martin, A. Argoitia, U. Landau, A. B. Anderson, J. C. Angus, *Electrochem. Soc.* **1996**, *143*, L133 – L136.

[11] T. Ndlovu, O. A. Arotiba, S. Sampath, R. W. Krause, B. B. Mamba, *Int. J. Electrochem. Sci.* **2012**, *7*, 9441 – 9453.

[12] R. F. Teófilo, H. J. Ceragioli, A. C. Peterlevitz, L. M. Da Silva, F. S. Damos, M. M. C. Ferreira, V. Baranauskas, L. T. Kubota, *J. Solid State Electrochem.* **2007,** *11*, 1449 – 1457.

[13] S. A. Alves, F. L. Migliorini, M. R. Baldan, N. G. Ferreira, M. R. V. Lanza, *ECS Transactions* **2012**, *43*, 191 – 197.

Appendix 2: Copyright Licenses

JOHN WILEY AND SONS LICENSE TERMS AND CONDITIONS

Apr 17, 2015

This Agreement between Isaiah Gyan ("You") and John Wiley and Sons ("John Wiley and Sons") consists of your license details and the terms and conditions provided by John Wiley and Sons and Copyright Clearance Center.

License Number	3611550882706
License date	Apr 17, 2015
Licensed Content Publisher	John Wiley and Sons
Licensed Content Publication	ChemElectroChem
Licensed Content Title	A Study of the Electrochemical Properties of a New Graphitic Material: GUITAR
Licensed Content Author	Isaiah O. Gyan,Peter M. Wojcik,D. Eric Aston,David N. McIlroy,I. Francis Cheng
Licensed Content Date	Feb 12, 2015
Pages	1
Type of use	Dissertation/Thesis
Requestor type	Author of this Wiley article
Format	Print and electronic
Portion	Full article
Will you be translating?	No
Title of your thesis / dissertation	Graphite from the University of Idaho Thermolyzed Asphalt Reaction (GUITAR): Fundamental Electrochemical Characterizations
Expected completion date	May 2015
Expected size (number of pages)	150
Requestor Location	Isaiah Gyan 327 Lauder Apt 1304 MOSCOW, ID 83843 United States Attn: Isaiah Gyan
Billing Type	Invoice
Billing Address	Isaiah Gyan 327 Lauder Apt 1304

MOSCOW, ID 83843
United States
Attn: Isaiah Gyan

Total	0.00 USD

ELSEVIER LICENSE
TERMS AND CONDITIONS

Apr 23, 2015

This is a License Agreement between Isaiah O Gyan ("You") and Elsevier ("Elsevier") provided by Copyright Clearance Center ("CCC"). The license consists of your order details, the terms and conditions provided by Elsevier, and the payment terms and conditions.

All payments must be made in full to CCC. For payment instructions, please see information listed at the bottom of this form.

Supplier	Elsevier Limited The Boulevard,Langford Lane Kidlington,Oxford,OX5 1GB,UK
Registered Company Number	1982084
Customer name	Isaiah O Gyan
Customer address	Department of Chemistry, Ren 26 Moscow, ID 83843
License number	3614620602116
License date	Apr 23, 2015
Licensed content publisher	Elsevier
Licensed content publication	Microchemical Journal
Licensed content title	Electrochemical study of biologically relevant molecules at electrodes constructed from GUITAR, a new carbon allotrope
Licensed content author	None
Licensed content date	September 2015
Licensed content volume number	122
Licensed content issue number	n/a
Number of pages	6
Start Page	39
End Page	44
Type of Use	reuse in a thesis/dissertation
Portion	full article
Format	both print and electronic
Are you the author of this Elsevier article?	Yes

Will you be translating?	No
Title of your thesis/dissertation	Graphite from the University of Idaho Thermolyzed Asphalt Reaction (GUITAR): Fundamental Electrochemical Characterizations
Expected completion date	May 2015
Estimated size (number of pages)	150
Elsevier VAT number	GB 494 6272 12
Permissions price	0.00 USD
VAT/Local Sales Tax	0.00 USD / 0.00 GBP
Total	0.00 USD
Terms and Conditions	